

MECHANISTIC APPROACHES TO RADIONUCLIDE SORPTION MODELING

Prepared for

Nuclear Regulatory Commission
Contract NRC-02-88-005

Prepared by

Center for Nuclear Waste Regulatory Analyses
San Antonio, Texas

September 1993



MECHANISTIC APPROACHES TO RADIONUCLIDE SORPTION MODELING

Prepared for

**Nuclear Regulatory Commission
Contract NRC-02-88-005**

Prepared by

David R. Turner

*Center for Nuclear Waste Regulatory Analyses
San Antonio, Texas*

September 1993

170009

*WM-11
ASG-1
NHIS
9/1*

*Delete all dirt
except
CF
NRC Pol
Nurecs Full Text
Nurecs Abstract*

ABSTRACT

Surface complexation models (SCMs) of differing complexity have been developed and applied to contaminant sorption. Three commonly used models include the Diffuse Layer (DLM), Constant Capacitance (CCM), and Triple Layer (TLM) Models. Only recently have such approaches been applied to radionuclide sorption processes. In order to compare the performance of the different models, it is necessary to generate a set of uniform SCM parameters that share common reference values. Such an approach has been developed for one model for one surface. To compare different models and to take advantage of newly available radionuclide sorption data, this approach needs to be expanded.

Using the numerical nonlinear parameter optimization code, FITEQL (Version 2.0) to interpret available potentiometric titration data, the current study provides the necessary model-dependent parameters to describe the acid-base behavior of a number of simple (hydr)oxides. Several adjustable parameters were fixed *a priori* to minimize the number of adjustable parameters and the likelihood of a nonunique fit. With these values as a necessary first step, it is possible to model available radionuclide sorption data both for simple and more complex minerals. In general, an approach has been adopted such that the simplest models that can describe the observed sorption behavior are used. Typical applications of these methods are described for U(VI) sorption on goethite and kaolinite and Np(V) sorption on biotite. These modeling results show promise for extension to other systems. Ideally, extension of this approach will lead to a set of parameters based on common methodologies and reference points. This, in turn, will allow for the direct comparison and evaluation of model performance.

CONTENTS

Section	Page
FIGURES	iv
TABLES	vi
ACKNOWLEDGES	vii
1 INTRODUCTION	1-1
1.1 TECHNICAL OBJECTIVES	1-1
1.2 INTRODUCTION	1-1
2 SORPTION MODELING AND ACID-BASE BEHAVIOR OF THE MINERAL SURFACE ..	2-1
2.1 SURFACE COMPLEXATION MODELS	2-1
2.1.1 General Model Features	2-1
2.1.2 Diffuse Layer Model	2-4
2.1.3 Constant Capacitance Model	2-5
2.1.4 Triple Layer Model	2-5
2.1.5 SCM Model Strengths and Weaknesses	2-6
2.2 SCM PARAMETER ESTIMATION	2-7
2.2.1 Mineral Acid-Base Behavior	2-7
2.2.2 Previous Work	2-7
2.3 POTENTIOMETRIC TITRATION DATA	2-9
2.3.1 Data Interpretation	2-10
2.3.2 Parameter Estimation Using FITEQL, Version 2.0	2-12
2.4 DISCUSSION OF RESULTS	2-13
2.5 MINERAL ACID-BASE BEHAVIOR — SUMMARY AND CONCLUSIONS	2-18
3 GEOCHEMICAL MODELING OF RADIONUCLIDES WITH MINTEQA2, VERSION 3.11	3-1
3.1 INTRODUCTION AND CODE DESCRIPTION	3-1
3.2 DATA SOURCES	3-1
3.3 DATABASE COMPARISON	3-2
4 RADIONUCLIDE SORPTION CONSTANTS	4-1
4.1 INTRODUCTION	4-1
4.2 SORPTION ON SIMPLE OXIDES: URANIUM SORPTION ON GOETHITE — AN EXAMPLE	4-1
4.2.1 Controlled Atmosphere (No CO ₂) Experiments	4-2
4.2.2 Modeling Sorption in the U(VI)-H ₂ O-CO ₂ -Goethite System	4-11
4.2.3 Effect of Data Set Size	4-19
4.3 MODELING OF COMPLEX ROCK-FORMING MINERALS	4-20
4.4 RADIONUCLIDE SORPTION MODELING — SUMMARY AND CONCLUSIONS ..	4-21
5 SUMMARY AND CONCLUSIONS	5-1
6 REFERENCES	6-1

FIGURES

Figure	Page	
2-1	Schematic diagram of the mineral-water interface ($T=25\text{ }^{\circ}\text{C}$) as represented in the (a) DLM, (b) CCM, and (c) TLM	2-3
2-2	SCM modeling results as compared to experimental potentiometric titration data. Results are shown for the model and mineral as indicated. Solid lines calculated using the weighted acidity constants given in Table 2-3. Dashed lines use best-fit acidity constants as calculated by FITEQL (Westall, 1982a, b)	2-16
2-3	Comparison of modeling results. DLM and TLM results calculated using weighted acidity constant values given in Table 2-3	2-17
2-4	Actual pH_{ZPC} vs calculated pH_{ZPC} . Actual values and uncertainty are from values given in Table 2-2. Calculated values are determined for the CCM and DLM using the values for $\log K_+$ and $\log K_-$ obtained using FITEQL and Eq. (2-12)	2-19
3-1	$\text{U(VI)}_{\text{T}} = 2 \times 10^{-6}\text{ M}$, No CO_2 , $I=0.1\text{ M NaNO}_3$, $T=25\text{ }^{\circ}\text{C}$; (a) U(VI) Speciation predicted by THERMO.DBS database as distributed with MINTEQA2. Uranium data from Langmuir (1978). (b) U(VI) speciation as predicted by the expanded MINTEQA2 database	3-4
3-2	$\text{U(VI)}_{\text{T}} = 2 \times 10^{-5}\text{ M}$, No CO_2 , $I=0.1\text{ M NaNO}_3$, $T=25\text{ }^{\circ}\text{C}$; (a) U(VI) Speciation predicted by THERMO.DBS database as distributed with MINTEQA2. Uranium data from Langmuir (1978). (b) U(VI) speciation as predicted by the expanded MINTEQA2 database. Uranium data from EQ3/6 database	3-4
3-3	$\text{U(VI)}_{\text{T}} = 2 \times 10^{-6}\text{ M}$, variable CO_2 , $I=0.1\text{ M NaNO}_3$, $\text{pH}=6.9$, $T=25\text{ }^{\circ}\text{C}$; (a) U(VI) speciation predicted by THERMO.DBS database as distributed with MINTEQA2. Uranium data from Langmuir (1978). (b) U(VI) speciation as predicted by the expanded MINTEQA2 database	3-5
3-4	Variable U(VI)_{T} , $p(\text{CO}_2) = 10^{-3.48}\text{ atm}$, $I=0.1\text{ M NaNO}_3$, $\text{pH}=6.9$, $T=25\text{ }^{\circ}\text{C}$; (a) U(VI) speciation predicted by THERMO.DBS database as distributed with MINTEQA2. Uranium data from Langmuir (1978). (b) U(VI) speciation as predicted by the expanded MINTEQA2 database	3-5
3-5	$\text{U(VI)}_{\text{T}}=2 \times 10^{-5}\text{ M}$, No CO_2 , $I=0.1\text{ M NaNO}_3$, $T=25\text{ }^{\circ}\text{C}$. U(VI) speciation predicted by EQ3 (solid lines) and MINTEQA2 (dashed lines)	3-6
3-6	$\text{U(VI)}_{\text{T}}=2 \times 10^{-5}\text{ M}$, $p(\text{CO}_2)=10^{-3.48}\text{ atm}$, $I=0.1\text{ M NaNO}_3$, $T=25\text{ }^{\circ}\text{C}$. U(VI) speciation predicted by EQ3 (solid lines) and MINTEQA2 (dashed lines)	3-6
4-1	Controlled atmosphere (No CO_2) experimental data for the U(VI)- H_2O -Goethite system. Data are from Tripathi (1984) and Hsi and Langmuir (1985)	4-3
4-2	SCM modeling results. (a) DLM; (b) CCM; (c) TLM. Parameters from Tables 2-2, 2-3, 4-1. Sorption data from Tripathi (1984). $\text{U(VI)}_{\text{T}}=1.05 \times 10^{-6}\text{ M}$, No CO_2 , 0.1 M NaNO_3	4-9
4-3	SCM modeling results. (a) DLM; (b) CCM; (c) TLM. Parameters from Tables 2-2, 2-3, and 4-2. Sorption data from Hsi and Langmuir (1985). $\text{U(VI)}_{\text{T}}=10^{-5}\text{ M}$, No CO_2 , 0.1 M NaNO_3	4-10
4-4	Experimental data for the U(VI)- H_2O - CO_2 -Goethite system. Data are from Tripathi (1984) and Hsi and Langmuir (1985)	4-12

FIGURES (Cont'd)

Figure		Page
4-5	SCM modeling results. (a) DLM; (b) CCM; (c) TLM. Parameters from Tables 2-2, 2-3, 4-4. Sorption data from Tripathi (1984). $U(VI)_T = 1.05 \times 10^{-6}$ M, $p(CO_2) = 10^{-3.48}$ atm, 0.1 M $NaNO_3$	4-15
4-6	SCM modeling results. (a) DLM; (b) CCM; (c) TLM. Parameters from Tables 2-2, 2-3, 4-5. Sorption data from Hsi and Langmuir (1985). $U(VI)_T = 10^{-5}$ M, $C_T = 0.01$ M, 0.1 M $NaNO_3$	4-16
4-7	SCM modeling results for the $U(VI)-H_2O-CO_2$ -Goethite system assuming three surface complexes: $XOH_2-UO_2(CO_3)_2^-$; $XOH_2-UO_2(CO_3)_3^{3-}$; and $XOH_2-(UO_2)_2CO_3(OH)_3^0$. Parameters from Tables 2-2, 2-3. (a) DLM with data from Tripathi (1984); log K from Tables 4-4 and 4-6; and (b) TLM with data from Hsi and Langmuir (1985)	4-18
4-8	DLM modeling results for: (a) $U(VI)$ -Kaolinite sorption (Payne et al., 1992); and (b) $Np(V)$ -Biotite sorption (Nakayama and Sakamoto, 1991). Postulated surface species are as indicated, binding constants are from Tables 4-8 and 4-9	4-23

TABLES

Table	Page
2-1	Potential sources of experimental sorption data for SCM parameter estimation 2-2
2-2	Mineral properties used in interpreting potentiometric titration with data sources 2-10
2-3	Best estimate values for SCM constants – simple (hydr)oxides 2-15
3-1	Sources for EQ3 (Data.com.r16, 26Jun92) equilibrium constant data adapted to MINTEQA2 3-3
4-1	Weighted Log K values for forming the indicated surface complexes in the (VI)-H ₂ O-Goethite system (No-CO ₂) derived from Tripathi (1984) data using FITEQL. Mineral properties and acidity constants are listed in Tables 2-2 and 2-3 4-5
4-2	Log K values for forming the indicated surface complexes in the U(VI)-H ₂ O-Goethite system (No-CO ₂) derived from Hsi and Langmuir (1985) data using FITEQL. Mineral properties and acidity constants are listed in Tables 2-2 and 2-3 4-6
4-3	Weighted log K values for forming the indicated surface complexes in the U(VI)-H ₂ O-Goethite system (No-CO ₂) determined by combining the results from Tripathi (1984) and Hsi and Langmuir (1985) 4-7
4-4	Weighted log K values for forming the indicated surface complexes in the U(VI)-H ₂ O-CO ₂ -Goethite system derived from Tripathi (1984) data using FITEQL. Mineral properties and acidity constants are listed in Tables 2-2 and 2-3 4-13
4-5	Log K values for forming the indicated surface complexes in the U(VI)-H ₂ O-CO ₂ -Goethite system derived from Hsi and Langmuir (1985) data using FITEQL. Mineral properties and acidity constants are listed in Tables 2-2 and 2-3 4-17
4-6	Weighted log K values for forming the indicated surface complexes in the U(VI)-H ₂ O-CO ₂ -Goethite system determined by combining the data of Tripathi (1984) and Hsi and Langmuir (1985). Mineral properties and acidity constants are listed in Tables 2-2 and 2-3 4-19
4-7	Effect of data set size (number of measurements) on log K estimated using FITEQL. Data from Tripathi (1984). Mineral properties and acidity constants are listed in Tables 2-2 and 2-3 4-20
4-8	Log K values the DLM for forming the indicated surface complexes in the U(VI)-Kaolinite system derived from Payne et al. (1992) data using FITEQL. Acidity constants are from Table 2-3 4-22
4-9	Log K values the DLM for forming the indicated surface complexes in the Np(V)-Biotite system derived from Nakayama and Sakamoto (1991) data using FITEQL. Acidity constants are from Table 2-3 4-22

ACKNOWLEDGMENTS

This report was prepared to document work performed by the Center for Nuclear Waste Regulatory Analyses (CNWRA) for the U.S. Nuclear Regulatory Commission (NRC) under Contract No. NRC-02-88-005. The activities reported herein were performed on behalf of the NRC Office of Nuclear Regulatory Research (RES), Division of Regulatory Applications. George F. Birchard is the NRC project manager, and H. Lawrence McKague is project manager at CNWRA. The report is an independent product of CNWRA and does not necessarily reflect the views or regulatory position of the NRC.

The author would like to thank Roberto Pabalan and Budhi Sagar for technical and programmatic review of this document. The author also wishes to thank Stephen Sassman, Tim Griffin, and Todd Dietrich who provided invaluable assistance in conducting the computer modeling reported in this study. Able secretarial support was provided by Esther Cantu.

1 INTRODUCTION

1.1 TECHNICAL OBJECTIVES

A fundamental concern in evaluating the suitability of Yucca Mountain, Nevada, as a repository for high-level nuclear wastes (HLW) is the possibility of radionuclide migration to the accessible environment as dissolved constituents in groundwaters. An important mechanism for attenuating radionuclide migration is sorption of radionuclides on minerals encountered along the flow paths. Sorption is specifically referred to in 10 CFR 60.122(b) as a favorable geochemical condition that will tend to inhibit radionuclide migration and "... favorably affect the ability of the geologic repository to isolate the waste...". Conversely, geochemical processes that "... would reduce sorption of radionuclides..." are listed [10 CFR 60.122(c)(8)] as potentially adverse conditions that could reduce the effectiveness of the natural barrier system.

To support the U.S. Nuclear Regulatory Commission's (NRC) HLW program, the Center for Nuclear Waste Regulatory Analyses (CNWRA) is conducting research activities under the Sorption Modeling for HLW Performance Assessment Research Project. The broad objectives are to develop a sufficient understanding of radionuclide transport issues so that timely preclicensing guidance can be provided to the U.S. Department of Energy (DOE) and to establish a sound basis that will be available for evaluating the DOE license application. Specifically, the results will be used in addressing NRC needs in evaluating the use of K_d 's in modeling sorption.

1.2 INTRODUCTION

Sorption is generally incorporated into performance assessment (PA) models through the use of an empirical linear sorption isotherm, which assumes that sorption of a given radionuclide is instantaneous, reversible, and increases linearly with the concentration in solution. The advantage to this approach lies in its computational simplicity, representing solute/rock interaction through a single lumped sorption coefficient, (K_d). The limitations to this approach have been discussed in detail elsewhere (Reardon, 1981; Kent et al., 1988; Davis and Kent, 1990; Pabalan and Turner, 1992). In general, such an approach cannot consider changes in system chemistry or variations in the mineral-water interface. For example, traditional applications assign the sorption coefficient as a physical property of the geologic medium of interest. Because many radionuclides are known to exhibit complex pH-dependent sorption behavior (Kohler et al., 1992), however, strict application of an empirical K_d approach would require a different sorption coefficient for each change in the physical and/or chemical system. This can quickly lead to an excessive experimental burden to represent the heterogeneous conditions likely to be encountered in the geologic environment of interest. Complex sorption behavior also makes it difficult to determine which radionuclides are strongly sorbed, as K_d can vary over several orders of magnitude with fairly small changes in chemical conditions (Rundberg, 1992).

As an alternative, it is desirable to develop more mechanistic approaches to sorption that use geochemical principles to simulate changes in the system and model complex sorption behavior (Davis and Kent, 1990). However, the complexity and computational requirements of such models tend to work against their ready incorporation in PA codes. Therefore, practical application of mechanistic sorption models requires that a balance be struck between model completeness, robustness, and computational

efficiency, streamlining the model where possible. Comparison and evaluation of different modeling approaches is a necessary part of this process.

Surface complexation models (SCMs) represent one type of mechanistic approach that has been used to model contaminant sorption on oxide surfaces over a wide range of chemical conditions (e.g., pH, ionic strength, total concentration of adsorbate) (Sanchez et al., 1985; Girvin et al., 1991; Payne et al., 1992). In modeling surface phenomena based on chemistry changes in the bulk solution, these equilibrium models are distinctive in that they include representations of the electrostatic interactions at the mineral-water interface. More commonly used SCMs include: Triple Layer (TLMs), Diffuse Layer (DLMs), and Constant Capacitance (CCMs) Models (Westall and Hohl, 1980; Hayes et al., 1990; Davis and Kent, 1990). The application of these models requires a set of model-specific parameters representing the system chemistry and the properties of the adsorbent; the number of parameters varies with the complexity of the model.

The objectives of this report are to investigate SCMs as mechanistic alternatives to empirical approaches for possible incorporation into PA codes. This report includes an introduction of different modeling approaches and identification of necessary input parameters. Methods for determining values of these parameters and possible sources for the necessary data are identified. A systematic approach is taken towards selecting a uniform set of parameters so that the results of individual models can be compared and contrasted. Finally, as an example, uranium and neptunium sorption data are interpreted using this uniform approach to determine values for application of different SCMs to the prediction of complex radionuclide sorption behavior.

2 SORPTION MODELING AND ACID-BASE BEHAVIOR OF THE MINERAL SURFACE

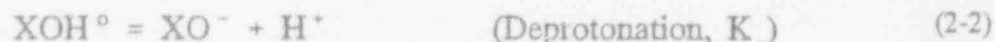
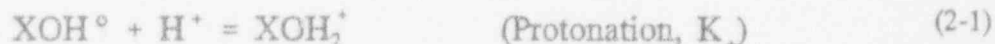
Many studies have been conducted during the past several decades to examine the complex sorption behavior of toxic elements, such as Zn^{2+} , Cd^{2+} , Pb^{2+} , Hg^{2+} , and CrO_4^{2-} , on a number of different mineral surfaces. SCMs have largely been developed and refined as a mechanistic approach to investigating these systems. Given the increasing concern with radioactive waste, similar experiments have begun to be performed for key radionuclides (especially actinides), with the results only recently reaching the open literature. Table 2-1 is a listing of some of the available data identified in the current study. In order to take full advantage of this research, there is a need to apply SCM approaches to data interpretation.

2.1 SURFACE COMPLEXATION MODELS

The surface charge of many minerals, primarily (hydr)oxides, is known to vary as a function of pH (Kent et al., 1988; Davis and Kent, 1990). SCMs deal with this pH-dependence by assuming a surface comprised of hydroxyl groups (XOH^0). By adding a hydrogen ion (protonation), a positively charged surface site, XOH_2^+ is developed. Conversely, losing a proton (deprotonation) leads to the development of a negatively charged surface (XO^-). At low pH, the XOH_2^+ sites are more abundant, and the surface is positively charged. At higher pH, the XO^- sites are more numerous, and the net surface charge is negative. At some intermediate pH referred to as the zero point of charge (pH_{ZPC}), the number of XO^- and XOH_2^+ sites will balance, and the surface will not exhibit any net charge. Therefore, depending on the pH, the electrostatic attraction from these sites can lead to the specific adsorption of cations and anions from solution. Surface adsorption can then be described using a combination of equilibrium protonation/deprotonation and complexation reactions (Davis and Leckie, 1978; Hayes et al., 1990).

2.1.1 General Model Features

To describe the acid-base behavior of a mineral surface, equilibrium protonation/deprotonation reactions are written in the form



where K_+ and K_- are referred to as intrinsic surface acidity constants. Eqs. (2-1) and (2-2) clearly show the pH dependence of surface charge development.

Electrical work done in moving ions across the zone of charge influence adjacent to the interface will affect the activity of aqueous species near the charged surface relative to its activity in the bulk solution. The change in activity due to electrostatic forces is governed by the Boltzmann relation

Table 2-1. Potential sources of experimental sorption data for SCM parameter estimation

I. URANIUM							
Hematite	Goethite	HFO	Al ₂ O ₃	Zeolite	Clay/Mica	TiO ₂	Magnetite
a	a,b,c	a,d	e	f	e,d,g	h,i	i
II. PLUTONIUM							
Goethite	Al ₂ O ₃						
j	k						
III. NEPTUNIUM							
Hematite	Goethite	HFO	Clay/Mica	SiO ₂	Al ₂ O ₃		
c,l	l	m	c	n	k		
IV. AMERICIUM							
SiO ₂	Al ₂ O ₃	Clay/Mica					
n,o	k,n	p					
V. THORIUM							
Goethite	SiO ₂	Al ₂ O ₃	MnO ₂	Clay/Mica			
q,r	n,s	k	q	s			
[a] Hsi and Langmuir (1985); [b] Tripathi (1984); [c] Kohler et al. (1992); [d] Payne et al. (1992); [e] Current experimental program at CNWRA; [f] Pabalan et al. (1993); [g] Della Mea et al. (1992); [h] Lieser and Thybusch (1988); [i] Venkatamarani and Gupta (1991); [j] Sanchez et al. (1985); [k] Righetto et al. (1988); [l] Nakayama and Sakamoto (1991); [m] Girvin et al. (1991); [n] Righetto et al. (1991); [o] Moulin et al. (1992); [p] Stammose and Dolo (1990); [q] Hunter et al. (1988); [r] LaFlamme and Murray (1987); [s] Riese (1982)							

$$a_{i,s} = a_i \left[e^{\frac{-\psi_j F}{RT}} \right]^z \quad (2-3)$$

where $a_{i,s}$ is the activity of a given ion, i , in the aqueous phase near the charged surface, a_i is the activity in the bulk solution, $e^{-\psi_j F/RT}$ is the Boltzmann factor, ψ_j is the electrostatic potential of the J th layer, z is the valence of the ion, F and R are the Faraday ($J/volt$ equiv) and ideal gas ($J/K \cdot mole$) constants, respectively, and T is absolute temperature (K). This correction is incorporated into the mass action expressions for surface reactions.

In all SCMs, the particle surface with specific charge σ_s (coulombs) is separated from the bulk solution by a diffuse layer of nonspecifically bound counterions. The models differ in how the mineral water interface is divided between the charged surface and the bulk solution, and in the charge-potential relationships used for the different layers (Figure 2-1). A general sorption reaction can be written as

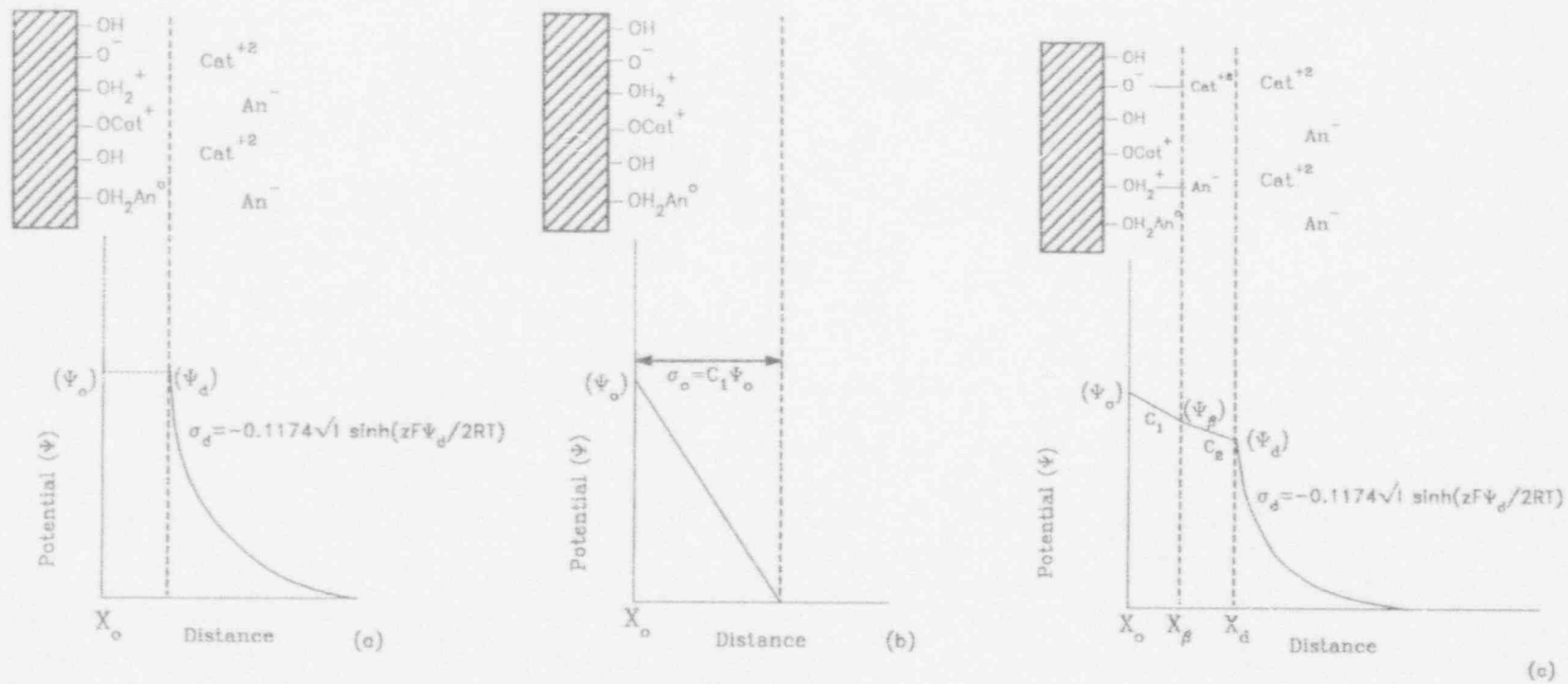


Figure 2-1. Schematic diagram of the mineral-water interface ($T=25\text{ }^\circ\text{C}$) as represented in the (a) DLM, (b) CCM, and (c) TLM (Modified from Hayes et al., 1991).



where XOH° represents a neutral surface site, and C^{z+} is a sorbing cation. The corresponding equilibrium constant for this reaction, K_C is commonly called a sorption or binding constant. Depending on the model, the mass action expression for K_C is

$$K_C = \left(\frac{[\text{XO} \cdot \text{C}^{(z-1)+}] [\text{H}^+] e^{-\Psi_j F / RT}}{[\text{XOH}^\circ] [\text{C}^{z+}] (e^{-\Psi_j F / RT})^z} \right) \quad (2-5)$$

where Ψ_j is the electrostatic potential (volts) of layer J which depends on how the model represents the mineral-water interface. A similar construction is used for describing anion (A^{z-}) adsorption (K_A) and intrinsic surface acidity constants (K_+ , K_-).

Mass balance for the total concentration of available surface sites (T_{XOH} in moles of sites/l) is

$$T_{\text{XOH}} = \frac{(N_s) \times (A_{\text{SP}}) \times (c_s) \times 10^{18} \text{ nm}^2/\text{m}^2}{6.023 \times 10^{23} \text{ sites/mole}} \quad (2-6)$$

where N_s is site density (sites/nm²), A_{SP} (m²/g) is specific surface area of the mineral, and c_s is the solid mass of the adsorbent in suspension (g/l).

These mass action, mass balance and charge-potential relations can be used in a manner analogous to that employed by geochemical speciation codes (Westall and Hohl, 1980; Allison et al., 1991). Eq. (2-6) is combined with charge-potential relationships specific to a given model, and a set of mass-action relationships analogous to Eq. (2-5) are used to describe concentration distributions of surface and aqueous species as a function of solution chemistry and surface charge.

2.1.2 Diffuse Layer Model

The DLM assumes that protonation/deprotonation and adsorption only occur in one plane at the surface-solution interface (Figure 2-1a), and that only those ions specifically adsorbed in this "o-plane" contribute to the total surface charge (i.e., $\sigma_s = \sigma_o$). Protonation and deprotonation of the surface sites are represented by the reactions given in Eqs. (2-1) and (2-2). Background electrolytes, such as Na^+ and NO_3^- , are assumed to be inert and not adsorb at the surface. For the adsorption of the contaminants M^+ and A^- , the general form of these reactions is



where the mass action equilibrium constants are represented by $K_{\text{M}+}$ and $K_{\text{A}-}$, respectively, and defined by an equation similar in form to Eq. (2-5) given above.

In the DLM, the Stern-Grahame extension of the Gouy-Chapman relationship (Davis and Kent, 1990) for symmetrical electrolytes is used to describe the interdependence between electrolyte concentration (ionic strength), charge ($\sigma_d = -\sigma_o = -\sigma_s$ at the boundary with the o-plane), and electrostatic potential ($\Psi_d = \Psi_o$) such that

$$-\sigma_o = \sigma_d = -\left(\sqrt{8\epsilon\epsilon_oIRT}\right) \left[\sinh \frac{(z\Psi_d F)}{2RT}\right] \quad (2-8)$$

where F , R , z , and T are as defined above, ϵ is the dielectric constant, ϵ_o is the permittivity in free space (8.85×10^{-12} coulombs²/J·m), and I is solution ionic strength.

2.1.3 Constant Capacitance Model

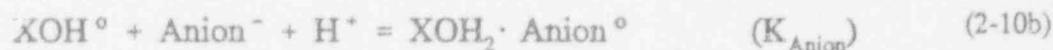
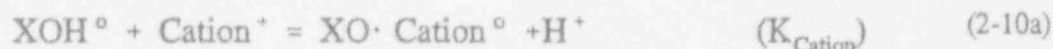
Like the DLM, the CCM also assumes a 1-layer interface, and the reactions, mass balance, and mass action used to describe surface phenomena are the same as those presented for the DLM. In contrast to the DLM, the CCM assumes that the charged surface is separated from the bulk solution by a layer of constant capacitance (Figure 2-1b). Based on this assumption, surface charge ($\sigma_d = -\sigma_o = -\sigma_s$) is related to surface potential ($\Psi_o = \Psi_d$) through the simple linear equation

$$-\sigma_o = \sigma_d = C_1 \Psi_o \quad (2-9)$$

where C_1 (Farads/m²) is a constant capacitance term. This relationship results in a linear potential gradient from the charged substrate to the bulk solution. The constant capacitance approach is limited to a specific ionic strength, however, and changes in ionic strength require recalculation of C_1 . Generally, the constant capacitance term is not provided as a characteristic property of a given system, but is applied instead as an empirical parameter fit to the data (Westall and Hohl, 1980; Hayes et al., 1990). This has the advantage of providing a better fit to a given data set, but at the expense of the theoretical basis of the model.

2.1.4 Triple Layer Model

Unlike the DLM and CCM, the TLM divides the mineral-water interface into three layers (Figure 2-1c). In its original construction (Davis et al., 1978), protonation/deprotonation of surface sites (K_+ and K_-) is restricted to the innermost o-plane, while specifically adsorbed ions are typically assigned to the β -plane (i.e., outer-sphere complexes). Subsequent modifications (Hayes and Leckie, 1987) provide for inner-sphere complexes to describe strongly bound metals. The outermost layer, the d-plane, is made up of a diffuse region of counterions extending into the bulk solution. Also, unlike the DLM and CCM, the TLM allows for adsorption of the background electrolyte. This leads to the introduction of an additional set of reactions such that



where K_{Cation} and K_{Anion} represent the equilibrium constants for adsorption of the background cation (e.g., Na^+) and anion (e.g., NO_3^-), respectively.

Surface charges in the TLM are designated σ_o and σ_β for the o- and β -layers, respectively. At the boundary between the intermediate β -layer and the diffuse outer d-layer, the diffuse layer charge (σ_d) is defined such that $\sigma_o + \sigma_\beta + \sigma_d = 0$. Charge-potential relations for the different layers are

$$\sigma_o = (\psi_o + \psi_\beta)C_1 \quad (2-11a)$$

$$\sigma_o + \sigma_\beta = (\psi_\beta + \psi_d)C_2 = -\sigma_d \quad (2-11b)$$

$$\sigma_d = -(\sqrt{8\epsilon\epsilon_o IRT}) \left[\sinh \frac{(z\psi_d F)}{2RT} \right] \quad (2-11c)$$

where C_1 , and C_2 (Farads/m²) are constant capacitances associated with the areas between the o- and β -planes and β - and d-planes, respectively. I , z , ψ_d , F , R , T , ϵ , and ϵ_o are as defined previously.

2.1.5 SCM Model Strengths and Weaknesses

Not surprisingly, each of the different SCMs considered here has strengths and weaknesses. Relative to empirical K_d models, the strength of all SCMs is the ability to handle changes in chemistry in a quantitative fashion to predict complex sorption behavior. The major drawback of the models is the complexity inherent in their construction, limiting practical applications in PA. This complexity is reflected in the number of adjustable parameters used in each model. The DLM is the simplest model, and requires only four types of adjustable parameters: Acidity constants for Protonation/Deprotonation (K_+ , K_-); Sorbing Radionuclides (such as $K_{UO_2^{2+}}$); and Site Density (N_s). Because it uses the Gouy-Chapman expression for charge-potential relationships [Eq. 2-8], this model is applicable at a variety of ionic strength conditions (Hayes et al., 1990), although it was developed for application to fairly dilute solutions (Davis and Kent, 1990). The CCM shares the same parameters as the DLM but adds a capacitance term (C_1) for charge-potential relationships [Eq. 2-9]. The CCM was developed for application to more concentrated solutions, and the capacitance is determined at a single ionic strength; therefore, in a strict sense, the CCM acidity constants are only valid at one ionic strength and new capacitances and surface equilibrium constants are necessary if conditions change. As the most elaborate model, the TLM requires seven types of adjustable parameters; the four offered by the DLM plus: Binding Constants for Sorbing Background Electrolytes (K_{Cation} and K_{Anion} such as K_{Na^+} , $K_{NO_3^-}$) and Capacitances for the inner and outer layers (C_1 and C_2 , respectively). Like the DLM, the TLM uses the Gouy-Chapman relationship and is also applicable at different ionic strengths. The TLM is also able to handle ionic strength effects through its provisions for background electrolyte adsorption.

The values of these parameters are imperfectly known, and in practice they have tended to be used as multiple fitting parameters specific to a particular data set (Sanchez et al., 1985; Hsi and Langmuir, 1985; LaFlamme and Murray, 1987). Given the number of parameters involved, this will almost certainly lead to nonunique fits to the data. Also, because of both fundamental differences in how the models treat the mineral-water interface and the tendency to use model-specific nonstandard parameters, it is difficult to compare directly the results of different studies, and it is even more difficult to compare the performance of different models for a given data set (Westall and Hohl, 1980).

One recently advocated approach to addressing these problems is the adoption of a "standard" set of parameters that is uniformly applied in all systems (Davis and Kent, 1990; Hayes et al., 1991; Bradbury and Baeyens, 1992, 1993; Mesuere, 1992). While this approach may not truly represent the exact physical, electrostatic, and chemical processes operating at the mineral-water interface, it does limit the number of adjustable parameters and serves to establish a baseline that will allow future direct comparison of modeling results and the evaluation of model performance. In addition, such an approach may be desirable from the point of view of developing simple, flexible sorption models with internally consistent databases for PA.

2.2 SCM PARAMETER ESTIMATION

2.2.1 Mineral Acid-Base Behavior

Although the ultimate goal of this research is to use a uniform approach to obtain the necessary equilibrium (or binding) constants for sorption reactions that involve the radionuclides themselves, a more basic first step is necessary. This involves deriving acidity constants that describe the acid-base chemistry of the mineral surface that is responsible for generating the sorption sites. Therefore, to demonstrate the feasibility of a uniform approach, one objective of this report was to obtain potentiometric titration data from readily available peer-reviewed literature for different (hydr)oxides and to interpret these data following, where possible, the techniques developed by Dzombak and Morel (1990) and Hayes et al. (1990; 1991). In this fashion, a consistent set of constants that characterize the acid-base behavior of each mineral can be developed for each of the three SCMs described earlier. These parameters are necessary to construct the mass balance/mass action equations used by geochemical sorption/speciation programs, such as MINEQL (Westall et al., 1976), MINTEQA2 (Allison et al., 1991), and HYDRAQL (Papelis et al., 1988). Once these parameters are in place, it will be possible to move to the next step of obtaining binding constants for the sorption of radionuclides, not only for simple (hydr)oxides but also for more complex rock-forming minerals, through a combination of several types of sites (Rai et al., 1988).

The required acidity constants for an SCM are determined by fitting potentiometric titration data. One approach uses graphical methods to extract values (Kent et al., 1988). An alternative approach, recommended in several recent studies (Dzombak and Morel, 1990; Dzombak and Hayes, 1992), is numerical nonlinear optimization. Westall (1982a,b) developed the iterative nonlinear least-squares optimization program, FITEQL, Version 2.0, to determine constants for several electrostatic models, including the DLM, CCM, and TLM. The code requires data describing the physical properties of the solid surface and reactions for the chemical equilibrium model with corresponding log K values. Serial sorption-pH or potentiometric titration data are also entered. In calculating acidity constants, FITEQL seeks to minimize the difference between experimental values and those calculated based on mass action constraints for those components where both the free and total concentrations are known. The numerical procedures employed in FITEQL and the details of program input are described in more detail elsewhere (Westall, 1982a,b; Dzombak and Morel, 1990).

2.2.2 Previous Work

Where possible, the approaches developed in previous work are used in this study to derive SCM parameters. The following is a brief description covering some of the major points made by these studies.

- Westall and Hohl (1980)

In one of the first studies to compare and contrast different SCM approaches, Westall and Hohl (1980) introduced the procedures for parameter optimization used in the FITEQL code. In the cases investigated by the authors, all models were able to represent the data well, but the different acidity constants used were dependent on the model considered and also on the other model parameters used. The authors also stressed that, although the optimal parameters may provide the best-fit to the data, they may not necessarily represent the actual conditions at the mineral-water interface.

- Smith and Jenne (1988; 1991; 1992)

Smith and Jenne (1988; 1991; 1992) investigated the application of the TLM to δ -MnO₂ and goethite. Based on a literature review of studies using this model (mostly pre-1988), the authors developed a set of parameters for $\log K_+$, $\log K_-$, $\log K_{\text{Cation}}$, and $\log K_{\text{Anion}}$. By writing complexation reactions as an interaction of contaminants with charged sites rather than neutral surface sites, the authors also suggested a transformation to develop surface complexation constants that are less variable than traditional binding constants reported among different investigations. Based on hydrolysis constants and acidity constants, Smith and Jenne (1991) used this approach to predict missing binding constants for several contaminants, including thorium.

- Hayes et al. (1990; 1991)

Hayes et al. (1990; 1991) used FITEQL to perform a sensitivity analysis of potentiometric titration data for rutile, goethite, and α -Al₂O₃. The authors considered the DLM, CCM, and TLM models and investigated the effect of varying different parameters on the goodness-of-fit calculated by FITEQL. Based on the results of these analyses, Hayes et al. (1991) recommended a set of "standard" parameters for each mineral for each of the three models considered.

- Dzombak and Morel (1990)

In perhaps the most extensive study of available data, Dzombak and Morel (1990) investigated the application of the DLM to available sorption data on ferrihydrite [Fe(OH)₃]. The authors developed a consistent set of parameters (site density, surface area, acidity constants) and used FITEQL to reinterpret sorption data for a large number of cationic and anionic toxic chemicals (e.g., Zn, Cd, Pb, SeO₄⁻). The model developed by Dzombak and Morel (1990) also includes an equilibrium precipitation model.

- Mesuere (1992) and Mesuere and Fish (1992)

Mesuere (1992) and Mesuere and Fish (1992) used a similar approach to Dzombak and Morel (1990) to develop a consistent database for goethite (α -FeOOH) for both the DLM and TLM. After examining the open literature for information on the surface properties and acid-base behavior of goethite, the authors used FITEQL to determine a set of acidity constants for both models. These parameters were then used to determine complexation reactions and binding constants for CrO₄²⁻ and oxalate. Both models were able to fit the experimental data well. These model constants were then used to examine binary mixtures of chromate and oxalate.

Again, model fits of the data were reasonably good, although results deteriorated for very dilute systems.

- Bradbury and Baeyens (1992; 1993)

Bradbury and Baeyens (1992; 1993) used the DLM model parameters recommended for ferrihydrite by Dzombak and Morel (1990). The model was applied to neptunyl (NpO_2^+)-ferrihydrite sorption data from Girvin et al. (1991), and FITEQL was used to determine binding constants for selected neptunyl surface complexes. It does not appear that the acidity constants of Dzombak and Morel (1990) were corrected for ionic strength effects. The effects of competition with Ca^{2+} for surface sites on neptunium sorption were also investigated. The DLM and the model parameters obtained in this manner were used to interpret the sorption data of Allard (1982). Only surface area was changed to reflect the different minerals investigated. K_d values calculated in this manner were in fair agreement with trends in experimentally determined values, but there was a general tendency to overpredict sorption for minerals with $A_{SP} \leq 10 \text{ m}^2/\text{g}$.

2.3 POTENTIOMETRIC TITRATION DATA

Potentiometric titration procedures are described in detail elsewhere (Dzombak and Morel, 1990), but titration generally involves the incremental addition of known amounts of acid or base to a solid suspension of the mineral of interest while monitoring changes in solution pH. The ionic strength (I) of the suspension is adjusted to a desired value using a supporting background electrolyte, such as NaNO_3 , NaClO_4 , or KCl ; the experiment is performed under closed atmosphere conditions, purging the solution with an inert gas such as nitrogen or argon to eliminate CO_2 and the formation of carbonate and bicarbonate species that would otherwise contaminate the surface. Changes in pH between acid-base additions are monitored potentiometrically; pH equilibration is generally assumed when the pH drift falls below some threshold value (pH units/minute). Ideally, the time between additions is kept short (on the order of minutes) to focus on surface protonation/deprotonation. Longer times allow proton exchange with the interior of the solid or dissolution, resulting in continuous pH drift and hysteresis in the titration curves (Dzombak and Morel, 1990).

Potentiometric titration data and point-of-zero charge data were identified through several compilations (James and Parks, 1982; Smith and Jenne, 1988; Kent et al., 1988) and a search of the peer-reviewed literature. The sources for potentiometric titration data used in this study are listed in Table 2-2. In most cases, the original data were obtained, although in some cases, data compiled in survey reports were used [e.g., ferrihydrite titration data reported in Dzombak and Morel (1990)]. Generally, data were presented in graphical form only; figures were enlarged where necessary, and an electronic digitizing tablet linked to a personal computer was used to convert graphical data to numerical values in the appropriate coordinates [typically pH versus surface charge ($\mu\text{C}/\text{cm}^2$)]. Surface charge data were then converted to total H^+ with a spreadsheet application based on procedures described in Dzombak (1985). Several data sets identified were not used (Breeuwsma and Lyklema, 1973) due to uncertainty regarding experimental conditions that were necessary for data interpretation. This was particularly true for solid concentrations (c_s) and specific surface area (A_{SP}), which were necessary to convert surface charge data to total H^+ but were not always reported.

There is likely to be some error introduced in this procedure due to the accuracy of the digitizing tablet itself and the reproducibility attributable to the operator. Checks on reproducibility using endpoints on the graphs indicate that the digitization is generally reproducible within about 0.1 mm. The

Table 2-2. Mineral properties used in interpreting potentiometric titration with data sources

Mineral	Generalized A_{SP} (m^2/g)	pH_{ZPC} ($\pm 1 \sigma$)	Reference(s)
Goethite	50	8.0 ± 0.8 (n=11)	Hsi and Langmuir (1985); Hayes et al. (1990); Yates and Healy (1975); Balistrieri and Murray (1981); Mesuere (1992)
Ferrihydrite ^(a)	600	8.0 ± 0.1 (n=9)	Hsi and Langmuir (1985); Davis (1977); Swallow (1978); Yates (1975)
Magnetite	5	6.7 ± 0.1 (n=2)	Regazzoni et al. (1983)
amorphous- SiO_2	175	2.8 ± 0.3 (n=3)	Abendroth (1970); Bolt (1957)
$\alpha-Al_2O_3$	12	8.9 ± 0.4 (n=4)	Hayes et al. (1990)
$\gamma-Al_2O_3$	120	8.4 ± 0.3 (n=3)	Huang and Stumm (1972); Sprycha (1989)
$\delta-MnO_2$	270	1.9 ± 0.5 (n=7)	Murray (1974); Catts and Langmuir (1986)
TiO_2 (anatase)	(b)	6.1 ± 0.2 (n=2)	Sprycha (1984); Berube and de Bruyn (1968)
TiO_2 (rutile)	30	5.9 ± 0.3 (n=4)	Berube and de Bruyn (1968); Yates (1975)
(a)	Values recommended in Dzombak and Morel (1990) based on measured values reported in literature.		
(b)	The reported value of $16 m^2/g$ used with data of Sprycha (1984); $125 m^2/g$ used with data of Berube and de Bruyn (1968).		

absolute error will vary depending on the coordinate system and the size of the graph. No attempt was made to propagate this error through the calculations.

2.3.1 Data Interpretation

In the case of magnetite and $\alpha-Al_2O_3$, only one data set was modeled, and the reported A_{SP} , rounded to the nearest whole number, was used. In most cases, in which several studies were interpreted, each study reported following the same mineral preparation procedures. For example, each of the five goethite studies listed in Table 2-2 reported using the methods of Atkinson et al. (1967; 1968; 1972), leading to relatively close agreement in A_{SP} (45 to 66 m^2/g). In some cases (e.g., $\gamma-Al_2O_3$, am- SiO_2), commercial-grade materials were used, and reported surface area measurements agreed closely. In the case of anatase, however, different sources for minerals were used, and surface area measurements differed markedly. Sprycha (1984) used a commercial-grade TiO_2 with a measured A_{SP} of $16 m^2/g$. Berube and de Bruyn (1968), however, synthesized anatase, and obtained a measured A_{SP} of $125 m^2/g$.

To consider mass balance constraints on site availability, all SCMs require a single value for A_{SP} . However, surface area, generally determined in titration experiments by BET/ N_2 techniques, is subject to uncertainty and can vary from study to study, depending on grain size, how the mineral was prepared, outgassing of the sample prior to measurement, and how long the mineral was allowed to age (Yates, 1975). In addition, the use of a surface area measured on dry samples in a vacuum to represent the surface area of a mineral in suspension is uncertain, and in some cases, A_{SP} has been used as a fitting parameter (Davis, 1977; Hsi and Langmuir, 1985).

Dzombak and Morel (1990) acknowledged these uncertainties and selected a single generalized surface area of $600 \text{ m}^2/\text{g}$ for ferrihydrite (amorphous ferric oxide). Since one objective of this research is the development of a similar simplified uniform approach to modeling titration and sorption data for other minerals, the methods of Dzombak and Morel (1990) have been followed here; a single generalized A_{SP} , based on measured values reported in the literature (e.g., Kent et al., 1988), has been assumed for each mineral and applied consistently for each SCM considered (Table 2-2). Although information is undoubtedly lost in this simplification, the distinction in A_{SP} between minerals is maintained. In most cases the use of similar mineral preparation techniques between studies provides some support for this assumption. The difference between the generalized surface area and the reported surface area is on the order of 10 percent in most instances, probably within the limits of uncertainty on the measurement itself. One exception has been the titration data for anatase. In this case, the relative difference in reported surface area is so large (16 versus $125 \text{ m}^2/\text{g}$) that the individual A_{SP} values were maintained. This resulted in good agreement between the acidity constants calculated for anatase using the data of Sprycha (1984) and Berube and de Bruyn (1968). Nevertheless, the uncertainty in the determined acidity constants due to differences in surface area should be kept in mind.

Site Density (N_s). Site densities reported for simple (hydr)oxides typically range between 1-20 sites/ nm^2 (Kent et al., 1988; Davis and Kent, 1990). Based on a sensitivity analysis of titration data using the CCMs, DLMs, and TLMs, Hayes et al. (1990) suggested that model results were relatively insensitive to differences in site density and proposed a constant site density of 10 sites/ nm^2 . The study of Mesuere (1992), however, suggested that, for a broader pH range, goethite titration data were sensitive to N_s and were better modeled by assuming a small site density of 1.5 sites/ nm^2 for the DLM and 5 sites/ nm^2 for the TLM. Based on a literature survey, Dzombak and Morel (1990) recommended a total site density of 2.31 sites/ nm^2 for ferrihydrite. Since the goal of this study was a uniform application rather than taking a best-fit approach, the recommendation of Davis and Kent (1990) was followed, and the site density of Dzombak and Morel (1990) was assumed for all minerals. Because there does not appear to be a physical reason for assuming different site densities for different models, the same site density has also been maintained for the different SCMs.

Also implicit in the approach taken here is the equivalence of all sites. Other studies (Benjamin and Leckie, 1981; Dzombak and Morel, 1990) have employed heterogeneous sites to explain observed sorption behavior. Since simplification is one desired goal of this study, and because of a lack of data on site heterogeneities for many of the minerals considered here, a single site type was assumed.

Capacitances. All three models require values for N_s and A_{SP} to construct the mass balance relationships. In addition, the CCM and TLM require capacitances to describe the charge-potential relationships across one or more model-defined planes at the mineral-water interface. The CCM requires a single value. Based on the sensitivity analysis of Hayes et al. (1990), this has been set at $1.0 \text{ F}/\text{m}^2$. The TLM requires capacitances for its two inner layers. By convention (Hayes et al., 1990), the outer β -layer capacitance

(C_2) is set at 0.2 F/m^2 . As with the CCM, the sensitivity analysis of Hayes et al. (1990) has been used to set the inner o-layer capacitance at 0.8 F/m^2 . The DLM does not require capacitance values.

Chemical Equilibrium Model. In addition to the model-dependent surface reactions, the chemical equilibrium model is relatively simple for potentiometric titration data, and only requires the dissociation constant, K_w , for water. At zero ionic strength ($I=0 \text{ M}$), $K_w \approx 14.0$ at $25 \text{ }^\circ\text{C}$. However, the data selected for this study covered a range in ionic strength from 0.0004 to 1 M , and the mass action required correction for ionic strength effects on activity. This was done using the Davies equation in a manner analogous to that outlined in Dzombak and Morel (1990). Although the Davies equation is only valid for fairly dilute solutions, this was generally appropriate, since the titrations were run at dilute concentrations where $I \leq 0.1 \text{ M}$ in most cases. An additional concern is the dissolution of the solid which can be considered by adding the equilibrium constants for aqueous species involving the dissolved metals. This can be mitigated to some extent by using rapid titration steps as discussed previously. In the present study, it was assumed that the solubility of the solids was negligible at the temperatures ($25 \text{ }^\circ\text{C}$) and times (minutes) being considered, and the chemical equilibrium model was not modified to consider dissolved metals.

2.3.2 Parameter Estimation Using FITEQL, Version 2.0

Several studies advocating a uniform approach to SCM applications (Dzombak and Morel, 1990; Hayes et al., 1990; Mesuere, 1992) have used Version 2.0 of the FITEQL parameter estimation code (Westall, 1982a,b) to determine the necessary model parameters. This study also used FITEQL, Version 2.0 to interpret the gathered titration data. For the DLM and CCM models, values were determined for $\log K_+$ and $\log K_-$ simultaneously. However, unlike the single-layer DLM and CCM, the TLM allows for sorption of the background electrolyte (Na^+ and NO_3^- , for example). This leads to four equilibrium constants, K_+ , K_- , K_{Cation} , and K_{Anion} to describe the interface. While FITEQL can, in theory, fit these four constants simultaneously, in practice the code does not converge unless two of these can be specified. The relationship between K_+ , K_- , and pH_{ZPC} can be expressed

$$(\log K_+ - \log K_-)/2 = \text{pH}_{\text{ZPC}} \quad (2-12)$$

and the sensitivity analysis of Hayes et al. (1990) recommended a value for ΔpK such that

$$\Delta\text{pK} = -[\log K_+ + \log K_-] = 4.0 \quad (2-13)$$

In this fashion, if pH_{ZPC} is known for a given mineral, values can be set for the TLM acidity constants and FITEQL can be used to solve for K_{Cation} and K_{Anion} . Turning again to the peer-reviewed literature, values for pH_{ZPC} were obtained for the different minerals considered. In general, the differences between values reported for a given mineral were small, and a mean value was chosen for pH_{ZPC} . The values used are reported in Table 2-2. It should also be noted that $\delta\text{-MnO}_2$ and amorphous- SiO_2 have such low pH_{ZPC} that most of the available titration data is at $\text{pH} > \text{pH}_{\text{ZPC}}$. In this range, only deprotonation and adsorption of cationic background electrolytes are assumed to be significant (Kent et al., 1988), and the FITEQL runs were set up to determine equilibrium constants (K_- and K_{Cation}) for only these reactions.

Output from FITEQL includes a "goodness-of-fit" parameter (V_y) and standard deviations for the estimated parameters (Westall, 1982a,b). These values are determined based on the experimental error

specified in the optimization run and on the size of the data set. For example, because the chemical system is not as well constrained, goodness-of-fit and parameter uncertainty generally deteriorate for smaller data sets (Dzombak and Morel, 1990). In most cases, error is not reported for potentiometric titration data, and the approach of Hayes et al. (1990) has been adopted with only slight modification. Relative error has been assumed to be ± 1 percent (0.01), while absolute error has been assumed to be 1×10^{-8} M instead of the 2×10^{-8} M used by Hayes et al. (1990). Their sensitivity analyses indicated that the dissimilarities in acidity constants due to differences in experimental error are negligible, but the calculated uncertainty in the estimated values increases with increasing error. The goodness-of-fit parameter generated by FITEQL can be used as a measure of how well the data are described by the assumed chemical and adsorption models. In a strict sense, however, goodness-of-fit cannot be compared directly unless the experimental error limits imposed on the problem are known.

2.4 DISCUSSION OF RESULTS

After interpretation of the data, the chief objective of this parameter estimation exercise was to combine the results for separate potentiometric titration data sets into a single set of weighted values for the desired SCM parameters (K_+ , K_- , K_{Cation} , and K_{Anion}). This involved combining experiments performed at different ionic strengths using different background electrolytes. In a strict sense, this approach is not valid for the CCM. This is because there is no ionic strength correction in the charge-potential relationship and, in theory, the capacitance used should be adjusted for each ionic strength (Hayes et al., 1990; 1991). By arbitrarily fixing the capacitance used in the model at a single value, the calculated equilibrium constants are adjusted by FITEQL to fit the data. The resultant values are, therefore, valid only for the ionic strength at which the data were measured. Also implicit in this approach is the assumption that different background electrolytes behave in an identical manner and have no effect on the modeling results. While this is probably reasonable for the simple CCM and DLM models that assume an inert background electrolyte, it is likely to be an oversimplification in the TLM.

The values resulting from the FITEQL analysis were tabulated for each study at each ionic strength considered. In some cases, the numerical scheme did not converge. For the DLM and TLM, the method of Dzombak and Morel (1990) was used to obtain convergence for one of the values. This involved fixing one of the constants using values obtained from runs at other ionic strengths in the data set, and rerunning the input file to fit the remaining parameter. In almost all cases, convergence was achieved quickly. Because of its lack of ionic strength dependence, however, this was not done for the CCM. For some data sets, plotting the \log_{10} of the CCM acidity constants ($\log K_+$ and $\log K_-$) versus \log_{10} of the ionic strength resulted in a linear relationship. The correlation was reasonably strong ($r^2 \geq 0.8$) and could be used to extrapolate CCM acidity constants for ionic strengths outside of the range of the experiments.

Dzombak and Morel (1990) proposed a scheme for deriving a single set of acidity constants for the DLM. This approach relies on using the standard deviation ($\sigma_{\log K}$) calculated by FITEQL from different data sets (e.g., titration data at different ionic strengths) to develop a weighting factor (w_i) according to the following relationship

$$w_i = \frac{(1/\sigma_{\log K})_i}{\sum (1/\sigma_{\log K})_i} \quad (2-14)$$

The weighting factor is then used to derive a "best-estimate" of the equilibrium constant of interest

$$\overline{\log K} = \sum w_i (\log K)_i \quad (2-15)$$

In this fashion, a parameter value with a lower standard deviation (i.e., a better fit) is more heavily weighted and will have more influence on the final value. Dzombak and Morel (1990) used this approach to combine acidity constants for different ferrihydrite data sets at different ionic strengths. This technique is valid for the DLM, which contains an ionic strength term in the charge-potential relationship. Because it also adjusts potential to reflect ionic strength, a similar approach should be valid for the TLM. Again, however, for the reasons given earlier, this approach is not valid for the CCM and was not used. The weighted results (DLM and TLM only) are presented in Table 2-3. To establish a common reference point, the values reported for the CCM are for $I=0.1$ M; the weighting scheme was applied if more than one analysis was available at this ionic strength. The 95 percent confidence limits are given in Table 2-3. These limits were calculated using the standard deviations generated by FITEQL and the methods outlined in Dzombak and Morel (1990). Generally, constants calculated at different ionic strengths within a given data set agreed very closely as shown by the relatively small uncertainty at the 95 percent confidence limit. This holds true even for different background electrolytes at the same concentration. For example, for the γ - Al_2O_3 data of Sprycha (1989), DLM- $\log K_+$ ranged from 6.17 to 7.02 and DLM- $\log K_-$ varied from -8.82 to -9.75. This was despite ionic strengths ranging from 0.001 to 0.1 M and background electrolytes (for $I=0.1$ M) that included NaBr, NaCl, KCl, CsCl, and NaI. Agreement between data sets was not as good, which is not surprising given the differences in data set size, laboratory procedure, equipment, and sample preparation (perhaps exemplified in differences in measured A_{SP}) that were noted for the different studies. Where it could be calculated, the uncertainty represented by these limits is much higher for the CCM than it is for the DLM and TLM. This results from the smaller number of data sets that are available to be combined to yield the single ionic strength values ($I=0.1$ M) reported for the CCM.

Figure 2-2 (a-f) shows model predictions using calculated acidity constants as compared to experimental data. Results using the best-fit (dashed lines) and the weighted (solid lines) values listed in Table 2-3 are shown. In most cases, the fit is very good for all three SCM considered. Not surprisingly, the best-fit models agree more closely with the observed values than the weighted values, but the difference is typically small. Direct comparison of model results for goethite (Figure 2-3) shows that all three models provide a reasonably good fit to the data. The DLM and TLM provide the best-fit and agree very closely in pH_{ZPC} (~ 8.0). The slightly worse fit for the CCM results from using acidity constants for $I=0.1$ M (Table 2-3).

One factor complicating data comparison is the different pH ranges covered in the experiments. If the coverage is not as extensive on one side of the pH_{ZPC} , the chemical equilibrium model will not be well constrained, and FITEQL will have more difficulty converging on equilibrium constants. One extreme example of this is δ - MnO_2 , where there are no data available below its low $\text{pH}_{ZPC} \sim 2.0$. In this case, as noted earlier, the protonation reaction and the anion adsorption reaction for the TLM (Table 2-3) are not constrained at all, and attempts to include them in the optimization led to convergence problems.

One of the trade-offs inherent in the simplified uniform approach adopted here is the implicit assumption of similar mineral morphology between studies embodied in using a single A_{SP} for a given mineral. Although a systematic analysis has not been performed here, it is important to recognize the uncertainty inherent in estimated acidity constants due to differences in surface area measurements. It would be possible to construct a more complete model by maintaining the exact A_{SP} reported for each

Table 2-3. Best estimate values for SCM constants - simple (hydr)oxides

Mineral	Model	N_S (sites/nm ²)	$\log K_+$ ($\pm 95\%$) _a	$\log K_-$ ($\pm 95\%$) _a	$\log K_{\text{Anion}}$ ($\pm 95\%$) _a	$\log K_{\text{Cation}}$ ($\pm 95\%$) _a
Goethite	CCM (0.1M)	2.31	6.47 \pm 0.72	-9.03 \pm 0.22	n.a.	n.a.
	DLM	*	7.35 \pm 0.11	-9.17 \pm 0.08	n.a.	n.a.
	TLM(b)	*	6.00	-10.00	8.78 \pm 0.13	-7.64 \pm 0.07
Ferrihydrite	CCM (0.1M)	2.31	7.35 \pm 1.08	-8.45 \pm 2.23	n.a.	n.a.
	DLM	*	7.29 \pm 0.10(c)	-8.93 \pm 0.07(c)	n.a.	n.a.
	TLM(b)	*	6.00	-10.00	8.43 \pm 0.04	-7.66 \pm 0.12
Magnetite	CCM (0.1M)(d)	2.31	6.26	-7.32	n.a.	n.a.
	DLM	*	6.72 \pm 0.02	-6.37 \pm 0.71	n.a.	n.a.
	TLM(b)	*	4.70	-8.70	7.95 \pm 0.11	-5.47 \pm 0.06
am-SiO ₂	CCM (0.1M)	2.31	(e)	-7.04 \pm 0.09	n.a.	n.a.
	DLM	*	(e)	-7.20 \pm 0.05	n.a.	n.a.
	TLM(b)	*	0.90	-4.90	(e)	-6.22 \pm 0.05
α -Al ₂ O ₃	CCM (0.1M)(d)	2.31	9.08	-8.32	n.a.	n.a.
	DLM	*	8.33 \pm 0.15	-9.73 \pm 0.12	n.a.	n.a.
	TLM(b)	*	6.80	-10.80	10.12 \pm 0.03	-7.73 \pm 0.07
γ -Al ₂ O ₃	CCM (0.1M)	2.31	6.92 \pm 0.06	-9.00 \pm 0.15	n.a.	n.a.
	DLM	*	6.85 \pm 0.06	-9.05 \pm 0.09	n.a.	n.a.
	TLM(b)	*	6.40	-10.40	8.28 \pm 0.05	-7.95 \pm 0.11
δ -MnO ₂	CCM (0.1M)	2.31	(e)	-2.14 \pm 24.7	n.a.	n.a.
	DLM	*	(e)	-3.27 \pm 0.73	n.a.	n.a.
	TLM(b)	*	-0.10	-3.9	(e)	-0.75 \pm 0.84
TiO ₂ (anatase)	CCM (0.1M)(d)	2.31	6.64	-5.60	n.a.	n.a.
	DLM	*	5.37 \pm 0.30	-5.92 \pm 0.12	n.a.	n.a.
	TLM(b)	*	4.10	-8.10	7.13 \pm 0.17	-4.59 \pm 0.10
TiO ₂ (rutile)	CCM (0.1M)(d)	2.31	3.91	-7.79	n.a.	n.a.
	DLM	*	4.23 \pm 0.09	-7.49 \pm 0.12	n.a.	n.a.
	TLM(b)	*	3.90	-7.90	5.24 \pm 0.08	-6.42 \pm 0.08

- n.a. Parameters not applicable to CCM and DLM models.
(a) 95 percent confidence interval based on FITEQL standard deviation and defined using the methods of Dzombak and Morel (1990).
(b) For TLM, $\log K_+$ and $\log K_-$ fixed by convention. See text for discussion.
(c) Dzombak and Morel (1990) DLM parameters for ferrihydrite.
(d) FITEQL did not converge at I=0.1 M. Extrapolated from $\log_{10}(I)$ vs $\log K_+$ and $\log K_-$.
(e) Not considered for δ -MnO₂ and Am-SiO₂.

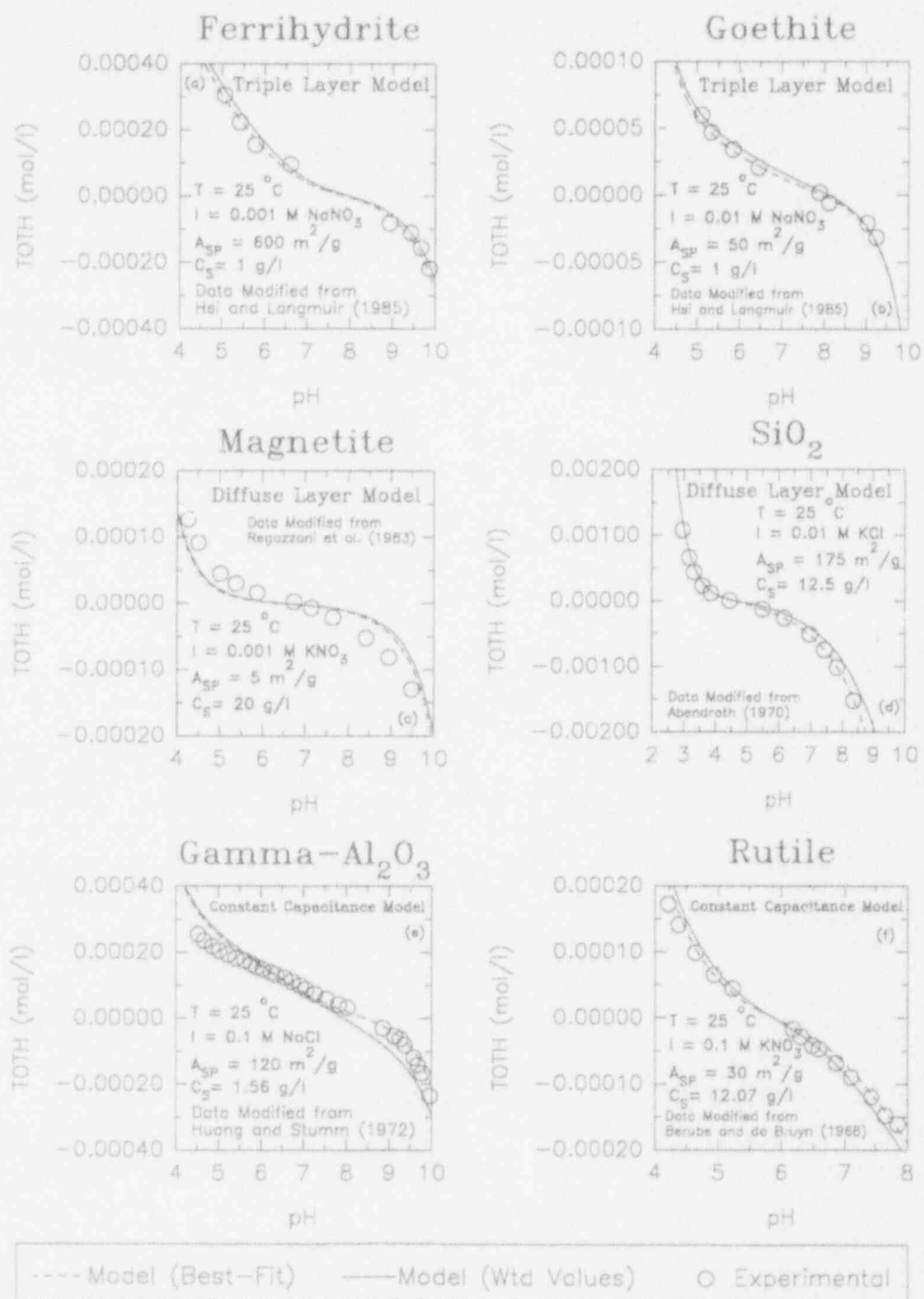


Figure 2-2. SCM modeling results as compared to experimental potentiometric titration data. Results are shown for the model and mineral as indicated. Solid lines calculated using the weighted acidity constants given in Table 2-3. Dashed lines use best-fit acidity constants as calculated by FITEQL (Westall, 1982a, b).

Model Comparison Goethite-Weighted Values

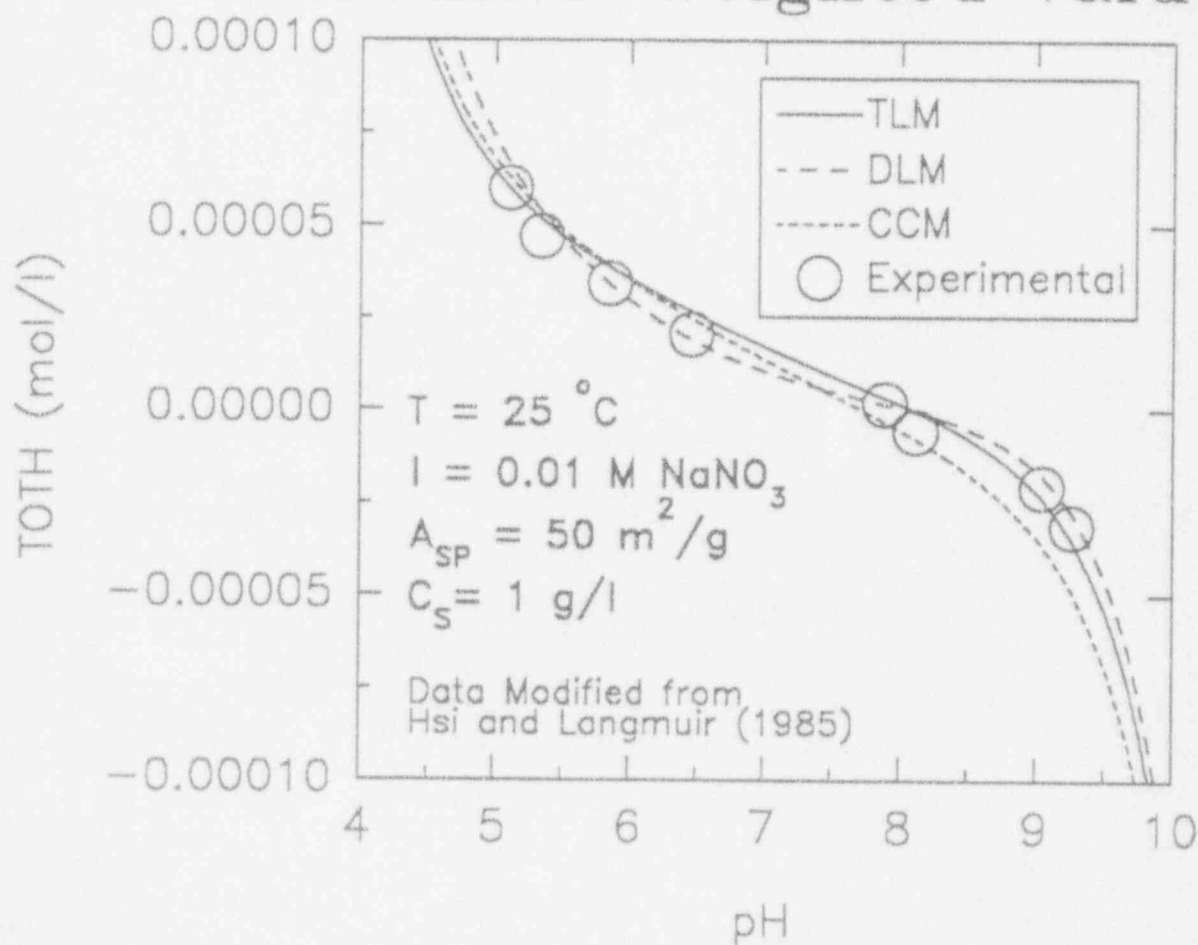


Figure 2-3. Comparison of modeling results. DLM and TLM results calculated using weighted acidity constant values given in Table 2-3. CCM acidity constants are for $I=0.1\text{ M}$, also given in Table 2-3.

of the titration studies through the data interpretation. However, because of the uncertainty in A_{SP} measurements, a single generalized value was used. This assumption is supported by the similarity in reported mineral preparation techniques and the generally close agreement between measured A_{SP} values. In addition, although some information is lost in this simplification, the general distinctions in A_{SP} between minerals are preserved. Also, relative to empirical models, the addition of geochemical considerations, such as aqueous speciation, pH, and partial gas pressures, to sorption models is the benefit received.

2.5 MINERAL ACID-BASE BEHAVIOR — SUMMARY AND CONCLUSIONS

Despite disparities in experimental conditions, the agreement in acidity constants (and binding constants for background electrolytes in the TLM) between different data sets for several minerals (e.g., goethite, ferrihydrite, $\gamma\text{-Al}_2\text{O}_3$, and am-SiO₂) for a given SCM was often within two orders of magnitude. This, with the relatively small uncertainty at 95 percent confidence for the DLM and TLM, supports combining these results into a single set of parameters. The similarity between the DLM and TLM constants calculated for goethite and ferrihydrite suggests that ferrinol (FeOH^\ominus) sites behave similarly for these two minerals despite differences in crystallinity, and it also indicates that they may be modeled using the same SCM parameters.

This modeling exercise also pointed up some of the limitations in the different SCMs. The CCM is perhaps the most restrictive of the three models in that it requires knowledge of the dependence of capacitance on ionic strength. For this reason, the type of generalized approach outlined here is not strictly applicable for the CCM. The TLM can model different ionic strengths, but it has a larger number of parameters and requires some means of fixing $\log K_+$ and $\log K_-$ to model titration data using FITEQL. This extra level of complexity tends to work against the ready incorporation of the TLM in PA codes (Hayes et al., 1990; 1991). The simplest model, the DLM, is able to model ionic strength changes and also has the fewest number of parameters to fit (Hayes et al., 1990). In some cases the fit is as good as, if not better than, the more complex TLM (Figure 2-3). As illustrated in Figure 2-4, comparison of pH_{ZPC} calculated using the acidity constants listed in Table 2-3 and measured mineral pH_{ZPC} (Table 2-2) indicates that the parameter values for both the CCM and DLM are reasonable, meeting the constraint set in Eq. (2-12).

Acidity constant values determined in this section are necessary before data on radionuclide sorption on simple (hydr)oxides can be interpreted using SCMs. As will be discussed in Section 4, it may also be possible to model more complex minerals by assuming some combination of these sites. It is important to remember, however, that, in an effort to establish a baseline, the constants in Table 2-3 were determined using fixed-site density, capacitances, and, in the case of the TLM, acidity constants. Although these parameters were selected, where possible, based on surveys of mineral properties, they may not be the same as properties reported for a given set of experimental data. For this reason, results cannot be compared directly to constants determined using a different set of parameters (Dzombak and Hayes, 1992). However, while there is some loss of conceptual (and numerical) accuracy in using a single set of parameters to model sorption data, this type of uniform approach is to be favored in trying to strike a balance between model completeness and PA needs for efficient modeling.

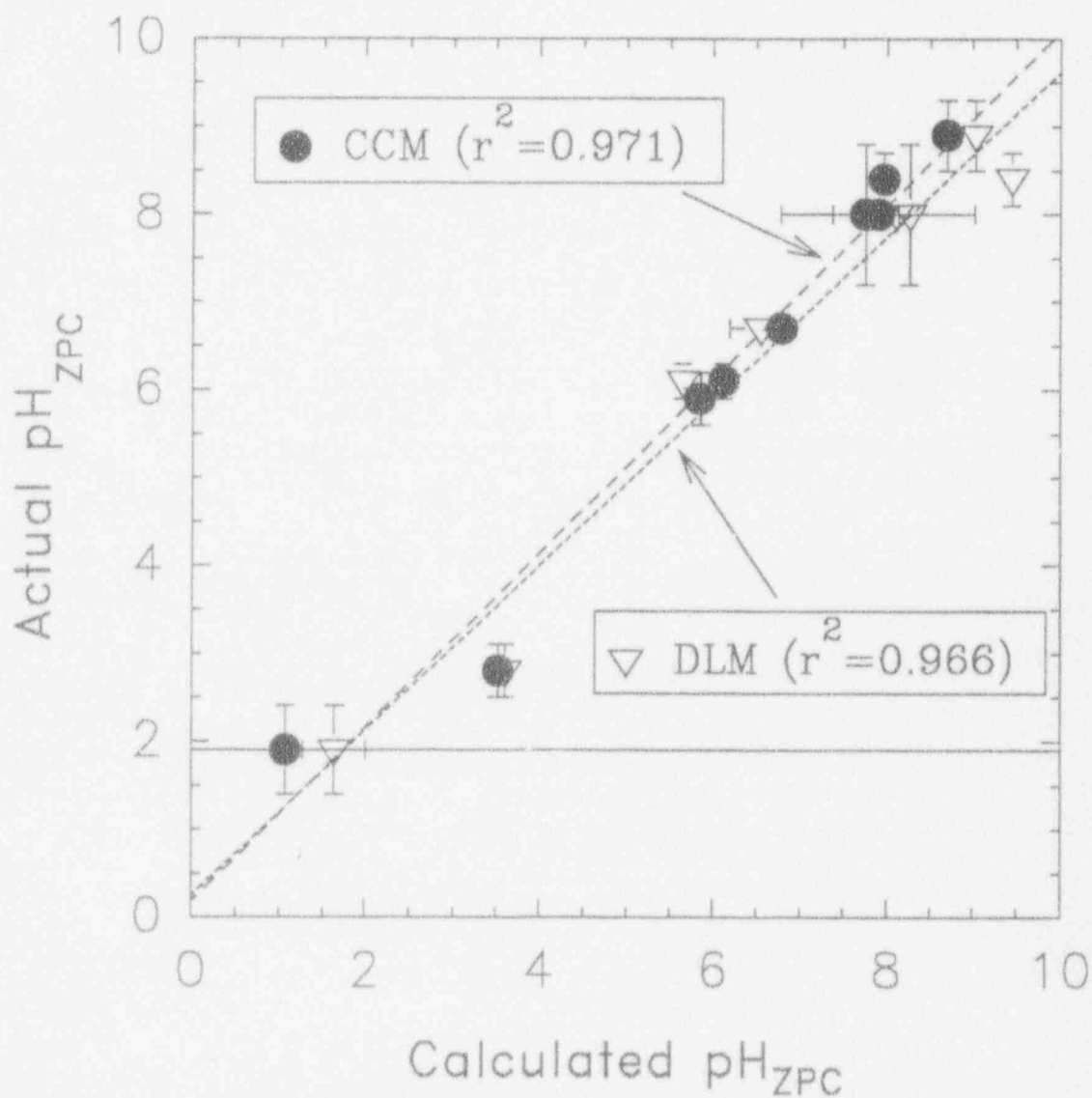


Figure 2-4. Actual pH_{ZPC} vs calculated pH_{ZPC} . Actual values and uncertainty are from values given in Table 2-2. Calculated values are determined for the CCM and DLM using the values for $\log K_+$ and $\log K_-$ obtained using FITEQL and Eq. (2-12). Uncertainty in the calculated values is obtained by combining and scaling the 95% error limits $[\alpha_+^2 + \alpha_-^2]^{0.5}/2$ reported in Table 2-3. Uncertainty limits are less than the symbol size in several cases.

3 GEOCHEMICAL MODELING OF RADIONUCLIDES WITH MINTEQA2, VERSION 3.11

3.1 INTRODUCTION AND CODE DESCRIPTION

In order to apply SCMs to radionuclide sorption, it is necessary to employ a geochemical code that is not only able to invoke different SCMs but also contains the necessary thermodynamic data for the radionuclides of interest. These data are necessary to run the model; any SCM binding constants calculated using FITEQL must also contain the same thermodynamic data in the chemical equilibrium model developed for FITEQL input.

Based on the mathematical approach of the MINEQL and FITEQL codes (Westall et al., 1976; Westall, 1982a,b), MINTEQA2 (Version 3.11, Allison et al., 1991) is a versatile geochemistry code for modeling sorption, offering seven different options, including empirical, electrostatic, and ion exchange models. In addition, precipitation/dissolution reactions can be considered based on an assumption of equilibrium. Equilibrium speciation is calculated using mass balance/mass action constraints. Extrapolation beyond 25 °C is generally accomplished using the van't Hoff equation, assuming constant enthalpies of reaction (ΔH_r). Construction of input files is simplified by the interactive preprocessor code, PRODEFA2.

3.2 DATA SOURCES

Kerrisk (1985) used U.S. Environmental Protection Agency (EPA) release limits specified in 40 CFR Part 191 and the anticipated makeup of HLW to identify important radionuclides. These include U, Am, Pu, Np, Th, Tc, Cs, Sr, Zr, Ra, and Sn. As released by the EPA, MINTEQA2 incorporates the thermodynamic database of WATEQ3 (Ball et al., 1981). As a result, the MINTEQA2 databases, THERMO.DBS (aqueous species), TYPE6.DBS (solids), and REDOX.DBS, provide extensive coverage of elements common in natural systems. Of the key radionuclides listed above, however, only uranium and strontium are currently available (Allison et al., 1991). Recent studies (Grenthe et al., 1992) suggest significant modifications are necessary to the uranium data. Until the MINTEQA2 databases are updated and expanded to include other important radionuclide species, the code cannot be used to investigate sorption of these radionuclides.

Many efforts have been and are continuing to be made to develop comprehensive, critically evaluated tabulations of thermodynamic data for important radionuclides (Tripathi, 1984; Phillips et al., 1988; Wolery et al., 1990; Cross and Ewart, 1991; Grenthe et al., 1992). In most cases, however, the data are not available in the proper format for use in MINTEQA2. Although it is beyond the intended scope of this research project to extensively evaluate thermodynamic data, it is possible to take advantage of these efforts to expand the existing MINTEQA2 databases to include key radionuclides.

The EQ3/6 code uses the same geochemical principles as MINTEQA2 to calculate equilibrium aqueous speciation. However, unlike MINTEQA2, EQ3/6 in its current form is unable to model sorption processes, except for recent modifications to consider ion exchange (Viani and Bruton, 1992). In a comparison of earlier versions of the two codes, Morrey et al. (1986) concluded that, given the same data, the codes produced similar speciation results. The latest release of the EQ3/6 database (Data0.com.r16, 26Jun92) includes an extensive, well-documented tabulation of data for radionuclides

listed above that draws on other critically evaluated databases (Grenthe et al., 1992). Because the EQ3/6 code will be used by the DOE in site characterization at Yucca Mountain (DOE, 1988; Section 8.3.5.19), its database was chosen as an initial source for much of the data used to expand and update the MINTEQA2 database. Like MINTEQA2, the EQ3/6 database includes 25 °C log K values referenced to a zero ionic strength reference state. Although not used by the code, the EQ3/6 database also tabulates enthalpies of formation (ΔH_f° in kcal or kJ/mole) for aqueous species, solids, gases, and redox reactions. For the selected radionuclides, original data sources are shown in Table 3-1.

Procedures described by Allison et al. (1991) were followed for reformatting data from EQ3/6 for use in MINTEQA2. Many of the reactions written in EQ3/6 must be recast in terms of component species used by MINTEQA2. This involved the selection of auxiliary reactions such as the dissociation of water, the formation of HCO_3^- from CO_3^{2-} , and the oxidation of water. Where possible, these data were selected from the MINTEQA2 database to provide consistency with other reactions. Upon inspection, however, the differences between EQ3/6 and MINTEQA2 data were very small for these common, more well characterized auxiliary reactions. A spreadsheet program was developed to calculate ΔH_f from the ΔH_f° values reported in the EQ3/6 data.

3.3 DATABASE COMPARISON

Uranium is the only actinide included in the original databases distributed with MINTEQA2, with data from Langmuir (1978). With the exception of some solids, these data have been replaced in this study by data from the recently released Nuclear Energy Agency (NEA) uranium database (Grenthe et al., 1992). Figures 3-1 through 3-4 illustrate some of the differences in predicted U(VI) speciation in a 0.1 M NaNO_3 solution that result from using the old and new MINTEQA2 databases. One prominent difference is the larger number of U-species available in the new database (Figures 3-1 and 3-2). At $\text{pH} < 5$, UO_2^{2+} decreases due to the presence of the new species, UO_2NO_3^+ . The relative importance of $(\text{UO}_2)_3(\text{OH})_5^+$ for $\text{pH} > 6$ is greatly reduced using the NEA data, and the newly entered species, $\text{UO}_2(\text{OH})_2^\circ$ and $\text{UO}_2(\text{OH})_3^-$, are predicted to dominate. For low $p(\text{CO}_2)$ at $\text{pH} = 6.9$, similar to values measured for J-13 water at Yucca Mountain, $(\text{UO}_2)_3(\text{OH})_5^+$ is eliminated and replaced by $\text{UO}_2(\text{OH})_2^\circ$ (Figure 3-3). Also, the importance of $\text{UO}_2\text{CO}_3^\circ$ is greatly reduced, and the new species $(\text{UO}_2)_2\text{CO}_3(\text{OH})_3^-$ is significant at atmospheric CO_2 values [$p(\text{CO}_2) = 10^{-3.48}$ atm]. Figure 3-4 demonstrates the changes in calculated speciation with the new database for varying total uranium concentration in the presence of atmospheric CO_2 with $\text{pH} = 6.9$. At low U(VI)_T , UO_2OH^+ , $\text{UO}_2\text{CO}_3^\circ$, and $\text{UO}_2(\text{CO}_3)_2^{2-}$ are the only species predicted to be present in significant quantities ($> 1\%$) using the original MINTEQA2 database. Using the new database, these species are reduced to less than 10 percent of U(VI)_T , and the dominant species is calculated to be $\text{UO}_2(\text{OH})_2^\circ$. A difference of particular interest with respect to modeling sorption is the introduction in the NEA data of anionic U(VI) species at alkaline pH. This may greatly influence the modeling of sorption of uranium on charged surfaces.

It should be noted, however, that, in spite of the great care taken in constructing the NEA database, there is some concern that the equilibrium constant used for the formation of $\text{UO}_2(\text{OH})_2^\circ$ ($\log K_{\text{UO}_2(\text{OH})_2^\circ} \leq -10.3$) should be considered as a maximum and that the actual value may be much smaller (Tripathi and Parks, 1992). Fuger (1992) proposes a value of $\log K_{\text{UO}_2(\text{OH})_2^\circ} = -13.0 \pm 0.25$, which greatly reduces the relative significance of $\text{UO}_2(\text{OH})_2^\circ$ from that shown in Figure 3-3. Nevertheless, for all subsequent calculations, it was decided to preserve the value of $\log K_{\text{UO}_2(\text{OH})_2^\circ} = -10.3$ used in the Data0.Com.R16 version of the EQ3/6 database.

Table 3-1. Sources for EQ3 (Data.com.r16, 26Jun92) equilibrium constant data adapted to MINTEQA2

Element	Data Source(s) †
Am	a, <u>b</u> ,c,d
Co	e,f,g,h, <u>i</u> ,j,k,l
Cs	<u>e</u> ,m,n
Eu	e, <u>o</u> ,p
Np	a, <u>q</u>
Pu	<u>r</u> ,s,t,u
Ra	e, <u>i</u>
Ru	<u>y</u> ,w
Sn	e,i,l, <u>x</u>
Sr	<u>e</u>
Tc	<u>y</u> ,z
Th	a, <u>f</u> ,g,i,m,aa,bb
U	i, <u>n</u> ,cc,dd,ee,ff,gg,hh,ii,jj,kk
Zr	f,j

†Underlined references are predominant data source for element of interest.

[a] Fuger and Oetting (1976); [b] Kerrisk (1984); [c] Kerrisk and Silva (1986); [d] Oetting et al. (1976); [e] Johnson et al. (1991); [f] Naumov et al. (1974); [g] Baes and Mesmer (1976); [h] Smith and Martell (1976); [i] Wagman et al. (1982); [j] Robie et al. (1979); [k] Garrels and Christ (1965); [l] Kubaschewski and Alcock (1979); [m] Cox et al. (1989); [n] Grenthe et al. (1992); [o] Rard (1987b); [p] Rard (1985b); [q] Lemire (1984); [r] Lemire and Tremaine (1980); [s] Schwab and Felmy (1982); [t] Nash and Cleveland (1984); [u] Morss (1986); [v] Rard (1985a); [w] Rard (1987a); [x] Jackson and Helgeson (1985); [y] Rard (1983); [z] Rard (1984); [aa] Langmuir and Herman (1980); [bb] Mills (1974); [cc] Langmuir (1978); [dd] Hemingway (1982); [ee] NEA (1989); [ff] NEA (1990); [gg] Rickard and Nriagu (1978); [hh] O'Hare et al. (1988); [ii] Tripathi (1984); [jj] Owens and Mayer (1964); [kk] Sverjensky (1990).

Adapting the EQ3/6 database to MINTEQA2 also allows comparison of speciation predicted by the two codes. Figures 3-5 and 3-6 show U(VI) speciation predicted by both EQ3 (the equilibrium speciation part of the EQ3/6 code) and MINTEQA2 as a function of pH. The match is very good in the absence of CO₂; with CO₂ present, the differences are slightly more pronounced, but the comparisons are still quite good. Because the thermodynamic data are identical, the slight variations are due to a combination of several factors related to differences in code design and model formulation.

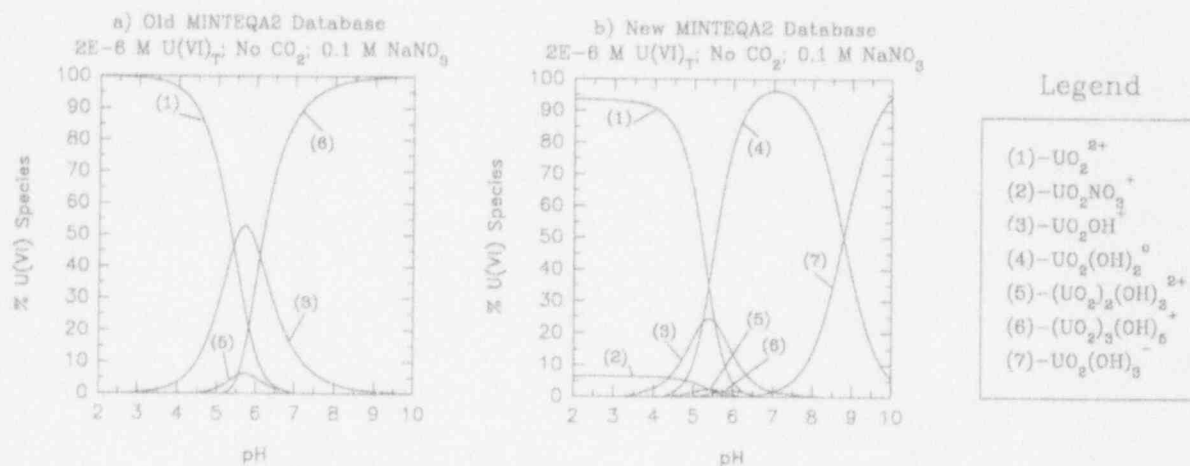


Figure 3-1. $U(VI)_T = 2 \times 10^{-6}$ M, No CO_2 , $I=0.1$ M $NaNO_3$, $T=25$ °C; (a) U(VI) Speciation predicted by THERMO.DBS database as distributed with MINTEQA2. Uranium data from Langmuir (1978). (b) U(VI) speciation as predicted by the expanded MINTEQA2 database. Uranium data from EQ3/6 database. MINTEQA2 does not report species present at less than 1% $U(VI)_T$.

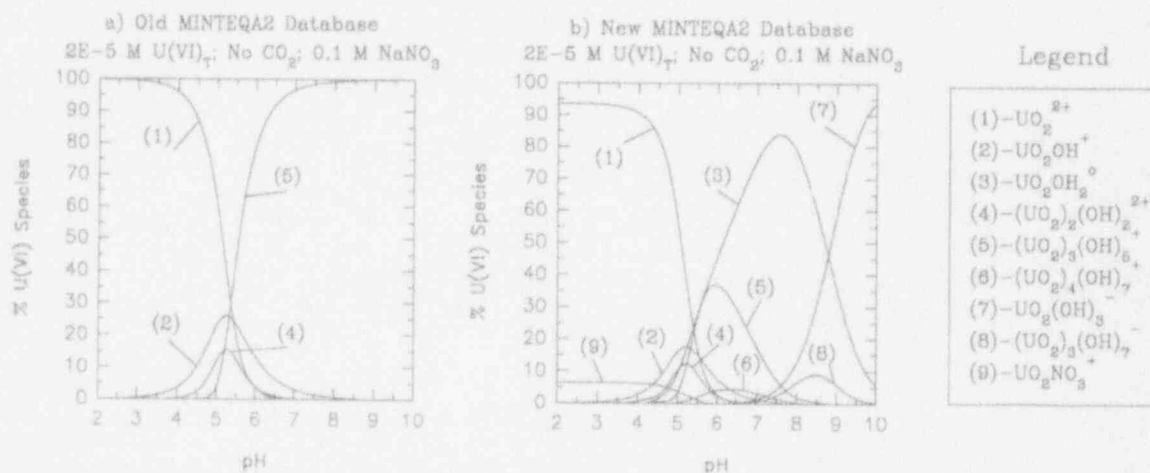


Figure 3-2. $U(VI)_T = 2 \times 10^{-5}$ M, No CO_2 , $I=0.1$ M $NaNO_3$, $T=25$ °C; (a) U(VI) Speciation predicted by THERMO.DBS database as distributed with MINTEQA2. Uranium data from Langmuir (1978). (b) U(VI) speciation as predicted by the expanded MINTEQA2 database. Uranium data from EQ3/6 database. MINTEQA2 does not report species present at less than 1% $U(VI)_T$.

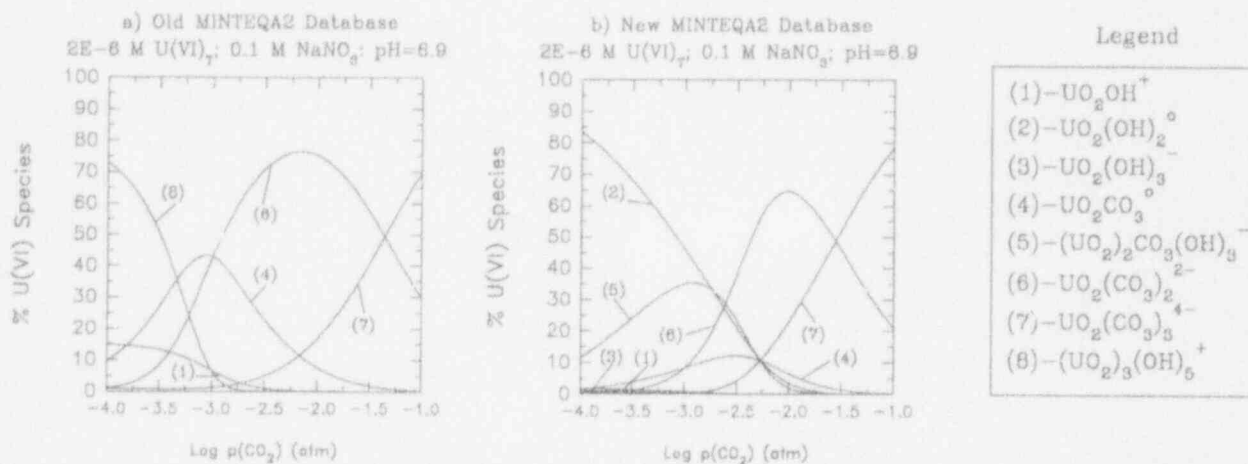


Figure 3-3. $U(VI)_T = 2 \times 10^{-6}$ M, variable CO_2 , $I=0.1$ M NaNO₃, pH=6.9, T=25 °C; (a) U(VI) speciation predicted by THERMO.DBS database as distributed with MINTEQA2. Uranium data from Langmuir (1978). (b) U(VI) speciation as predicted by the expanded MINTEQA2 database. Uranium data from EQ3/6 database. MINTEQA2 does not report species present at less than 1%.

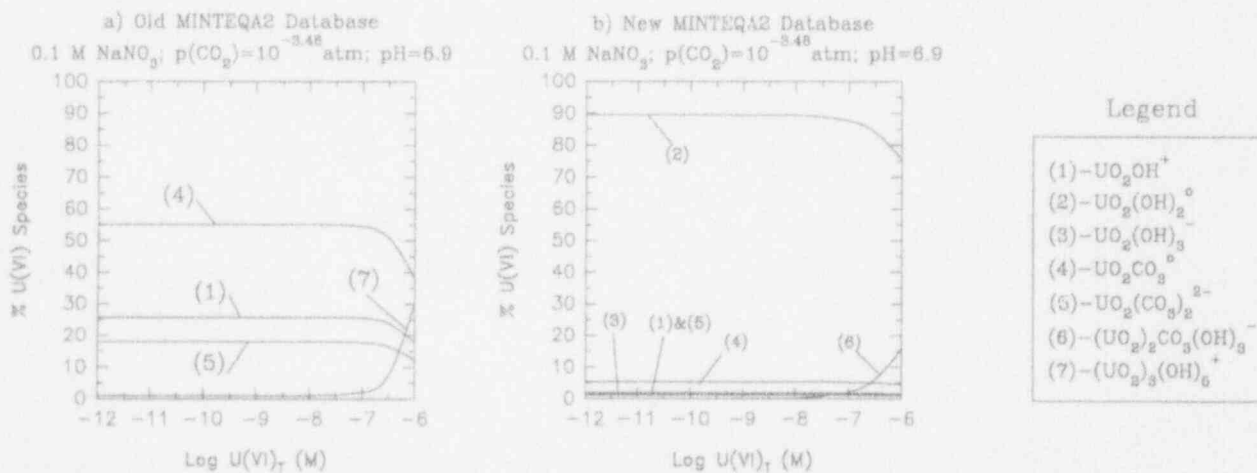


Figure 3-4. Variable $U(VI)_T$, $p(CO_2) = 10^{-3.48}$ atm, $I=0.1$ M NaNO₃, pH=6.9, T=25 °C; (a) U(VI) speciation predicted by THERMO.DBS database as distributed with MINTEQA2. Uranium data from Langmuir (1978). (b) U(VI) speciation as predicted by the expanded MINTEQA2 database. Uranium data from EQ3/6 database. MINTEQA2 does not report species present at less than 1%.

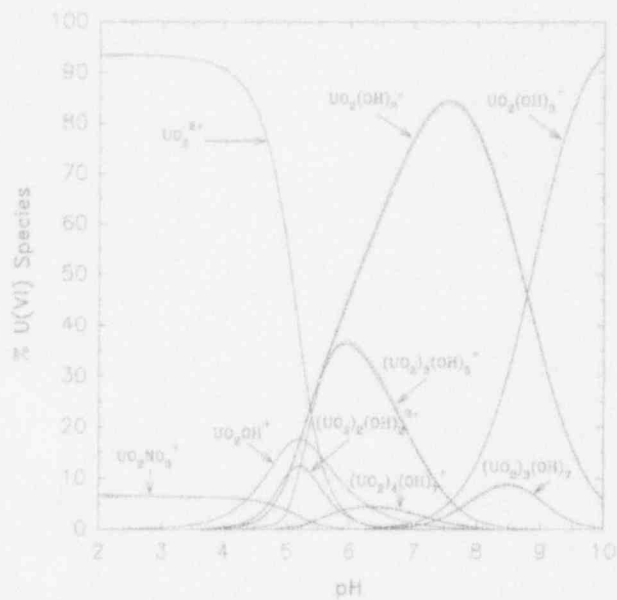


Figure 3-5. $U(VI)_T = 2 \times 10^{-5} \text{ M}$, No CO_2 , $I = 0.1 \text{ M NaNO}_3$, $T = 25 \text{ }^\circ\text{C}$. U(VI) speciation predicted by EQ3 (solid lines) and MINTEQA2 (dashed lines).

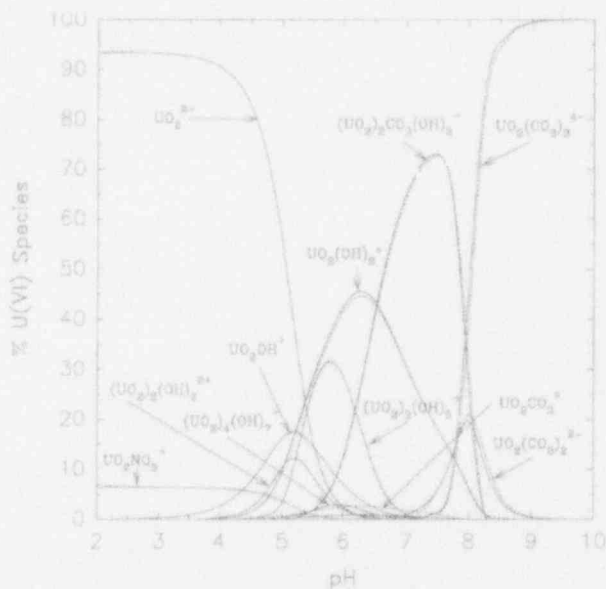


Figure 3-6. $U(VI)_T = 2 \times 10^{-5} \text{ M}$, $p(CO_2) = 10^{-3.48} \text{ atm}$, $I = 0.1 \text{ M NaNO}_3$, $T = 25 \text{ }^\circ\text{C}$. U(VI) speciation predicted by EQ3 (solid lines) and MINTEQA2 (dashed lines).

EQ3 and MINTEQA2 differ in how activity coefficients are corrected for ionic strength effects. EQ3 uses the "b-dot" extension of the Debye-Hückel relation, while MINTEQA2 defaults to the Davies equation (Allison et al., 1991). Also, the activity coefficient (γ_i) of neutral species is expressed in MINTEQA2 by the relationship, $\log \gamma_i = 0.1 I$, while EQ3 assumes $\gamma_i=1$ for uncharged species. Another difference is in the way the codes fix pH. EQ3 balances charge, adding enough acid or base species to adjust the pH to the desired values. As a result, the ionic strength (and therefore activity coefficients) will vary as a function of pH, particularly at extreme values where more acid or base is needed. This leads to an addition of species (such as NO_3^- and CO_3^{2-}) which can complex with U(VI), changing the speciation. In contrast, MINTEQA2 does not have a charge balance option and externally fixes pH without considering the addition of acid or base species. As a result of this approach, the background electrolytes remain fixed, and ionic strengths are largely independent of pH, varying from 0.1 M NaNO_3 only at the extreme values where H^+ and OH^- become significant.

For the speciation shown in Figure 3-6, the chief differences are at low $\text{pH} < 3$ where UO_2NO_3^+ is predicted to be greater by EQ3. This is due to a higher ionic strength and a slightly greater amount of NO_3^- in solution due to charge balancing. In the range $5.5 < \text{pH} < 8.5$, the difference is due to the activity coefficient of the neutral species, $\text{UO}_2(\text{OH})_2^0$ and UO_2CO_3^0 . In MINTEQA2, $\gamma_i = 10^{0.01} = 1.023$, while EQ3 assumes that $\gamma_i = 1.0$ for these species. As can be seen from Figure 3-6, the difference between the two codes is greatest for these species, reaching a maximum when $\text{UO}_2(\text{OH})_2^0$ becomes the predominant species. The disparity between the two codes is also pronounced for the charged uranyl carbonate species. This is due to the increased amounts of carbonate and bicarbonate in solution from the charge balance option of EQ3.

Despite differences in code construction, it is important to note that the differences are relatively small in the example shown. This indicates that the two codes are handling the chemical problem in a similar fashion, and, perhaps more importantly, it builds confidence in the reliability of the results.

4 RADIONUCLIDE SORPTION CONSTANTS

4.1 INTRODUCTION

The ultimate goal of this study is to determine the SCM binding constants necessary to model radionuclide sorption. The first step towards this has been discussed earlier in Section 2 in the development of the acidity constants necessary to describe the acid-base behavior of different minerals. It is now possible to take these parameters and, in a manner analogous to potentiometric titration data, use FITEQL to interpret existing sorption data and develop a set of weighted binding constants for a given radionuclide.

To do this, it is also necessary to gather existing radionuclide sorption data. These data should be from well characterized experiments covering a fairly wide pH range. A search of the open literature discovered a number of recently published studies that examine the sorption of actinides to a variety of minerals, both simple oxides such as goethite and more complex rock-forming minerals such as kaolinite and biotite. A listing of those potentially useful data found during the current investigation is given in Table 2-1.

4.2 SORPTION ON SIMPLE OXIDES: URANIUM SORPTION ON GOETHITE — AN EXAMPLE

As a means of demonstrating the procedures that can be used to determine the necessary radionuclide binding constants, U^{6+} [also UO_2^{2+} or U(VI)] sorption on goethite will be covered in some detail here. Uranium is an important constituent of the HLW to be stored at Yucca Mountain (Kerrisk, 1985), and goethite and other iron (hydr)oxides are common minerals in the Yucca Mountain System (Rogers and Meijer, 1993). In addition, the thermodynamic data of uranium has undergone a great deal of recent scrutiny to develop an internally consistent data set as part of the NEA-Thermodynamic Database (TDB) program (Wanner, 1988; Grenthe et al., 1992). With the input parameters developed above, FITEQL was used to fit U(VI)-Goethite sorption data reported by Tripathi (1984) and Hsi and Langmuir (1985) for controlled atmosphere (No CO_2) and H_2O-CO_2 systems (Table 2-1). The data of Kohler et al. (1992) were not used, because the total U(VI) concentration was not given.

In addition to the parameters describing the properties of the mineral and the acid-base behavior of the surface (Tables 2-2 and 2-3), FITEQL requires the input of a chemical equilibrium model for the system under investigation. As discussed in Section 2, this was fairly simple for the potentiometric titration data, requiring the dissociation constant of water corrected for ionic strength effects. However, with inclusion of trace metals, especially readily hydrolyzable elements such as Pu^{4+} and UO_2^{2+} , the chemical system becomes a good deal more complicated (see Section 3), and the equilibrium model requires equilibrium constants for the formation of aqueous species. For this reason, the resultant equilibrium constants for the surface complexation reactions are dependent on the quality and extent of the thermodynamic data available for the system of interest. Implicit in this statement is that the sorption constants derived using FITEQL are only valid for the thermodynamic data used in constructing the chemical equilibrium model.

The equilibrium constants used in the chemical equilibrium models submitted to FITEQL were selected from the CNWRA radionuclide database for MINTEQA2 as discussed in Section 3 and corrected for ionic strength effects using the Davies equation (Dzombak and Morel, 1990). Water is assumed to

be pure and assigned a unit activity coefficient. Because there is only limited theoretical understanding of the activity coefficients of surface species (Westall and Hohl, 1980), unit activity coefficients were assumed. Because the same data sources are used, sorption constants determined using FITEQL can be applied directly in MINTEQA2 to model uranium sorption once they are corrected back to a reference state of $I=0$ M.

The final part of the FITEQL input file is some estimate of the experimental uncertainty for the FITEQL error calculations. Although analytical precision is sometimes given, total laboratory uncertainty is not generally reported. For this reason, where error could not be determined, the approach of Dzombak and Morel (1990) was used; relative error was described, perhaps optimistically, as 1 percent relative to the lowest amount measured in solution. Relative error of ± 0.02 was assumed for pH. All standard deviations and uncertainties are reported relative to these values.

4.2.1 Controlled Atmosphere (No CO₂) Experiments

The controlled atmosphere data of Tripathi (1984) and Hsi and Langmuir (1985) are presented in Figure 4-1 and demonstrate some of the challenges involved in interpreting radionuclide sorption data, particularly data from separate laboratories. The data of Hsi and Langmuir were measured with $U(VI)_T = 10^{-5}$ M, while the data of Tripathi consist of six sets of experiments, with $U(VI)_T$ ranging from $10^{-5.4}$ to $10^{-7.1}$ M. It is apparent that, although the sorption behavior is similar in general detail, the location of the sorption edges defined by the data differs between the two studies. The sorption edge of Hsi and Langmuir (1985) agrees more closely with the data of Kohler et al. (1992); in the absence of more data on experimental conditions used by Kohler et al. (1992), however, this can only be a subjective observation and is difficult to justify as a basis for selection.

The difference between the two studies exceeds the reported uncertainty in the analytical methods, about ± 1 to 20 percent [depending on $U(VI)$ concentration] for Tripathi (1984) and ± 15 percent at 1 ppb for Hsi and Langmuir (1985). This may be due to the higher uranium concentrations (10^{-5} M) used by Hsi and Langmuir (1985), shifting the sorption edge to lower pH. However, data for $U(VI)$ -sorption on ferrihydrite exhibit smaller shifts that follow an opposite trend, with the sorption edge shifting to higher pH with increasing $U(VI)$ concentration (Payne et al., 1992). Also, the data of Tripathi (1984) indicate no trends of a similar magnitude for concentrations ranging from $10^{-5.4}$ to $10^{-7.1}$ M. Given the higher uranium concentrations, it is also possible that precipitation of U-solids could lead to the appearance of anomalously high sorption and could complicate the data of Hsi and Langmuir (1985), but mineral precipitation is not reported, nor is it predicted for the observed low pH values using the MINTEQA2 code. Differences in mineral characteristics may also be involved, but both studies report using the same mineral preparation techniques (Atkinson et al., 1967), and specific surface areas [$A_{SP} = 50$ m²/g and 45 m²/g for Tripathi (1984) and Hsi and Langmuir (1985), respectively] are similar.

Part of the discrepancy may be due to uranium loss to sinks other than goethite. Studies (Tripathi, 1984; Pabalan and Turner, 1993) report that potential uranium sinks exhibiting pH dependence in sorption experiments include the container walls (particularly polypropylene), pipettes, and filter assemblies. This is generally negligible at higher concentrations, but it can be significant for more dilute solutions in the range of 10^{-6} to 10^{-7} M. The data of Tripathi (1984) are corrected for losses to the container (polyethylene) walls, which shift the sorption edge down by as much as 20 percent for $U(VI)_T = 10^{-7.1}$ M at pH ≈ 5.4 . The experiments of Hsi and Langmuir (1985), conducted in capped polyethylene bottles, are not corrected for uranium loss, which may have resulted in an apparent shift in

Sorption of U(VI) on Goethite

Tripathi (1984); Hsi and Langmuir (1985)

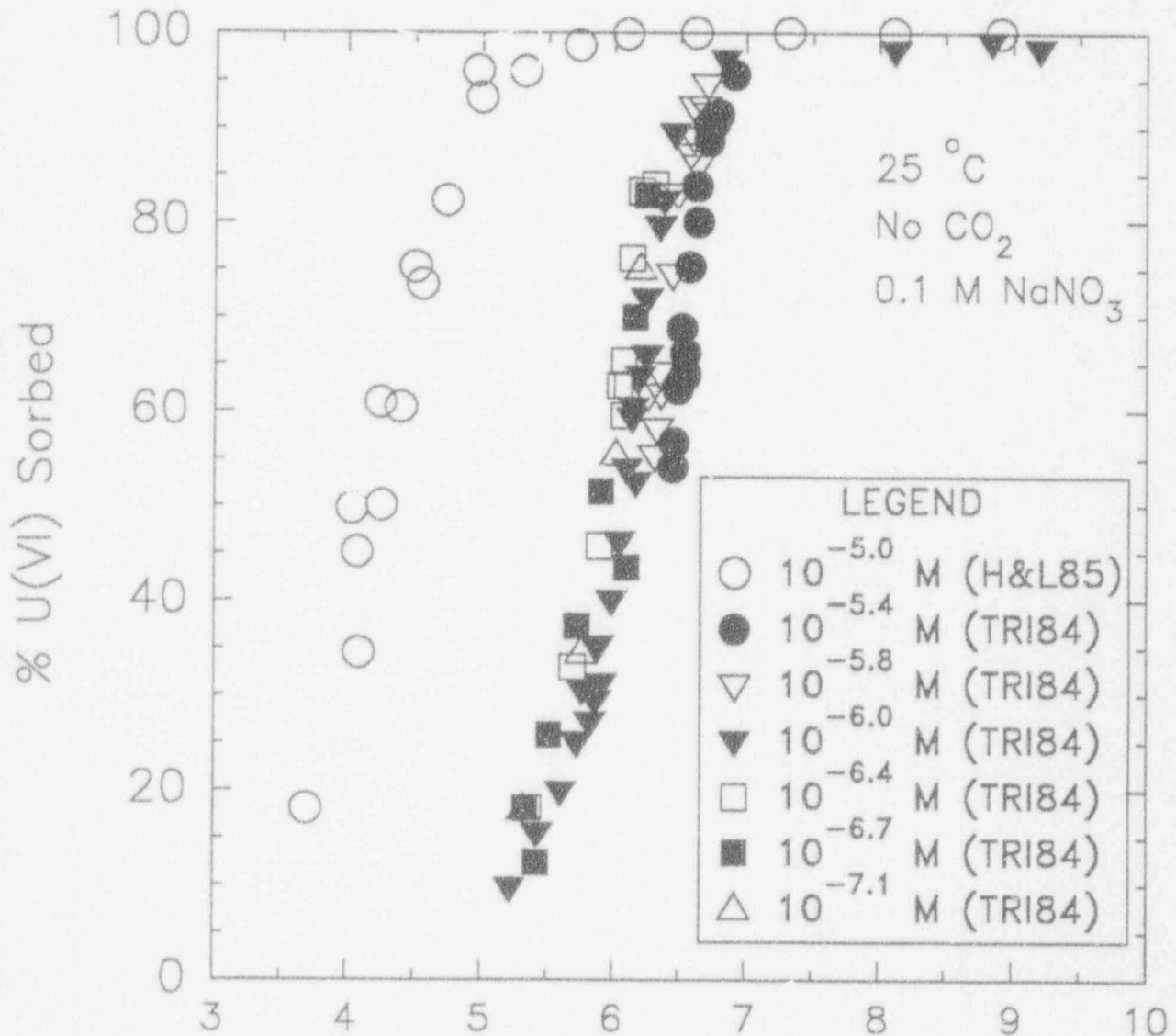
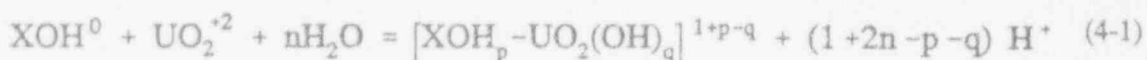


Figure 4-1. Controlled atmosphere (No CO₂) experimental data for the U(VI)-H₂O-Goethite system. Data are from Tripathi (1984) and Hsi and Langmuir (1985).

the sorption edge to lower pH, although there is no way to account for this effect in a quantitative fashion due to the lack of control data in their experiments.

In the absence of an objective way to select between the two available data sets or a clear way to correct quantitatively for the different effects contributing to the discrepancies between them, it was decided to accept the experimental results as reported, model the two data sets, and compare the resulting complexation parameters.

Since one objective of this exercise is to develop simple sorption models for PA, uranium sorption for the CO₂-free U(VI)-H₂O-Goethite system was modeled assuming monodentate complexation reactions involving only a single mononuclear uranyl hydroxide species [UO₂(OH)_n²⁻ⁿ] of the general form



Undoubtedly, the models could be further refined to produce a better fit to the data by invoking more than one surface complex, multidentate sorption, and/or consideration of polynuclear species such as was done by Kohler et al. (1992) and Payne and Waite (1991). However, to satisfy the need to develop simple models for PA, the principal of parsimony has generally been adopted, and the simplest model capable of reproducing the observed data has been preferred. While this type of approach may not reflect the actual surface complex that is formed (Manceau and Charlet, 1991), it allows comparison of different modeling strategies.

Once the chemical equilibrium model has been defined for the FITEQL input file, the serial sorption data can be entered. In most sorption studies, these data are reported in graphs as percent sorbed versus pH. As described in Section 2, these graphs have been enlarged where necessary, and an electronic digitizing tablet was used to convert graphical data to numerical values. Reproducibility was subject to the same limits discussed in Section 2.

For the U(VI)-H₂O-Goethite system (no CO₂), Tables 4-1 and 4-2 list the equilibrium constants (or binding constants) determined using FITEQL with the data of Tripathi (1984) and Hsi and Langmuir (1985), respectively. Table 4-3 lists weighted values determined by combining all data sets using the weighting scheme discussed above in Section 2. Since all experiments considered were performed with I=0.1 M, the CCM binding constants were also combined. It is important to remember that the equilibrium constants determined using FITEQL are conditional for the ionic strength considered. Prior to use in MINTEQA2, these must be converted back to the reference state of infinite dilution (I=0 M). This is accomplished using the Davies equation and is essentially the reverse of the procedure used to correct thermodynamic data to higher ionic strengths prior to constructing the FITEQL input file. This step is especially important for highly charged species such as Pu⁺⁴ and Am⁺³.

The relatively small uncertainties reported in Table 4-1 indicate that the binding constants determined for six different uranium concentrations used by Tripathi agree closely. Standard deviations for binding constants based on the data of Hsi and Langmuir (1985) are also relatively small (Table 4-2). Comparison of the sorption constants in Tables 4-1 and 4-2, however, shows the differences that result from modeling two different data sets. In general, the binding constants for the Tripathi data are smaller than those calculated for the Hsi and Langmuir data, especially for the more hydrolyzed surface species such as XOH·UO₂(OH)₄²⁻. This is due to a need to push the modeled sorption edge to higher pH to

Table 4-1. Weighted log K values for forming the indicated surface complexes in the U(VI)-H₂O-Goethite system (No-CO₂) derived from Tripathi (1984) data using FITEQL. Mineral properties and acidity constants are listed in Tables 2-2 and 2-3. U(VI)_T = 10^{-5.4}, 10^{-5.8}, 10⁻⁶, 10^{-6.4}, 10^{-6.7}, and 10^{-7.1} M. V_Y is the average measure of the goodness-of-fit as calculated by FITEQL. All things being equal, smaller values for V_Y indicate a better fit to the data. Uncertainties reflect 95% confidence limits determined using methods discussed in Dzombak and Morel (1990). Values corrected to I=0 M using Davies equation.

Surface Species	log K					
	TLM (± 95%)	V _Y (TLM)	CCM (± 95%)	V _Y (CCM)	DLM (± 95%)	V _Y (DLM)
XO-UO ₂ ⁺	-1.37±0.59	8.8	1.29±0.15	3.4	1.82±0.15	3.5
XOH-UO ₂ ²⁺	6.95±0.77	10.0	8.55±0.24	4.8	9.49±0.24	5.5
XO-UO ₂ OH ⁰	-7.61±0.27	4.7	-5.94±0.09	2.1	-5.85±0.08	1.8
XOH-UO ₂ OH ⁺	-0.04±0.81	6.6	1.29±0.15	3.4	1.82±0.15	3.5
XO-UO ₂ (OH) ₂ ⁻	-13.62±0.17	1.6	-13.17±0.06	1.0	-13.54±0.05	0.8
XOH-UO ₂ (OH) ₂ ⁰	-5.80±0.09	1.5	-5.94±0.09	2.1	-5.85±0.08	1.8
XOH ₂ -UO ₂ (OH) ₂ ⁺	2.32±0.19	2.3	1.29±0.15	3.4	1.82±0.15	3.5
XOH-UO ₂ (OH) ₃ ⁻	-11.87±0.06	0.4	-13.17±0.06	1.0	-13.54±0.05	0.8
XOH ₂ -UO ₂ (OH) ₃ ⁰	-4.07±0.04	0.4	-5.94±0.09	2.1	-5.85±0.08	1.8
XOH-UO ₂ (OH) ₄ ²⁻	-17.70±0.16	0.5	-20.35±0.06	0.6	-21.20±0.04	0.5
XOH ₂ -UO ₂ (OH) ₄ ⁻	-10.15±0.05	0.5	-13.17±0.06	1.0	-13.54±0.05	0.8

Table 4-2. Log K values for forming the indicated surface complexes in the U(VI)-H₂O-Goethite system (No-CO₂) derived from Hsi and Langmuir (1985) data using FITEQL. Mineral properties and acidity constants are listed in Tables 2-2 and 2-3. V_Y is the measure of the goodness-of-fit as calculated by FITEQL. All things being equal, smaller values for V_Y indicate a better fit to the data. Indicated uncertainties are one standard deviation ($\pm 1 \sigma$) in log K as reported by FITEQL. U(VI)_T = 10⁻⁵ M. Values corrected to I=0 M using Davies equation.

Surface Species	log K					
	TLM ($\pm 1\sigma_{\log K}$)	V _Y (TLM)	CCM ($\pm 1\sigma_{\log K}$)	V _Y (CCM)	DLM ($\pm 1\sigma_{\log K}$)	V _Y (DLM)
XO-UO ₂ ⁺	-3.17 \pm 0.04	45.0	2.69 \pm 0.04	1.9	3.13 \pm 0.04	1.6
XOH-UO ₂ ²⁺	6.57 \pm 0.06	43.3	9.56 \pm 0.03	8.3	9.86 \pm 0.03	10.8
XO-UO ₂ OH ^o	-7.33 \pm 0.03	14.7	-4.08 \pm 0.04	2.0	-3.76 \pm 0.04	3.9
XOH-UO ₂ OH ⁺	0.97 \pm 0.04	18.3	2.69 \pm 0.04	1.9	3.13 \pm 0.04	1.6
XO-UO ₂ (OH) ₂ ⁻	-11.38 \pm 0.05	0.8	-10.77 \pm 0.04	2.4	-10.19 \pm 0.05	6.0
XOH-UO ₂ (OH) ₂ ^o	-3.99 \pm 0.04	2.0	-4.08 \pm 0.04	2.0	-3.76 \pm 0.04	3.9
XOH ₂ -UO ₂ (OH) ₂ ⁺	4.29 \pm 0.05	0.7	2.69 \pm 0.04	1.9	3.13 \pm 0.04	1.6
XOH-UO ₂ (OH) ₃ ⁻	-7.98 \pm 0.05	2.5	-10.77 \pm 0.04	2.4	-10.19 \pm 0.05	6.0
XOH ₂ -UO ₂ (OH) ₃ ^o	-0.55 \pm 0.05	4.9	-4.30 \pm 0.04	2.0	-3.76 \pm 0.04	1.6
XOH-UO ₂ (OH) ₄ ²⁻	-11.40 \pm 0.07	1.7	-17.39 \pm 0.05	2.2	-16.80 \pm 0.06	7.3
XOH ₂ -UO ₂ (OH) ₄ ⁻	-4.50 \pm 0.06	4.8	-10.88 \pm 0.04	2.0	-10.19 \pm 0.05	6.0

Table 4-3. Weighted log K values for forming the indicated surface complexes in the U(VI)-H₂O-Goethite system (No-CO₂) determined by combining the results from Tripathi (1984) and Hsi and Langmuir (1985). Mineral properties and acidity constants are listed in Tables 2-2 and 2-3. Experimental conditions for data listed in captions for Tables 4-1 and 4-2. Weighting techniques are from Dzombak and Morel (1990) and described previously in Section 2. Uncertainties reflect 95 percent confidence limits determined using methods discussed in Dzombak and Morel (1990). Values corrected to I=0 M using Davies equation.

Surface Species	log K		
	TLM (± 95%)	CCM (± 95%)	DLM (± 95)
XO-UO ₂ ⁺	-0.02±0.84	1.65±0.07	2.15±0.06
XOH-UO ₂ ²⁺	6.87±0.32	8.82±0.06	9.61±0.03
XO-UO ₂ OH ^o	-7.53±0.04	-5.50±0.10	-5.36±0.14
XOH-UO ₂ OH ⁺	0.23±0.37	1.65±0.07	2.15±0.06
XO-UO ₂ (OH) ₂ ⁻	-13.12±0.15	-12.62±0.16	-12.89±0.27
XOH-UO ₂ (OH) ₂ ^o	-5.37±0.10	-5.50±0.10	-5.36±0.14
XOH ₂ -UO ₂ (OH) ₂ ⁺	2.76±0.12	1.65±0.07	2.15±0.06
XOH-UO ₂ (OH) ₃ ⁻	-11.03±0.40	-12.62±0.16	-12.89±0.27
XOH ₂ -UO ₂ (OH) ₃ ^o	-3.30±0.33	-5.50±0.10	-5.36±0.14
XOH-UO ₂ (OH) ₄ ²⁻	-16.39±1.03	-19.68±0.24	-20.40±0.45
XOH ₂ -UO ₂ (OH) ₄ ⁻	-8.97±0.81	-12.62±0.16	-12.89±0.27

match the data of Tripathi (1984); assuming formation of a single-surface complex, smaller log K values can accomplish this. The weighted binding constants given in Table 4-3 illustrate one problem with combining data from different studies. In this particular case, the results of Tripathi (1984) for six different uranium concentrations cluster at one set of values as compared to a single concentration reported by Hsi and Langmuir (1985). Therefore, all things being equal in terms of experimental error, the weighted constants exhibit a bias towards the values of Tripathi due to the relative sizes of the data sets. Consequences of this bias will be demonstrated in the modeling results.

In addition to variations between data sets, it is apparent that the resultant values are model dependent. Because both protonation and deprotonation of surface sites and specific adsorption of uranyl (UO₂²⁺) species are assumed to occur in the same plane for the DLM, the electrostatic correction applied to the mass action represented in Eq. (4-1) is the same for like-charged surface complexes. As a result, if the activity of HQ is assumed to be unity, the binding constants determined in the fitting exercise are

the same (e.g., the log K is identical for $\text{XOH-UO}_2(\text{OH})_2^0$ and $\text{XO-UO}_2\text{OH}^0$). This is also true for the CCM. In addition, the three surface complexes formed assuming a neutral aqueous species, $\text{UO}_2(\text{OH})_2^0$, result in similar binding constants for all three models. This is due to the fact that, for a neutral species, there is no electrostatic correction for specific uranyl adsorption, and the β -plane in the TLM does not require an electrostatic component. Under these conditions, all three models "behave" as a single-plane model, and the entire surface charge is assumed to be due to inner-sphere protonation and deprotonation. The slight variations between the three SCMs (less than an order of magnitude) are due to differences in the charge-potential relationship assumed by the different models.

After generating the values listed in Tables 4-1 through 4-3, the MINTEQA2 geochemical code (Allison et al., 1991) was used to model sorption in the CO_2 -free U(VI)-Goethite system. Comparison to U(VI) speciation in the absence of goethite, similar to that presented in Section 3, was used as a guide in determining which uranyl-hydroxy species might be appropriate in the pH range of the sorption edge. However, there is not always a direct correspondence. Several authors have proposed that sorption at the surface enhances hydrolysis, leading to more hydrolyzed species at the surface at a given pH than would be expected in the bulk solution alone (Davis and Leckie, 1979). It should also be remembered that SCMs treat reactions at the surface in a fashion equivalent to aqueous speciation reactions in solution. As a result, surface sites, introduced as an additional component, effectively "compete" with the solution for available uranium. Due to mass balance constraints, uranium in solution is reduced by the amount sorbed on the solids. Since a surface such as goethite acts as a uranium sink over at least part of the pH range considered, the aqueous speciation predicted in the presence of a solid will differ from that predicted for a pristine U(VI)- H_2O - CO_2 system.

The resultant fits to the $\text{U(VI)}_{\text{T}} = 1.051 \times 10^{-6}$ M data of Tripathi (1984) are shown in Figure 4-2. For clarity, and because the CCM and the DLM consider like-charged surface complexes to be the same, only one example of each type of charged-surface complex (i.e., 2+, 1+, 0, 1-, and 2-) is shown. For the Tripathi data, the TLM model fits the observed data very well, assuming a single complex of the form $\text{XOH-UO}_2(\text{OH})_4^{2-}$ and provides the best-fit to the data for all three models. This is understandable given the greater complexity and larger number of parameters in the TLM. However, the simplest model, the DLM, produces a reasonable fit to the data assuming the formation of $\text{XOH-UO}_2(\text{OH})_4^{2-}$. Like the CCM, the fit to the data is reasonable up to a pH of about 6, but falls short of the sorption maximum, Γ_{max} . All three models are able to reproduce the general aspects of the observed sorption behavior over a pH range (3 to 10) that spans the entire range of pH values measured in waters at Yucca Mountain.

Similar to Figure 4-2, modeling results for the data of Hsi and Langmuir (1985) are shown in Figure 4-3. In contrast to the modeling results for the data of Tripathi (1984), all three models are capable of reproducing the observed sorption behavior very well, assuming a single-surface complex. None of the models can match the observed data assuming either XOH-UO_2^{2+} or $\text{XOH-UO}_2\text{OH}^+$ complexes. However, the results are very good assuming either $\text{XOH-UO}_2(\text{OH})_2^0$, $\text{XOH-UO}_2(\text{OH})_3^-$, or $\text{XOH-UO}_2(\text{OH})_3^{2-}$ surface species. There is a slight tailing of sorption at $\text{pH} > 9$ for $\text{XOH-UO}_2(\text{OH})_2^0$, consistent with experimental observations (Hsi and Langmuir, 1985). In addition, data from Hsi and Langmuir (1985) indicated that between 2 and 2.66 protons (H^+) were released for each uranyl ion adsorbed, suggesting that perhaps the neutral surface complex formed according to the reaction

SORPTION OF U(VI) ON GOETHITE

Experimental data from Tripathi (1984)

$$U(VI)_T = 10^{-6} \text{ M}; 0.1 \text{ M NaNO}_3; \text{ No CO}_2$$

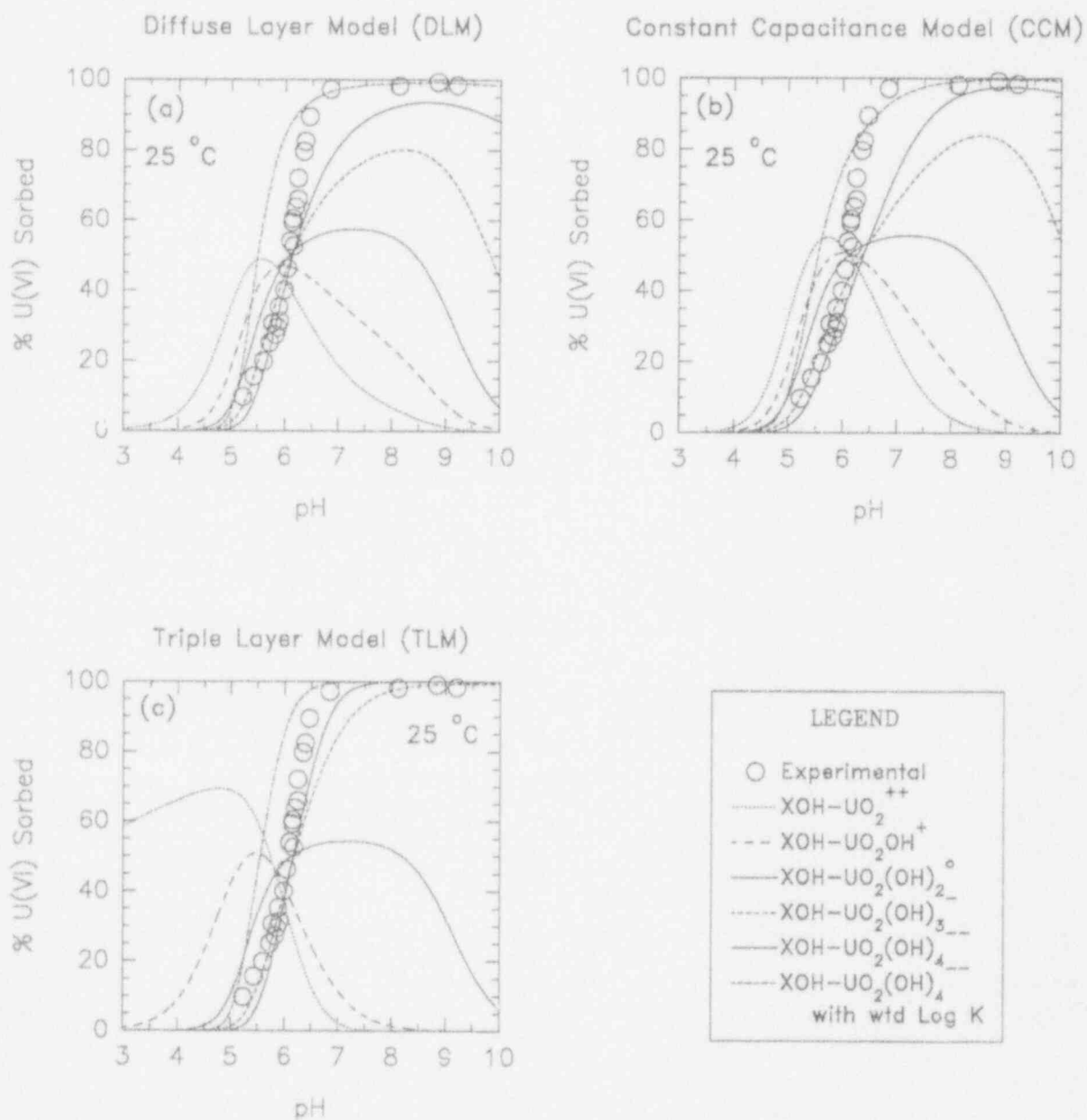


Figure 4-2. SCM modeling results. (a) DLM; (b) CCM; (c) TLM. Parameters from Tables 2-2, 2-3, 4-1. Sorption data from Tripathi (1984). $U(VI)_T = 1.05 \times 10^{-6} \text{ M}$, No CO_2 , 0.1 M $NaNO_3$.

SORPTION OF U(VI) ON GOETHITE

Experimental data from Hsi & Langmuir (1985)

$$U(VI)_T = 10^{-5} \text{ M}; 0.1 \text{ M NaNO}_3; \text{ No CO}_2$$

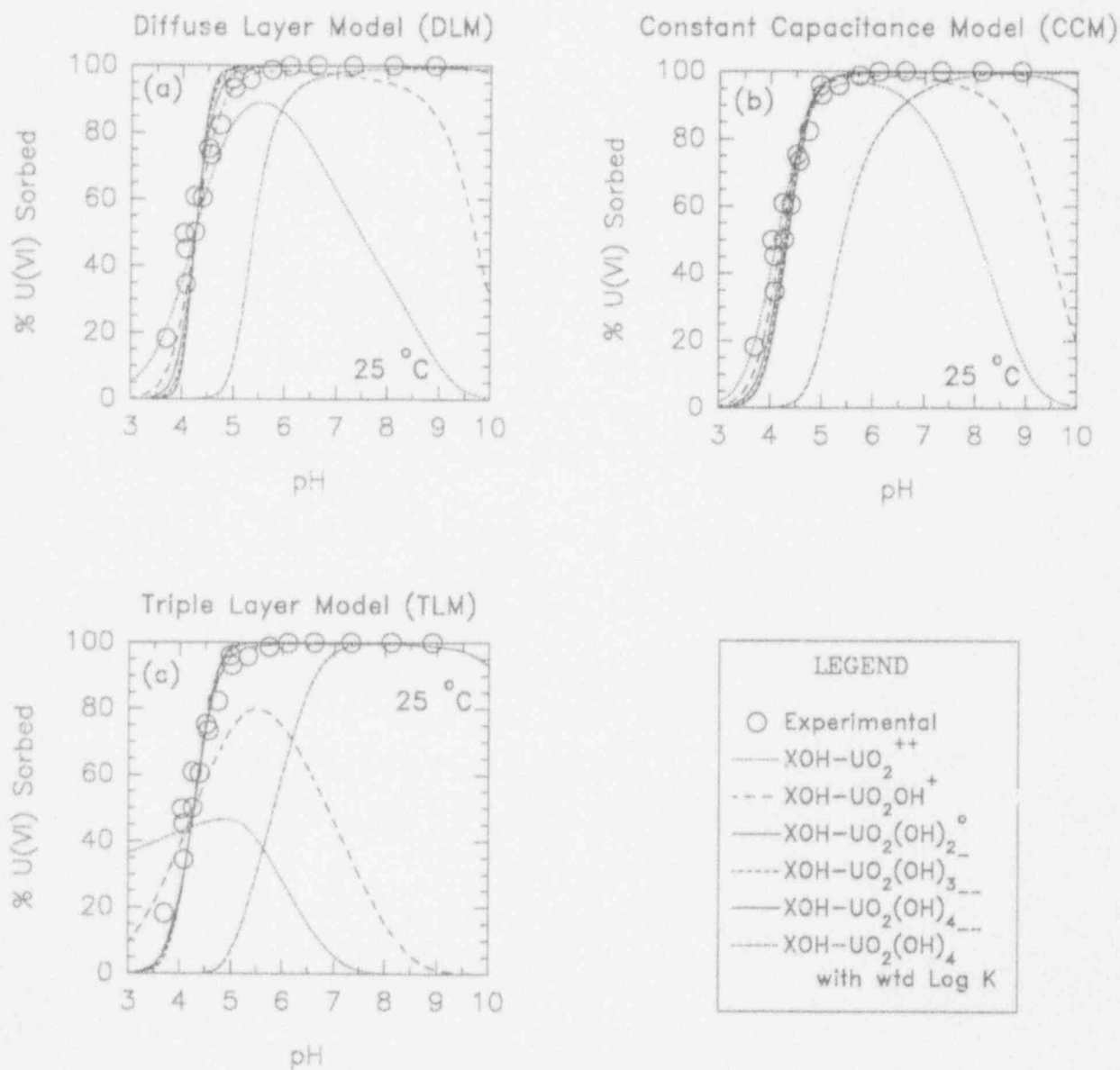
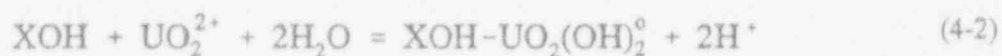


Figure 4-3. SCM modeling results. (a) DLM; (b) CCM; (c) TLM. Parameters from Tables 2-2, 2-3, and 4-2. Sorption data from Hsi and Langmuir (1985). $U(VI)_T=10^{-5}M$, No CO_2 , 0.1 M $NaNO_3$.



is most appropriate. It is important to remember that in addition to Eq. 4-2, the formation of $\text{XO-UO}_2\text{OH}^0$ and $\text{XOH}_2\text{-UO}_2(\text{OH})_3^0$ also release two protons. As discussed above, the single layer DLM and CCM cannot distinguish between reactions forming these three neutral surface species, and the fits will be identical to that shown in Figure 4-3.

Both Figures 4-2 and 4-3 show sorption predicted using the weighted $\log_5 K_{\text{UO}_2(\text{OH})_4^{2-}}$ from Table 4-3. In Figure 4-3, it can be seen that the model is not as good as that assuming the best-fit values, and predicts a sorption edge that is about 1-2 pH units higher than observed. The fit to the observed data is better in Figure 4-2, but this is due to the bias of the weighted values towards the values determined for the Tripathi (1984) data as described earlier.

4.2.2 Modeling Sorption in the U(VI)-H₂O-CO₂-Goethite System

Several studies of actinide sorption (LaFlamme and Murray, 1987; Kohler et al., 1992; Payne et al., 1992) have shown that introduction of $\text{CO}_2/\text{CO}_3^{2-}$ leads to the development of a desorption edge at higher pH. The data of Tripathi (1984) and Hsi and Langmuir (1985) also show these characteristics (Figure 4-4). This desorption has been attributed to both competition for sites by CO_3^{2-} and HCO_3^- (LaFlamme and Murray, 1987) and the competition for uranium by uranyl-(hydroxy)-carbonate complexes (Tripathi, 1984; Kohler et al., 1992). Payne et al. (1992) were able to provide an excellent fit to U(VI)-CO₂ sorption data for ferrihydrite using the two-site, double-diffuse-layer model of Dzombak and Morel (1990) without invoking site competition. Zachara et al. (1987) suggest that sorption of CO_3^{2-} , HCO_3^- , and H_2CO_3^0 reduces chromate (CrO_4^{2-}) adsorption at $p(\text{CO}_2) = 10^{-2.46}$ atm, indicating that competition for sorption sites by carbonate species may be significant in soils where $p(\text{CO}_2)$ is elevated. Dzombak and Morel (1990) conclude that CO_3^{2-} and HCO_3^- sorb only weakly, if at all, unless total carbonate concentrations are much greater than that which would occur in a system open to atmospheric CO₂ [$p(\text{CO}_2) = 10^{-3.48}$ atm]. Finally, control experiments in Hsi (1981) were unable to detect any sorption of carbon species on goethite at $C_T = 10^{-4}$ M.

The approach described in the previous section was used with the different SCMs to investigate the feasibility of modeling the effect of $\text{CO}_2/\text{CO}_3^{2-}$ on U(VI)-sorption on goethite (Tripathi, 1984; Hsi and Langmuir, 1985). Uranium speciation calculations for the U(VI)-CO₂-H₂O system indicate the formation of several uranyl-(hydroxy)-carbonato species over the pH range represented by the sorption data (see Section 3). These species may adsorb at the mineral-water interface. As with the controlled atmosphere experiments, the formation of a single monodentate surface complex was assumed. In a method analogous to that described for the controlled atmosphere experiments (Section 4.2.2), the data shown in Figure 4-4 were interpreted using FITEQL and the parameters in Tables 2-2 and 2-3 to determine binding constants (Tables 4-4 through 4-6). Also included in the analysis was the surface complex, $\text{XOH-UO}_2(\text{OH})_4^{2-}$, that generally gave the best-fit to the controlled atmosphere data.

The sorption-pH curves, calculated using MINTEQA2 and the parameters in Tables 4-3 and 4-4 are compared to the data of Tripathi (1984) in Figure 4-5. For the DLM and CCM, assuming the formation of $\text{XOH}_2\text{-UO}_2(\text{CO}_3)_3^{3-}$ best simulates the general aspects of the data, but none of the curves reproduce the observed data exactly, particularly for the TLM. This is perhaps not surprising given the added level of complexity in the observed sorption behavior. In general, the complexes that provide the

Sorption of U(VI) on Goethite

Tripathi (1984); Hsi and Langmuir (1985)

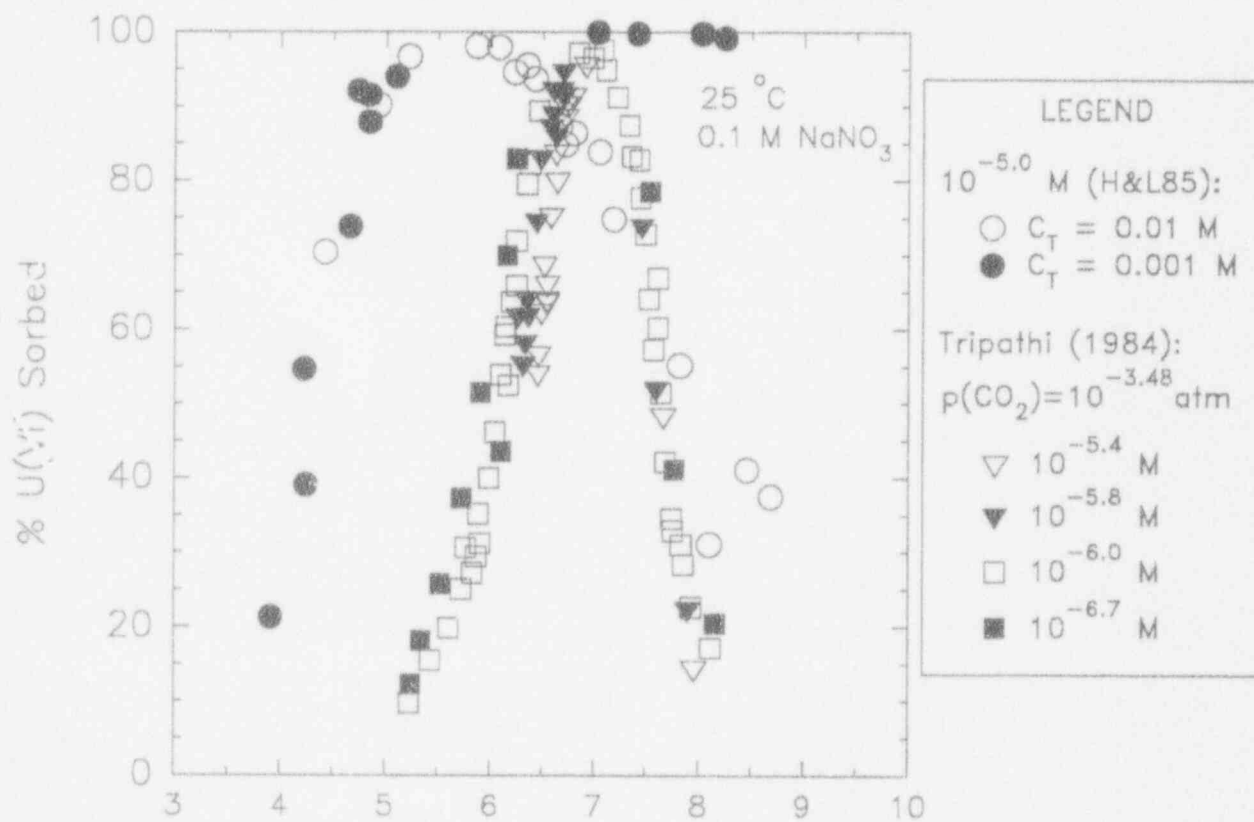


Figure 4-4. Experimental data for the U(VI)-H₂O-CO₂-Goethite system. Data are from Tripathi (1984) and Hsi and Langmuir (1985).

Table 4-4. Weighted log K values for forming the indicated surface complexes in the U(VI)-H₂O-CO₂-Goethite system derived from Tripathi (1984) data using FITEQL. Mineral properties and acidity constants are listed in Tables 2-2 and 2-3. U(VI)_T = 10^{-5.4}, 10^{-5.8}, 10⁻⁶, 10^{-6.7} M; p(CO₂) = 10^{-3.48} atm. V_Y is the average measure of the goodness-of-fit as calculated by FITEQL. All things being equal, smaller values for V_Y indicate a better fit to the data. Uncertainties reflect 95% confidence limits determined using methods discussed in Dzombak and Morel (1990). Values corrected to I=0 M using Davies equation.

Surface Species	log K					
	TLM (± 95%)	V _Y (TLM)	CCM (± 95%)	V _Y (CCM)	DLM (± 95%)	V _Y (DLM)
XOH-UO ₂ CO ₃ ⁰	16.03±0.17	2.3	15.88±0.16	2.2	15.95±0.15	2.0
XOH ₂ -UO ₂ (CO ₃) ₂ ⁻	31.97±0.91	5.3	30.16±0.22	1.1	29.81±0.21	0.7
XOH ₂ -UO ₂ (CO ₃) ₃ ³⁻	40.47±2.90	7.0	37.33±0.25	2.1	36.08±0.14	0.8
XOH ₂ -(UO ₂) ₂ CO ₃ (OH) ₃ ⁰	13.22±0.54	2.8	11.72±0.20	1.6	11.78±0.21	1.5
XOH-UO ₂ (OH) ₄ ²⁻	-17.63±0.37	9.6	-20.48±0.20	8.6	-21.47±0.17	7.6

best-fit to the sorption/desorption edges fall short of the sorption maximum. If the sorption maximum is reached, as with the case of the surface complex, $\text{XOH-UO}_2(\text{OH})_4^{2-}$, and assuming the weighted binding constant from Table 4-3, the sorption envelope defined by the sorption and desorption edges tends to be too wide.

The modeling efforts with the data of Hsi and Langmuir (1985) are shown in Figure 4-6. Binding constants are listed in Tables 4-3 and 4-5. The observed sorption envelope defined by the data is generally wider than that of Tripathi (1984); as a result, the calculated binding constants are typically larger (Table 4-5). The agreement between the binding constants determined based on data for two carbonate concentrations ($C_T=0.01$ and 0.001 M) is reasonable, with the exception of $\text{XOH}_2\text{-UO}_2(\text{CO}_3)_3^{3-}$ and $\text{XOH-UO}_2(\text{OH})_4^{2-}$. This is due to the absence of a desorption edge for the data at the lower carbonate concentration, which results in sorption behavior that closely resembles the controlled atmosphere data. In this case, FITEQL seeks to match the sorption edge at the low pH values without the twin constraint of the desorption edge at higher pH. For this reason, the binding constants for these two species at $C_T=0.001$ M are considerably larger than for $C_T = 0.01$ M. In fact, the binding constant determined at the lower carbon concentration assuming formation of $\text{XOH-UO}_2(\text{OH})_4^{2-}$ at the surface is very similar to that determined for the controlled atmosphere experiments (Table 4-2). It is also worth noting that the goodness-of-fit parameter V_y is smaller for $\text{XOH-UO}_2(\text{OH})_4^{2-}$ than for the uranyl-carbonate species. This would typically indicate a better fit for $\text{XOH-UO}_2(\text{OH})_4^{2-}$, but this is clearly not the case (Figure 4-6). This seems to be related to additional error assumed for carbonate in writing the complexation reactions to include U(VI)-CO_3 .

As with the controlled atmosphere experiments, the results of modeling the data of Hsi and Langmuir (1985) using the DLM and CCM are relatively insensitive to the postulated surface complex. All of the surface complexes match the sorption maximum, but they tend to overpredict the sorption edge and underpredict the desorption edge. In addition, the models appear to impart too much pH dependence on the sorption behavior, leading to sorption/desorption edges that are steeper than observed values. In contrast to the model results for the data of Tripathi (1984), assuming the single-surface complex, $\text{XOH-UO}_2(\text{OH})_4^{2-}$, does not fit the observed data of Hsi and Langmuir (1985) at all for the higher carbonate concentration ($C_T = 0.01$ M).

An improved fit can be obtained for both data sets by postulating more than one surface species. For example, assuming a combination of the three surface species, $\text{XOH}_2\text{-(UO}_2)_2\text{CO}_3(\text{OH})_3^0$, $\text{XOH}_2\text{-UO}_2(\text{CO}_3)_2^-$, and $\text{XOH}_2\text{-UO}_2(\text{CO}_3)_3^{3-}$, results in a much closer fit (Figure 4-7). Using the weighted values from Table 4-6 results in a slight improvement in the fit to the Tripathi (1984) data, but a significant worsening in the fit to the data of Hsi and Langmuir (1985), which again shows the effects of the bias towards the larger data set of Tripathi (1984). As another example, Kohler et al. (1992) obtained an excellent fit to U(VI)-Goethite sorption data using a TLM and assuming the formation of four surface complexes, $\text{XO-UO}_2\text{OH}^0$, $\text{XO-(UO}_2)_3(\text{OH})_5^0$, $\text{XOH}_2\text{-UO}_2(\text{CO}_3)_2^-$, and $\text{XOH}_2\text{-UO}_2(\text{CO}_3)_3^{3-}$.

Although such approaches have been demonstrated to provide an improved fit to the data set, it should be kept in mind that there is generally little information available on actual surface species. In addition, the added level of complexity introduced by multiple surface species may work against the practical application of SCMs in PA.

SORPTION OF U(VI) ON GOETHITE

Experimental data from Tripathi (1984)

$$U(VI)_T = 10^{-6} \text{ M}; 0.1 \text{ M NaNO}_3; p(\text{CO}_2) = 10^{-3.48} \text{ atm}$$

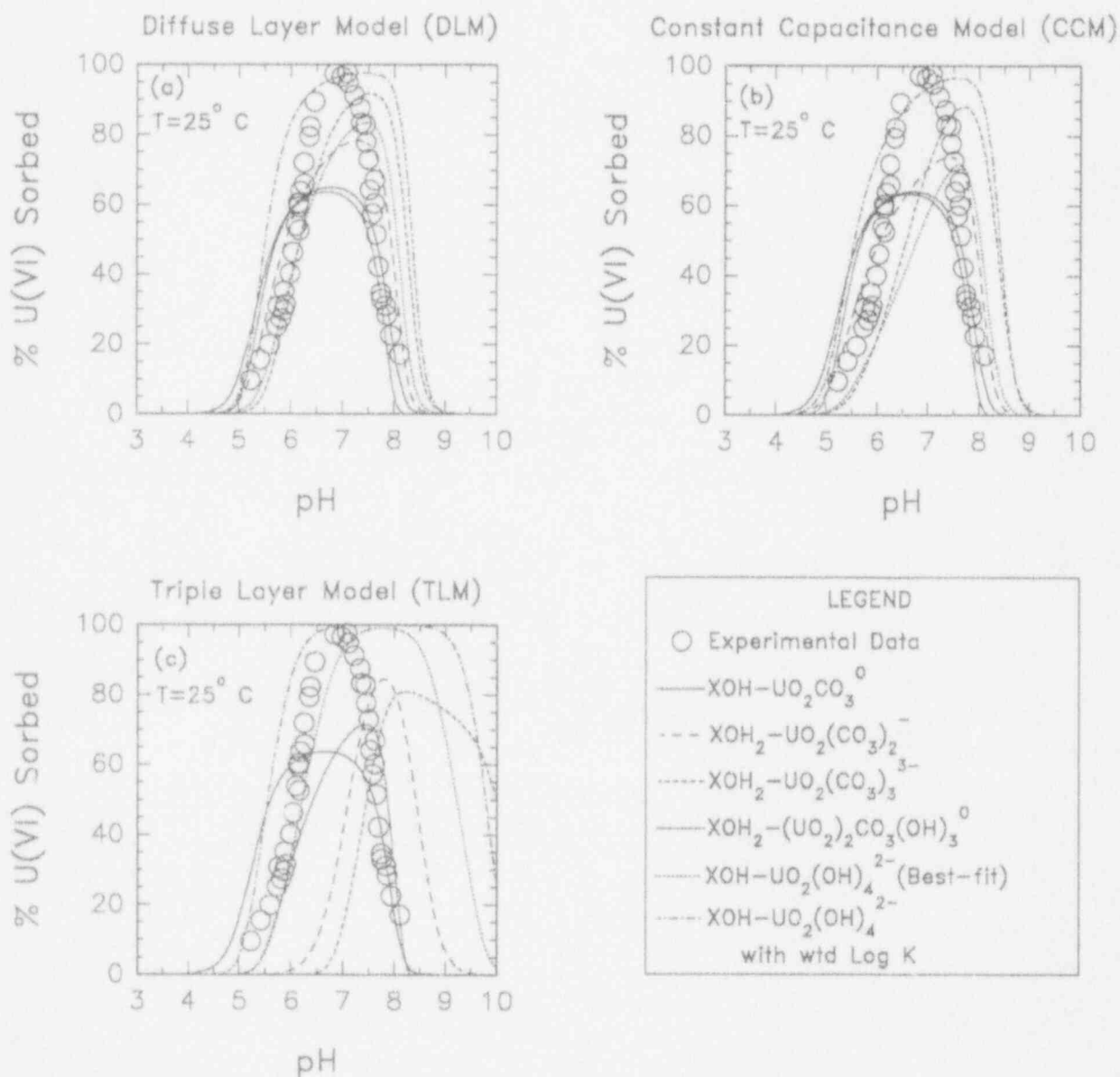


Figure 4-5. SCM modeling results. (a) DLM; (b) CCM; (c) TLM. Parameters from Tables 2-2, 2-3, 4-4. Sorption data from Tripathi (1984). $U(VI)_T = 1.05 \times 10^{-6} \text{ M}$, $p(\text{CO}_2) = 10^{-3.48} \text{ atm}$, 0.1 M NaNO_3 .

SORPTION OF U(VI) ON GOETHITE

Experimental data from Hsi & Langmuir (1985)

$$U(VI)_T = 10^{-5} \text{ M}; 0.1 \text{ M NaNO}_3; C_T = 0.01 \text{ M}$$

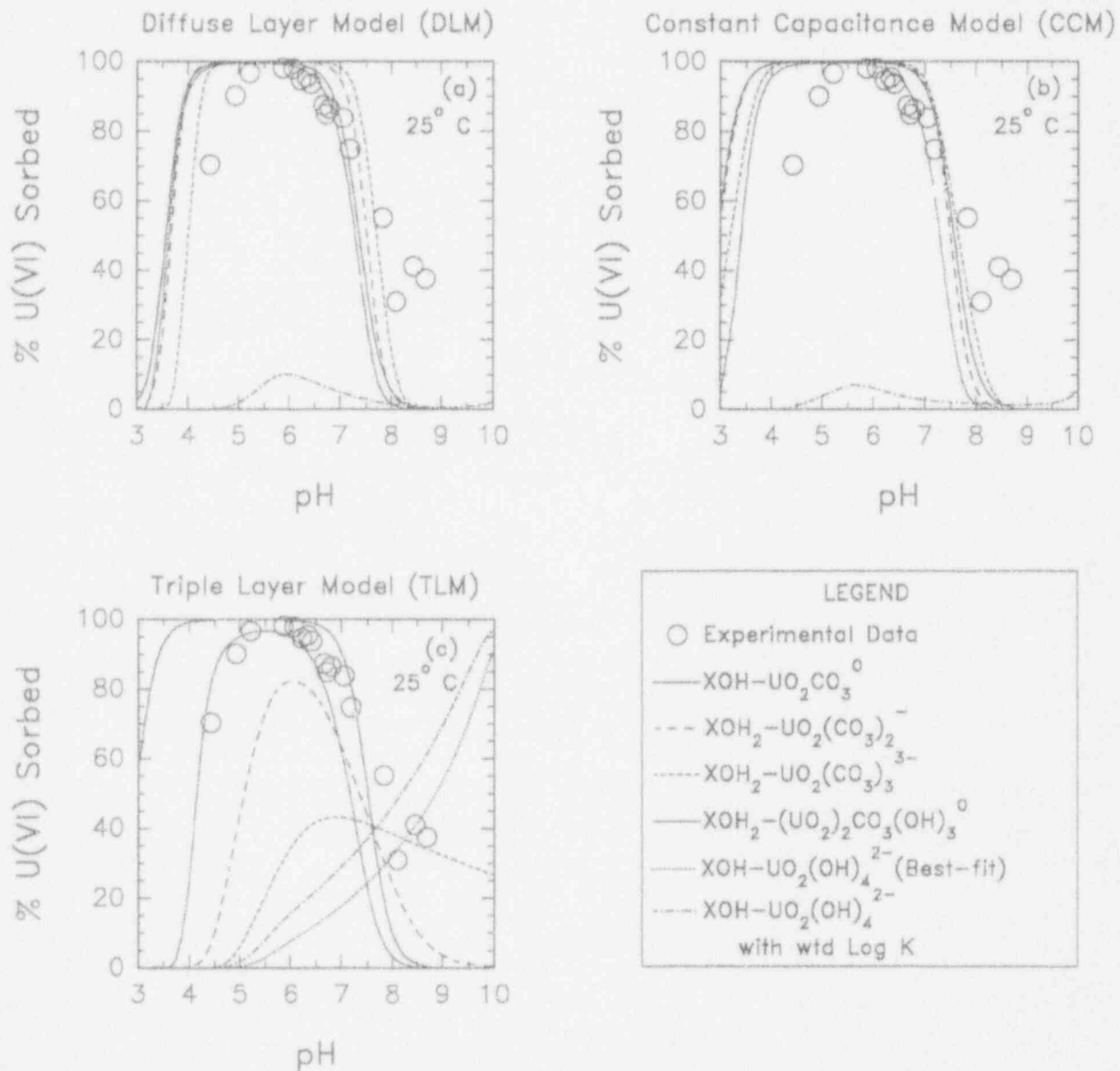


Figure 4-6. SCM modeling results. (a) DLM; (b) CCM; (c) TLM. Parameters from Tables 2-2, 2-3, 4-5. Sorption data from Hsi and Langmuir (1985). $U(VI)_T=10^{-5} \text{ M}$, $C_T=0.01 \text{ M}$, 0.1 M NaNO_3 .

Table 4-5. Log K values for forming the indicated surface complexes in the U(VI)-H₂O-CO₂-Goethite system derived from Hsi and Langmuir (1985) data using FITEQL. Mineral properties and acidity constants are listed in Tables 2-2 and 2-3. Indicated uncertainties are one standard deviation ($\pm 1 \sigma$) in log K as reported by FITEQL. The number in brackets, [V_Y], is the measure of the goodness-of-fit as calculated by FITEQL. All things being equal, smaller values for V_Y indicate a better fit to the data. U(VI)_T = 10⁻⁵ M; C_T = 0.01 M and 0.001 M as indicated. Values corrected to I = 0 M using Davies equation.

Surface Species	log K					
	TLM ($\pm 1\sigma_{\log K}$) [V _Y]		CCM ($\pm 1\sigma_{\log K}$) [V _Y]		DLM ($\pm 1\sigma_{\log K}$) [V _Y]	
	10 ⁻³ M	10 ⁻² M	10 ⁻³ M	10 ⁻² M	10 ⁻³ M	10 ⁻² M
XOH-UO ₂ CO ₃ ⁰	17.00±0.03 [0.6]	17.37±0.05 [12.7]	16.90±0.03 [0.6]	17.37±0.06 [13.7]	17.43±0.04 [1.0]	17.12±0.06 [14.1]
XOH ₂ -UO ₂ (CO ₃) ₂ ⁻	28.78±0.03 [90.2]	30.74±0.04 [24.0]	28.17±0.02 [79.5]	29.65±0.05 [12.0]	27.80±0.02 [80.5]	29.53±0.05 [12.4]
XOH ₂ -UO ₂ (CO ₃) ₃ ³⁻	52.49±0.11 [0.6]	38.28±0.07 [49.0]	39.32±0.05 [0.4]	35.30±0.05 [10.8]	40.00±0.07 [2.4]	34.29±0.06 [17.0]
XOH ₂ -(UO ₂) ₂ CO ₃ (OH) ₃ ⁰	17.37±0.07 [2.2]	15.61±0.07 [12.7]	13.85±0.06 [1.4]	15.10±0.09 [14.4]	14.38±0.07 [1.9]	15.14±0.09 [14.4]
XOH-UO ₂ (OH) ₄ ²⁻	-11.81±0.10 [0.2]	-17.12±0.06 [14.9]	-17.63±0.06 [0.3]	-22.47±0.05 [3.1]	-16.98±0.08 [1.1]	-22.96±0.05 [4.9]

SORPTION OF U(VI) ON GOETHITE

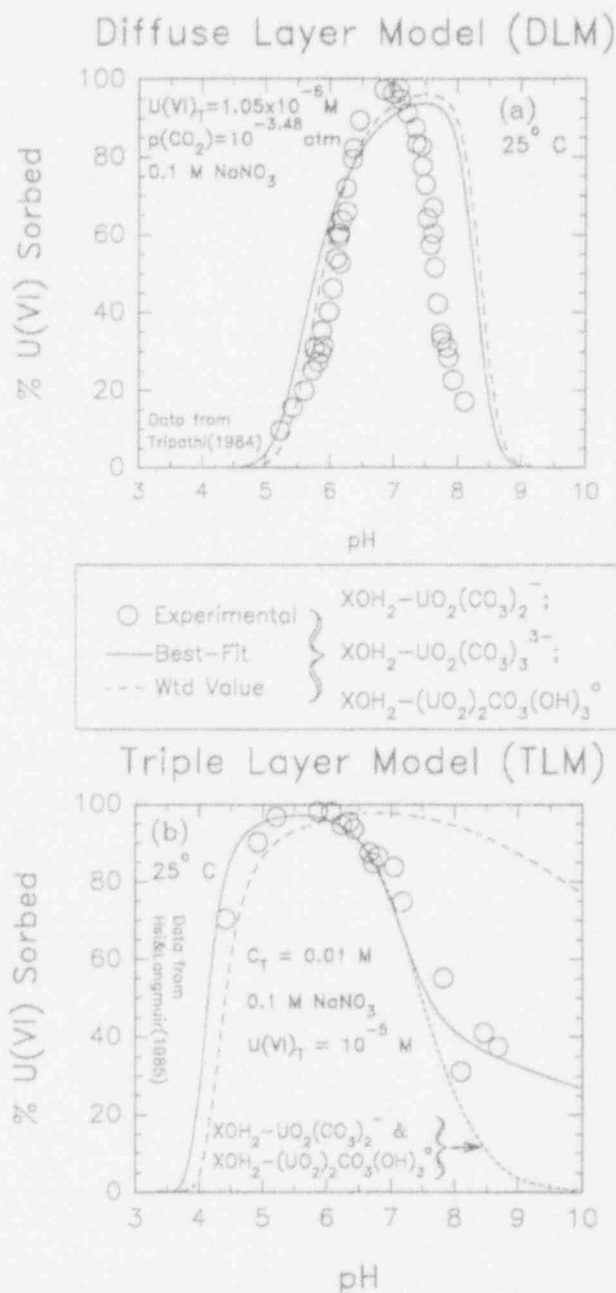


Figure 4-7. SCM modeling results for the U(VI)-H₂O-CO₂-Goethite system assuming three surface complexes: $XOH_2-UO_2(CO_3)_2^-$; $XOH_2-UO_2(CO_3)_3^{3-}$; and $XOH_2-(UO_2)_2CO_3(OH)_3^0$. Parameters from Tables 2-2, 2-3. (a) DLM with data from Tripathi (1984); log K from Tables 4-4 and 4-6; and (b) TLM with data from Hsi and Langmuir (1985). The short dashed line represents modeling assuming only $XOH_2-UO_2(CO_3)_2^-$ and $XOH_2-(UO_2)_2CO_3(OH)_3^0$ as surface species; log K from Tables 4-5 and 4-6.

Table 4-6. Weighted log *K* values for forming the indicated surface complexes in the U(VI)-H₂O-CO₂-Goethite system determined by combining the data of Tripathi (1984) and Hsi and Langmuir (1985). Mineral properties and acidity constants are listed in Tables 2-2 and 2-3. Experimental conditions for data listed in captions for Tables 4-4 and 4-5. Weighting techniques are from Dzombak and Morel (1990) and described previously in Section 2. Uncertainties represent 95 percent confidence limits determined using methods discussed in Dzombak and Morel (1990). Values corrected to *I*=0 M using Davies equation.

Surface Species	log <i>K</i>		
	TLM (± 95%)	CCM (± 95%)	DLM (± 95%)
XOH-UO ₂ CO ₃ ⁰	16.37±0.29	16.22±0.29	16.32±0.32
XOH ₂ -UO ₂ (CO ₃) ₂ ⁻	30.89±0.75	29.51±0.47	29.15±0.49
XOH ₂ -UO ₂ (CO ₃) ₃ ³⁻	41.98±2.76	37.34±0.63	36.28±0.85
XOH ₂ -(UO ₂) ₂ CO ₃ (OH) ₃ ⁰	14.54±0.92	12.50±0.65	12.62±0.70
XOH-UO ₂ (OH) ₄ ²⁻	-16.59±1.10	-20.41±0.78	-21.23±0.91

4.2.3 Effect of Data Set Size

Another concern in PA is that the number of data points that are necessary to allow an adequate description of the system under consideration should not be excessive. As a first-order attempt to address this concern, the controlled atmosphere data of Tripathi (1984) for U(VI)_T=1.05×10⁻⁶ M was divided into progressively smaller subsets, and FITEQL was used to calculate DLM binding constants for the U(VI)-H₂O-Goethite (no CO₂) system. In an attempt to avoid bias towards a particular pH range, the original 25 data points (see Figure 4-1) were arranged from lowest to highest pH; progressively smaller subsets were then extracted, first by selecting every other data point (*m*=13 points), every third data point (*m*=9), and finally every fifth data point (*m*=5). This initial approach is simplistic, but it does assure that most of the experimental pH range is sampled. The binding constants calculated using FITEQL are listed in Table 4-7. All other parameters were held constant at the values listed in Tables 2-2 and 2-3 for the DLM. Calculated log *K* values for all surface complexes were similar for all subsets of the data. However, as represented by the standard deviation calculated by FITEQL, the uncertainty in the value increased slightly with a decreasing number of data points. This is not surprising, as the geochemical system is less well constrained by a smaller data set.

From this analysis, it is clear that a few carefully selected data points are sufficient to model the location of the sorption edge for the U(VI)-H₂O system. Similar sorption behavior has been observed (Sanchez et al., 1985; LaFlamme and Murray, 1987; Girvin et al., 1991) for other important actinides such as Am, Np, Pu, Th; it seems reasonable to expect similar results for these systems. Although the uncertainty in the calculated binding constants is slightly greater for smaller data sets, it is not excessive and does offer some guidance in the ability to predict complex sorption behavior with a reasonable number of data points. However, it is critical that experiments are performed over a broad enough range

Table 4-7. Effect of data set size (number of measurements) on log K estimated using FITEQL. Data from Tripathi (1984). Mineral properties and acidity constants are listed in Tables 2-2 and 2-3. Indicated uncertainties are one standard deviation ($\pm 1 \sigma$) in log K as reported by FITEQL. $U(VI)_T = 1.05 \times 10^{-6}$ M, No CO_2 . Values corrected to $I=0$ M using Davies equation.

Surface Species	DLM - log K ($\pm 1\sigma_{\log k}$)			
	m=25	m=13	m=9	m=5
XO- UO_2^+	1.64 \pm 0.042	1.62 \pm 0.059	1.62 \pm 0.071	1.58 \pm 0.090
XOH- UO_2^{2+}	9.21 \pm 0.044	9.16 \pm 0.063	9.15 \pm 0.075	9.10 \pm 0.096
XO- UO_2OH^0	-5.97 \pm 0.042	-5.96 \pm 0.058	-5.94 \pm 0.071	-6.01 \pm 0.094
XOH- UO_2OH^+	1.64 \pm 0.042	1.62 \pm 0.059	1.62 \pm 0.071	1.58 \pm 0.090
XO- $UO_2(OH)_2^-$	-13.65 \pm 0.045	-13.64 \pm 0.063	-13.62 \pm 0.077	-13.66 \pm 0.103
XOH- $UO_2(OH)_2^0$	-5.97 \pm 0.042	-5.96 \pm 0.058	-5.94 \pm 0.071	-6.01 \pm 0.094
XOH ₂ - $UO_2(OH)_2^+$	1.64 \pm 0.042	1.62 \pm 0.059	1.62 \pm 0.071	1.58 \pm 0.090
XOH- $UO_2(OH)_3^-$	-13.65 \pm 0.045	-13.64 \pm 0.063	-13.62 \pm 0.077	-13.66 \pm 0.103
XOH ₂ - $UO_2(OH)_3^0$	-5.97 \pm 0.042	-5.96 \pm 0.058	-5.94 \pm 0.071	-6.01 \pm 0.094
XOH- $UO_2(OH)_4^{2-}$	-21.32 \pm 0.050	-21.31 \pm 0.070	-21.30 \pm 0.087	-21.32 \pm 0.111
XOH ₂ - $UO_2(OH)_4^-$	-13.65 \pm 0.045	-13.64 \pm 0.063	-13.62 \pm 0.077	-13.66 \pm 0.103

in pH to adequately "sample" all aspects of the sorption behavior under consideration. This is especially important in the presence of CO_2 or other ligands that are known to produce a desorption edge at higher pH.

4.3 MODELING OF COMPLEX ROCK-FORMING MINERALS

Radionuclide sorption data are available for a number of common rock-forming minerals, such as clays and micas (Table 2-1) that, because of their abundance, may contribute significantly to sorption processes. In contrast to simple (hydr)oxides, only rarely are potentiometric titration data available for these minerals (Riese, 1982). However, because these minerals are more complex, the development of a surface charge may be due to more than one type of site.

One method of applying SCMs to more complex minerals has been used in several recent studies. Using a TLM, Rai et al. (1988) modeled chromate (CrO_4^{2-}) adsorption on kaolinite assuming a heterogeneous surface composed of stoichiometric proportions of silanol ($SiOH^0$) and aluminol ($AlOH^0$) sites. Similar approaches have been proposed to model radionuclide sorption on kaolinite, including uranium (Kohler et al., 1992), thorium, and radium (Riese, 1982).

The U(VI)-Kaolinite sorption data of Payne et al. (1992) and Np(V)-Biotite sorption data of Nakayama and Sakamoto (1991) were investigated using this approach. Surface areas for these minerals were taken from Allard et al. (1983). Stoichiometries for kaolinite $[\text{Al}_2\text{Si}_2\text{O}_5(\text{OH})_4]$ and biotite $[\text{K}(\text{Mg},\text{Fe})_3\text{AlSi}_3\text{O}_{10}(\text{OH})_2]$ yielded $\text{AlOH}^0:\text{SiOH}^0$ ratios of 1:1 and 1:3, respectively. The acidity constants from Table 2-3 for SiO_2 and $\alpha\text{-Al}_2\text{O}_3$ were used in these proportions, and binding constants were determined using FITEQL (Tables 4-8 and 4-9).

Contaminant speciation (especially for actinides) varies rapidly as a function of pH. For this reason, sorption edges that extend over wider pH ranges, such as those exhibited by the U(VI)-Kaolinite and Np(V)-Biotite data, tend to require more than one surface complex (Davis and Leckie, 1978; Dzombak and Morel, 1990). In both cases, more than one surface complex was necessary to fit the observed data. The resultant fit is quite good (Figure 4-8). However, as discussed in the previous section, the added complexity of multiple surface species tends to make the practical application of SCMs more difficult in PA.

4.4 RADIONUCLIDE SORPTION MODELING — SUMMARY AND CONCLUSIONS

Following the recommendations of Davis and Kent (1990), a first attempt has been made to apply a standard set of SCM parameters to radionuclide sorption. These parameters have been developed using a uniform approach based on the work of Dzombak and Morel (1990) for the CCM, DLM, and TLM. To demonstrate the approach, examples have been presented for a simple (hydr)oxide system, U(VI)-sorption on goethite (Tripathi, 1984; Hsi and Langmuir, 1985). The method has also been adapted to apply a SCM to radionuclide sorption on more complex rock-forming minerals such as U(VI)-kaolinite and Np(V)-biotite.

This modeling attempt is relevant to the HLW repository at Yucca Mountain, since both uranium and neptunium are anticipated to be important radionuclides in assessing repository performance (Kerrisk, 1985). The relatively well-characterized uranium system (Grenthe et al., 1992) is considered to be analogous to other important actinides (Pu, Np, Am, Th). Hematite and other iron (hydr)oxides, such as goethite, have been identified near Yucca Mountain and are ubiquitous minerals in many natural systems. Equilibrium speciation calculations indicate that J-13 well water is saturated with regard to several iron (hydr)oxides (Baca et al., 1992). In addition, kaolinite and biotite are reported in the Yucca Mountain environment (DOE, 1988).

Version 2.0 of the FITEQL parameter estimation code of Westall (1982a,b) was used to determine the necessary equilibrium constants for possible surface complexation reactions. The resultant constants were model-specific. Within the constraints of the conceptual model, the TLM was best able to fit data in the CO_2 -free data of Tripathi (1984) assuming a single $\text{XOH-}\text{UO}_2(\text{OH})_4^{2-}$ surface species. For the data of Hsi and Langmuir (1985), all three models proved capable of producing satisfactory fits. As with the Tripathi data, the $\text{XOH-}\text{UO}_2(\text{OH})_4^{2-}$ provides a good fit. However, fits were comparable for three different surface species. In the absence of independent data on actual surface species, proton release data suggest $\text{XOH-}\text{UO}_2(\text{OH})_2^0$ as a likely surface species.

Because of the twin constraints of a sorption edge at low pH and a desorption edge at higher pH, a single species is inadequate in most cases for U(VI)-Goethite sorption in the presence of carbon-bearing species. The fit can be greatly improved by invoking additional species. This does not add significantly to the computational burden for geochemical modeling, but it may limit the application of SCMs to PA.

Table 4-8. Log K values the DLM for forming the indicated surface complexes in the U(VI)-Kaolinite system derived from Payne et al. (1992) data using FITEQL. Acidity constants are from Table 2-3. For Kaolinite, assumed $A_{SP}=11 \text{ m}^2/\text{g}$ (Allard et al., 1983). Except as noted, indicated uncertainties are one standard deviation ($\pm 1\sigma$) in log K as reported by FITEQL. $U(VI)_T=10^{-6} \text{ M}$. Values corrected to $I=0 \text{ M}$ using Davies equation.

Surface Complex	DLM - log K ($\pm 1\sigma_{\log K}$) ^a
SiOH ₂ ⁺ AlOH ₂ ⁺	n.a. 8.33 ± 0.15
SiO ⁻ AlO ⁻	-7.20 ± 0.05 -9.73 ± 0.12
SiO-UO ₂ ⁺ AlO-UO ₂ ⁺	0.96 ± 0.04 2.18 ± 0.10
SiOH-UO ₂ ²⁺ AlOH-UO ₂ ²⁺	5.73 ± 0.16 9.20 ± 0.03
SiO-UO ₂ OH ⁰ AlO-UO ₂ OH ⁰	-5.84 ± 0.44 -4.74 ± 0.59

n.a. $pH_{ZPC} \approx 2.8$ for SiO₂; SiOH₂⁺ not considered in this pH range.

(a) Reported uncertainties represent 95 percent confidence limit for acidity constants. For uranium surface complexes, listed uncertainty represents standard deviation ($\pm 1\sigma$) in log K reported by FITEQL.

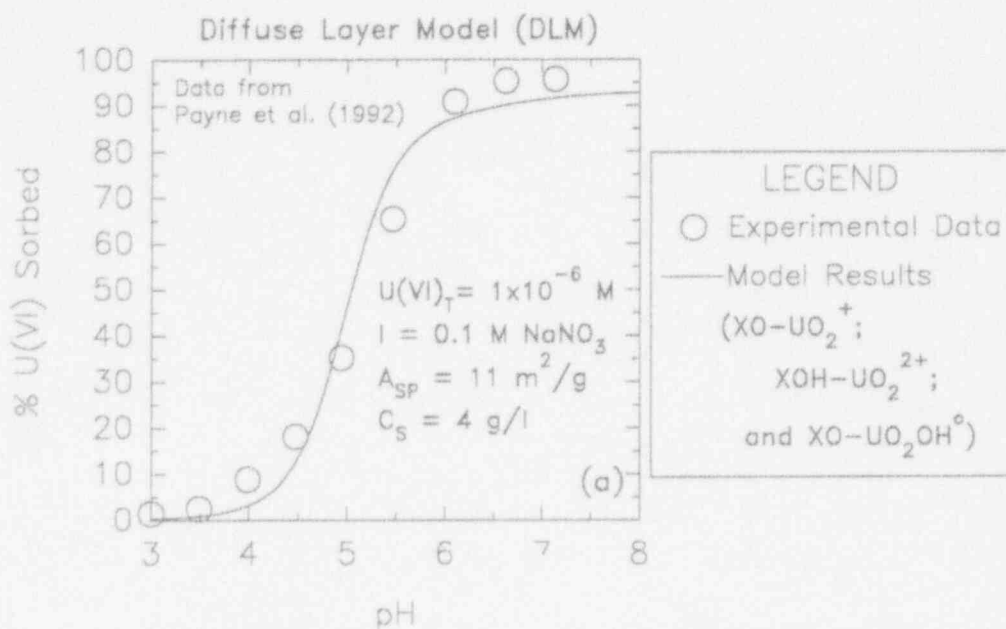
Table 4-9 Log K values the DLM for forming the indicated surface complexes in the Np(V)-Biotite system derived from Nakayama and Sakamoto (1991) data using FITEQL. Acidity constants are from Table 2-3. For Biotite, assumed $A_{SP}=8 \text{ m}^2/\text{g}$ (Allard et al., 1983). Except as noted, indicated uncertainties are one standard deviation ($\pm 1\sigma$) in log K as reported by FITEQL. $Np(V)_T=6 \times 10^{-6} \text{ M}$. Values corrected to $I=0 \text{ M}$ using Davies equation.

Surface Complex	DLM - log K ($\pm 1\sigma_{\log K}$) ^a
SiOH ₂ ⁺ AlOH ₂ ⁺	n.a. 8.33 ± 0.15
SiO ⁻ AlO ⁻	-7.20 ± 0.05 -9.73 ± 0.12
SiOH-NpO ₂ ⁺ AlOH-NpO ₂ ⁺	2.86 ± 0.06 4.15 ± 0.03
SiO-NpO ₂ OH ⁻ AlO-NpO ₂ OH ⁻	-11.58 ± 0.02 -12.39 ± 0.17

n.a. $pH_{ZPC} \approx 2.8$ for SiO₂; SiOH₂⁺ not considered in this pH range.

(a) Reported uncertainties represent 95 percent confidence limit for acidity constants. For uranium surface complexes, listed uncertainty represents standard deviation ($\pm 1\sigma$) in log K reported by FITEQL.

SORPTION OF U(VI) ON KAOLINITE



SORPTION OF Np(V) ON BIOTITE

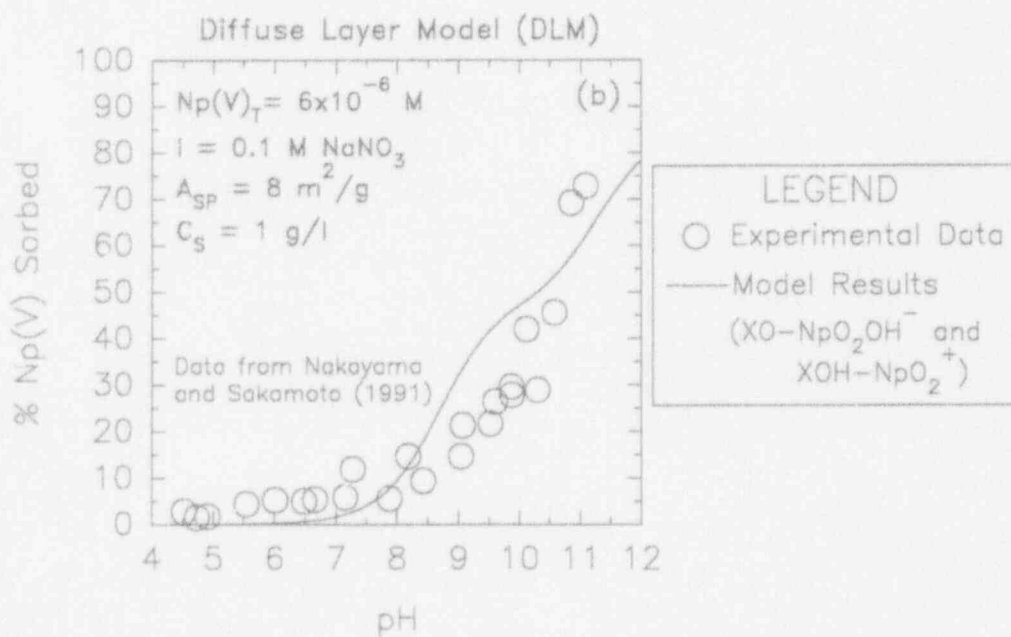


Figure 4-8. DLM modeling results for: (a)U(VI)-Kaolinite sorption (Payne et al., 1992); and (b) Np(V)-Biotite sorption (Nakayama and Sakamoto, 1991). Postulated surface species are as indicated, binding constants are from Tables 4-8 and 4-9.

5 SUMMARY AND CONCLUSIONS

Experimental sorption data indicate that radionuclide (especially actinide) sorption is a complex function of the physical and chemical conditions of the system under consideration. Current PA approaches tend to rely on empirical approaches to modeling radionuclide sorption. Because these models do not explicitly account for changes in system chemistry, extrapolation of laboratory data beyond experimental conditions is uncertain. The purpose of this study is to move towards a uniform mechanistic model for radionuclide sorption that allows for the prediction of complex sorption behavior.

SCMs represent one type of mechanistic approach to modeling sorption processes. Three models have been commonly used: DLM, CCM, and TLM. These models use similar approaches to correct for electrostatic effects at the charged mineral-water interface, but differ in how the interface is represented. The complexity of these models varies, with the types of adjustable parameters ranging from three for the DLM to seven for the TLM. Traditional applications rely on adjusting different parameters to match a given data set. Because of the number of parameters, this is likely to result in a nonunique fit and difficult comparisons between models and between studies.

To minimize these problems, recent efforts have focused on developing a "standard" set of model parameters. This has the benefit of providing a set of uniform SCM parameters that share common reference values. Dzombak and Morel (1990) used such an approach for applying the DLM to ferrihydrite sorption data. To compare different models and to take advantage of the available radionuclide sorption data (Table 2-1), this approach needs to be expanded. In an effort to do this, the current study has adopted many of the methods outlined in Dzombak and Morel (1990). Many simplifying assumptions have been made along the way as a means of minimizing the amount of "tweaking" used in the modeling exercise.

The first step involved using numerical parameter optimization methods (Westall, 1982a,b) to interpret available potentiometric titration data and to determine the acidity constants that are necessary to describe the acid-base behavior of the mineral surface. Data were obtained from the open, peer-reviewed literature. One simplifying step that has been taken here is to adopt for all minerals the site density of 2.31 sites/nm² determined by Dzombak and Morel (1990). Because it is rarely reported, an additional simplification has been made by assuming a uniform experimental uncertainty (Hayes et al., 1990). By interpreting each data set for each of the three SCMs listed above and then combining the resultant acidity constants using a weighting scheme proposed in Dzombak and Morel (1990), a set of uniform model-dependent acidity constants has been derived for a number of common simple (hydr)oxides. In general, all three models were able to simulate the observed acid-base behavior quite well. With these parameters in place, it is possible to move to the next step of applying SCMs to radionuclide sorption data.

A similar approach has been taken for interpreting radionuclide sorption data. The methods have been described in detail for sorption in the U(VI)-CO₂-H₂O-Goethite system. Two different data sets are available for this system (Tripathi, 1984; Hsi and Langmuir, 1985). Discrepancies between these studies illustrate some of the difficulties in interpreting radionuclide sorption data. At least part of the discrepancy is likely due to loss to the container wall (Pabalan and Turner, 1993), which has apparently been considered only for the data of Tripathi (1984). Assuming a single simple monodentate, mononuclear uranyl-hydroxy surface species is adequate to model observed sorption behavior for the controlled

atmosphere CO₂-free system for all three models, although the postulated species may be different for the two studies due to differences in the sorption edge. Weighted parameters are not able to model either data set satisfactorily, and there is a clear bias towards the larger data set.

The fit to the data can be improved by invoking additional surface complexes as has been done in other studies (Hsi and Langmuir, 1985; Kohler et al., 1992), but without independent methods of analysis, the validity of the postulated complexes would be uncertain. As can be seen from examining the derived binding constants, different surface complexes with identical charges have identical binding constants in the DLM and CCM. For this reason, these models are not able to distinguish between like-charged surface complexes. Although EXAFS work indicates the formation of bidentate mononuclear uranyl-hydroxy surface complexes (Manceau and Charlet, 1991), this work only exists for fairly concentrated solutions (millimolar) at single pH values. Additional EXAFS work will be required to ascertain the extent to which SCMs represent the mineral-water interface (Sposito, 1992). It must also be stressed that the parameters calculated in the fitting exercise are dependent on the thermodynamic data used in the geochemical equilibrium model, and actinide data are notoriously uncertain. Even for the uranium data from the extensively evaluated NEA database (Grenthe et al., 1992; Turner et al., 1993), several studies (Tripathi, 1984; Tripathi and Parks, 1992; Fuger, 1992) suggest that there is some uncertainty in the value used for UO₂(OH)₂⁰.

As should be apparent from this report, development of a uniform set of radionuclide binding constants proceeds through a logical progression of steps from potentiometric titration data to radionuclide sorption data. Combining data from different laboratories may be problematic, and deciding between data sets is not always straightforward. This effort has also pointed out inconsistencies in reporting data and experimental conditions in the literature. A number of data sets are not usable in this type of exercise merely because certain key pieces of information are missing. In addition, a more thorough reporting of experimental error would minimize the need to rely on assumed values; this would provide more accurate estimates for weighting factors. As noted by Dzombak and Morel (1990), the weighting scheme used allows for relatively easy updating of these data to incorporate new or revised data when they become available. However, any radionuclide binding constants are dependent on the acidity constants used in the FITEQL optimization run; if these acidity constants are modified by the incorporation of new potentiometric titration data or changes in parameter values assumed while interpreting the present data, all radionuclide binding constants must be reevaluated. In addition, the tabulated binding constants are dependent on the thermodynamic data available. Any significant changes in the data likewise require a recalculation of the necessary parameters.

For the purposes of PA, computational efficiency of sorption models is an important consideration. For the simple systems modeled in this study, computer runs using a DOS-compiled version of MINTEQA2 on an IBM 486 personal computer took about 4 or 5 seconds (real-time) for each pH value considered. Run-time would necessarily increase for more complex systems, but recompiling the source code to take advantage of 32-bit processors would presumably reduce run-time requirements. Although not modeled here, MINTEQA2 can also consider other processes such as precipitation and dissolution, but at present it is restricted to an assumption of thermodynamic equilibrium and cannot consider reaction kinetics.

The result of this exercise is a first step towards developing the database necessary for consistent application of mechanistic SCMs in a predictive way for PA, especially through the presentation of a comprehensive set of model-dependent acidity constants to describe mineral acid-base behavior. Future efforts will concentrate on using these parameters in conjunction with the FITEQL code to model other

available sorption data. In addition to simple (hydr)oxides, it should also be possible to apply these models to more complex rock-forming minerals as demonstrated for U(VI)-sorption on kaolinite and Np(V) sorption on biotite. Other minerals that can be considered in this fashion are clinoptilolite and montmorillonite, both key minerals in the Yucca Mountain environment.

From the point of view of describing the mineral-water interface, it must be emphasized that the results given here are dependent on the assumptions used in constructing the conceptual model. For the purposes of PA, a principle of parsimony was adopted in defining possible surface complexes in the U(VI)-H₂O-CO₂-Goethite system. Within this framework, the DLM was able to reproduce the general aspects of uranyl sorption behavior while using a far simpler representation of the mineral-water interface than the TLM. This may be preferred where simpler models are desirable to strike a balance between accuracy of the conceptual model and the computational resources required by geochemistry in PA calculations (Yeh and Tripathi, 1989).

The exercise has also demonstrated that, unlike an empirical K_d approach, SCMs are a relatively robust and flexible way to reproduce the general aspects of chemistry-dependent complex sorption behavior using a single set of parameters. As observed by others, the simplest SCM, the DLM is able to perform quite well in comparison to more complex models.

6 REFERENCES

- Abendroth, R.P. 1970. Behavior of pyrogenic silica in aqueous electrolytes. *Journal of Colloid and Interface Science* 34: 591-596.
- Allard, B. 1982. *Sorption of actinides in granite rock*. Report KBS 82-21, Göteborg, Sweden: Chalmers University of Technology.
- Allard, B., M. Karlsson, E-L Tullborg, and S.A. Larson. 1983. *Ion Exchange Capacities and Surface Areas of Some Major Components and Common Fracture Filling Materials of Igneous Rocks*. Report KBS 83-64. Göteborg, Sweden: Chalmers University of Technology.
- Allison, J.D., D.S. Brown, and K.J. Novo-Gradac. 1991. *MINTEQA2/PRODEFA2, A Geochemical Assessment Model for Environmental Systems: Version 3.0 User's Manual*. EPA/600/3-91/021. Athens, GA: U.S. Environmental Protection Agency.
- Atkinson, R.J., A.M. Posner, and J.P. Quirk. 1967. Adsorption of potential determining ions at the ferric oxide-aqueous electrolyte interface. *Journal of Physical Chemistry* 71: 550-558.
- Atkinson, R.J., A.M. Posner, and J.P. Quirk. 1968. Crystal nucleation in Fe(III) solutions and hydroxide gels. *Journal of Inorganic Nuclear Chemistry* 30: 2371-2381.
- Atkinson, R.J., A.M. Posner, and J.P. Quirk. 1972. Kinetics of isotopic exchange of phosphate at the α -FeOOH-aqueous solution interface. *Journal of Inorganic Nuclear Chemistry* 34: 2201-2211.
- Baca, R.G., D. Turner, and B. Sagar. 1992. Transport of radionuclides in colloidal form. *NRC High-Level Radioactive Waste Research at CNWRA January 1 Through June 30, 1992*. W.C. Patrick, ed. CNWRA 92-01S. San Antonio, TX: Center for Nuclear Waste Regulatory Analyses.
- Baes, C.F., and R.E. Mesmer. 1976. *The Hydrolysis of Cations*. New York, NY: Wiley-Interscience Publication, John Wiley and Sons.
- Balistreri, L., and J.W. Murray. 1981. The surface chemistry of goethite (α -FeOOH) in major ion sea water. *American Journal of Science* 281: 788-806.
- Ball, J.W., E.A. Jenne, and M.W. Cantrell. 1981. *WATEQ3—A Geochemical Model With Uranium Added*. USGS-OF-81-1183. Menlo Park, CA: U.S. Geological Survey.
- Benjamin, M.M., and J.O. Leckie. 1981. Multiple-site adsorption of Cd, Cu, Zn, and Pb on amorphous iron oxyhydroxide. *Journal of Colloid and Interface Science* 79: 209-221.
- Berube, Y.G., and P.L. de Bruyn. 1968. Adsorption at the rutile-solution interface. 1. Thermodynamic and experimental study. *Journal of Colloid and Interface Science* 27: 305-318.
- Bolt, G.H. 1957. Determination of the charge density of silica soils. *Journal of Physical Chemistry* 61: 1166-1169.

- Bradbury, M.H., and B. Baeyens. 1992. A mechanistic approach to the generation of sorption databases. *Radionuclide Sorption From the Safety Evaluation Perspective. Proceedings of an NEA Workshop*. Paris: Nuclear Energy Agency. Organization for Economic Cooperation and Development: 121-162.
- Bradbury, M.H., and B. Baeyens. 1993. A general application of surface complexation to modeling radionuclide sorption in natural systems. *Journal of Colloid and Interface Science* 158: 364-371.
- Breeuwsma, A., and J. Lyklema. 1973. Physical and chemical adsorption of ions in the electrical double layer on hematite (α -Fe₂O₃). *Journal of Colloid and Interface Science* 43: 437-448.
- Catts, J.G., and D. Langmuir. 1986. Adsorption of Cu, Pb and Zn by δ -MnO₂: Applicability of the site binding surface complexation model. *Applied Geochemistry* 1: 255-264.
- Cox, J.D., D.D. Wagman, and V.A. Medvedev, eds. 1989. *CODATA Key Values for Thermodynamics*. NY: Hemisphere Publishing.
- Cross, J.E., and F.T. Ewart. 1991. HATCHES—A thermodynamic database and management system. *Radiochimica Acta* 52/53: 421-422.
- Davis, J.A. 1977. *Adsorption of Trace Metals and Complexing Ligands at the Oxide/Water Interface*. Ph.D. Dissertation; Stanford, CA: Stanford University.
- Davis, J.A., and J.O. Leckie. 1978. Surface ionization and complexation at the oxide/water interface 2. Surface properties of amorphous iron oxyhydroxide and adsorption of metal ions. *Journal of Colloid and Interface Science* 67: 90-107.
- Davis, J.A., and J.O. Leckie. 1979. Speciation of adsorbed ions at the oxide water interface. *Chemical Modeling in Aqueous Systems, Speciation, Sorption, Solubility, and Kinetics*. E.A. Jenne, ed. Washington, DC, ACS Symposium Series 93. American Chemical Society: 299-317.
- Davis, J.A., R.O. James, and J.O. Leckie. 1978. Surface ionization and complexation at the oxide/water interface 1. Computation of electrical double layer properties in simple electrolytes. *Journal of Colloid and Interface Science* 63: 480-499.
- Davis, J.A., and D.B. Kent. 1990. Surface complexation modeling in aqueous geochemistry. *Reviews in Mineralogy: Volume 23. Mineral-Water Interface Geochemistry*. M.F. Hochella, Jr. and A.F. White, eds. Washington, DC: Mineralogical Society of America: 177-260.
- Della Mea, G., J.C. Dran, V. Moulin, J.C. Petit, J.D.F. Ramsay, and M. Theyssier. 1992. Scavenging properties of inorganic particles toward heavy elements. *Radiochimica Acta* 58/59: 219-223.
- Department of Energy (DOE). 1988. *Site Characterization Plan: Yucca Mountain Site, Nevada Research and Development Area, Nevada*. Office of Civilian Radioactive Waste Management (OCRWM). Washington, DC: DOE/RW-0199.

- Dzombak, D.A. 1985. *Toward a Uniform Model for the Sorption of Inorganic Ions on Hydrous Oxides*. Ph.D. Dissertation. Boston, MA: Massachusetts Institute of Technology.
- Dzombak, D.A., and F.M.M. Morel. 1990. *Surface Complexation Modeling: Hydrous Ferric Oxide*. NY: John Wiley and Sons.
- Dzombak, D.A., and K.F. Hayes. 1992. Comment on "Recalculation, evaluation, and prediction of surface complexation constants for metal adsorption on iron and manganese oxides." *Environmental Science and Technology* 26: 1251-1253.
- EPA (40 CFR Part 191). 1991. *Environmental Radiation Protection Standards for Management and Disposal of Spent Nuclear Fuel, High-Level and Transuranic Radioactive Wastes*. Title 40, Protection of Environment, Part 191. Washington, DC: U.S. Government Printing Office.
- Fuger, J., and F.L. Oetting. 1976. *The Chemical Thermodynamics of Actinide Elements and Compounds. Part 2. The Actinide Aqueous Ions*. Vienna, Austria: International Atomic Energy Agency.
- Fuger, J. 1992. Thermodynamic properties of actinide aqueous species relevant to geochemical problems. *Radiochimica Acta* 58/59: 81-91.
- Garrels, R.M., and C.L. Christ. 1965. *Solutions, Minerals, and Equilibria*. San Francisco, CA: Freeman, Cooper and Company.
- Girvin, D.C., L.L. Ames, A.P. Schwab, and J.E. McGarrah. 1991. Neptunium adsorption on synthetic amorphous iron oxyhydroxide. *Journal of Colloid and Interface Science* 141: 67-78.
- Grenthe, I., J. Fuger, R.J. Lemire, A.B. Muller, C. Nguyen-Trung, and H. Wanner. 1992. *Chemical Thermodynamics Series, Volume 1: Chemical Thermodynamics of Uranium*. Nuclear Energy Agency, Organization for Economic Cooperation and Development (OECD). NY: Elsevier.
- Hayes, K.F., and J.O. Leckie. 1987. Mechanism of lead ion adsorption at the goethite-water interface. J.A. Davis and K.F. Hayes, eds. *Geochemical Processes at Mineral Surfaces*. ACS Symposium Series 323. Washington, DC: American Chemical Society: 114-141.
- Hayes, K.F., G. Redden, W. Ela, and J.O. Leckie. 1990. *Application of Surface Complexation Models for Radionuclide Adsorption: Sensitivity Analysis of Model Input Parameters*. NUREG/CR-5547. Washington, DC: U.S. Nuclear Regulatory Commission.
- Hayes, K.F., G. Redden, W. Ela, and J.O. Leckie. 1991. Surface complexation models: An evaluation of model parameter estimation using FITEQL and oxide mineral titration data. *Journal of Colloid and Interface Science* 142: 448-469.
- Hemingway, B.S. 1982. *Thermodynamic Properties of Selected Uranium Compounds and Aqueous Species at 298.15 K and 1 Bar and at Higher Temperatures—Preliminary Models for the Origin of Coffinite Deposits*. U.S. Geological Survey Open-File Report, USGS-OFR-82-619. Reston, VA: U.S. Geological Survey.

- Hsi, C-K.D. 1981. *Sorption of Uranium(VI) by Iron Oxides*. Ph.D. Dissertation. Golden, CO: Colorado School of Mines.
- Hsi, C-K.D, and D. Langmuir. 1985. Adsorption of uranyl onto ferric oxyhydroxides: Application of the surface complexation site-binding model. *Geochimica et Cosmochimica Acta* 49: 1931-1941.
- Huang, C.P., and W. Stumm. 1972. The specific surface area of γ -Al₂O₃. *Surface Science* 32: 287-296.
- Hunter, K.A., D.J. Hawke, and L.K. Choo. 1988. Equilibrium adsorption of thorium by metal oxides in marine electrolytes. *Geochimica et Cosmochimica Acta* 52: 627-636.
- Jackson, K.J., and J.C. Helgeson. 1985. Chemical and thermodynamic constraints on the hydrothermal transport and deposition of tin. I. Calculation of the solubility of cassiterite at high pressures and temperatures. *Geochimica et Cosmochimica Acta* 49: 1-22.
- James, R.O., and G. Parks. 1982. Characterization of aqueous colloids by their electrical double-layer and intrinsic surface chemical properties. *Surface and Colloid Science* 12: 119-216.
- Johnson, J.W., E.H. Oelkers, and H.C. Helgeson. 1991. *SUPCRT92: A Software Package for Calculating the Standard Molal Thermodynamic Properties of Minerals, Gases, Aqueous Species, and Reactions from 1 to 5000 bars and 0 °C to 1000 °C*. Livermore, CA: Lawrence Livermore National Laboratory.
- Kent, D.B., V.S. Tripathi, N.B. Ball, J.O. Leckie, and M.D. Siegel. 1988. *Surface-Complexation Modeling of Radionuclide Adsorption in Subsurface Environments*. NUREG/CR-4807. Washington, D.C: U.S. Nuclear Regulatory Commission.
- Kerrisk, J.F. 1984. *Americium Thermodynamic Data for the EQ3/6 Data Base*. LA-10040-MS. Los Alamos, NM: Los Alamos National Laboratory.
- Kerrisk, J.F. 1985. *An Assessment of the Important Radionuclides in Nuclear Waste*. LA-10414-MS. Los Alamos, NM: Los Alamos National Laboratory.
- Kerrisk, J.F., and R.J. Silva. 1986. A Consistent Set of Thermodynamic Constants for Americium(III) Species with Hydroxyl and Carbonate. *Proceedings of the Workshop on Geochemical Modeling*. Fallen Leaf Lake, CA: 167-175.
- Kohler, M., E. Wieland, and J.O. Leckie. 1992. Metal-ligand-surface interactions during sorption of uranyl and neptunyl on oxides and silicates. *Proceedings of the 7th International Symposium on Water-Rock Interaction—WRI-7. Volume 1: Low Temperature Environments*. Y.K. Kharaka and A.S. Maest, eds. Rotterdam: A.A. Balkema.
- Krupka, K.M., R.L. Erikson, S.V. Mattigod, J.A. Schramke, and C.E. Cowan. 1988. *Thermochemical Data Used by the FASTCHEM Package*. EPRI-EA-5872. Palo Alto, CA: Electric Power Research Institute.

- Kubaschewski, O., and C.B. Alcock. 1979. *Metallurgical Thermochemistry*. 5th Ed. Oxford, UK: Pergamon Press.
- LaFlamme, B.D., and J.W. Murray. 1987. Solid/solution interaction: The effect of carbonate alkalinity on adsorbed thorium. *Geochimica et Cosmochimica Acta* 51: 243-250.
- Langmuir, D. 1978. Uranium solution-mineral equilibria at low temperatures with applications to sedimentary ore deposits. *Geochimica et Cosmochimica Acta* 42: 547-569.
- Langmuir, D., and J.S. Herman. 1980. The mobility of thorium in natural waters at low temperatures. *Geochimica et Cosmochimica Acta* 44: 1753-1766.
- Lemire, R.J. 1984. *An Assessment of the Thermodynamic Behavior of Neptunium in Water and Model Groundwater from 25 to 150 °C*. AECL-7817. Pinawa, Manitoba: Atomic Energy of Canada Limited.
- Lemire, R.J., and P.R. Tremaine. 1980. Uranium and plutonium equilibria in aqueous solutions to 200 °C. *Journal of Chemical Engineering Data* 25: 361-370.
- Lieser, K.H., and B. Thybusch. 1988. Sorption of uranyl ions on hydrous titanium dioxide. *Fresenius Zeitschrift für Analytisch Chemie* 332: 351-357.
- Manceau, A. and L. Charlet. Sorption and speciation of heavy metals at the oxide/water interface: From microscopic to macroscopic. *Environmental Pollution* 1: 401-408.
- Mesuere, K.L.G. 1992. *Adsorption and Dissolution Reactions Between Oxalate, Chromate, and an Iron Oxide Surface: Assessment of Current Modeling Concepts*. Ph.D. Dissertation. Beaverton, OR: Oregon Graduate Institute of Science and Technology.
- Mesuere, K.L.G., and W. Fish. 1992. Chromate and oxalate adsorption on goethite. 1. Calibration of surface complexation models. *Environmental Science and Technology* 26: 2357-2364.
- Mills, K.C. 1974. *Thermodynamic Data for Inorganic Sulphides, Selenides and Tellurides*. London, UK: Butterworths.
- Morrey, J.R., C.T. Kincaid, C.J. Hostetler, S.B. Yabusaki, and L.W. Vail. 1986. *Geohydrochemical Models for Solute Migration. Volume 3: Evaluation of Selected Computer Codes*. EPRI-EA-3417. Palo Alto, CA: Electric Power Research Institute.
- Morss, L.R. Thermodynamic properties. *The Chemistry of the Actinide Elements*, 2nd Ed. T.T. Katz, G. Seaborg, and L.R. Morss, eds. NY: Chapman and Hall: 1278-1360.
- Moulin, V., D. Stammose, and G. Ouzounian. 1992. Actinide sorption at oxide-water interfaces: Application to α alumina and amorphous silica. *Applied Geochemistry Supplemental Issue* 1: 163-166.

- Murray, J.W. 1974. The surface chemistry of hydrous manganese dioxide. *Journal of Colloid and Interface Science* 46: 357-371.
- Nakayama, S., and Y. Sakamoto. 1991. Sorption of neptunium on naturally-occurring iron-containing minerals. *Radiochimica Acta* 52/53: 153-157.
- Nash, K.L., and J.M. Cleveland. 1984. The thermodynamics of plutonium(IV) complexation by fluoride and its effect on plutonium (IV) speciation in natural waters. *Radiochimica Acta* 36: 129-134.
- NEA. 1989. *NEA-TDB: Chemical Thermodynamics of Uranium. Draft Report*. OECD Data Bank. Saclay, France: Nuclear Energy Agency.
- NEA. 1990. *NEA-TDB: Chemical Thermodynamics of Uranium. Draft Report*. OECD Data Bank. Saclay, France: Nuclear Energy Agency.
- Naumov, G.B., B.N. Ryzhenko, and I.L. Khodakovsky. 1974. *Handbook of Thermodynamic Data*. USGS-WRD-74-001, trans. NTIS-PB-226 722/AS. Springfield, VA: National Technical Information Service.
- Oetting, F.L., M.H. Rand, and R.J. Ackerman. 1976. *The Chemical Thermodynamics of Actinide Elements and Compounds, Part 1. The Actinide Elements*. Vienna, Austria: IAEA.
- O'Hare, P.A.G., B.M. Lewis, and S.N. Nguyen. 1988. *Thermochemistry of Uranium Compounds, XVII. Standard Molar Enthalpy of Formation at 298.15 K of Dehydrated Schoepite $UO_3 \cdot 0.9 H_2O$. Thermodynamics of Schoepite + Dehydrated Schoepite + Water*. UCRL-21053 s/c 610-007. Livermore, CA: Lawrence Livermore National Laboratories.
- Owens, B.B., and S.W. Mayer. 1964. The thermodynamic properties of uranyl sulphate. *Journal of Inorganic Nuclear Chemistry* 26: 501-507.
- Pabalan, R.T. and D.R. Turner. 1992. Sorption Modeling for HLW Performance Assessment. *Report on Research Activities for Calendar Year 1991*. W.C. Patrick, ed. CNWRA 91-01A. San Antonio, TX: Center for Nuclear Waste Regulatory Analyses: 8-1 to 8-66.
- Pabalan, R.T. and D.R. Turner. 1993. Sorption Modeling for HLW Performance Assessment. *NRC High-Level Radioactive Waste Research at CNWRA January Through June 1993*. B. Sagar, ed. CNWRA 92-02S. San Antonio, TX: Center for Nuclear Waste Regulatory Analyses: 8-1 to 8-18.
- Pabalan, R.T., J.D. Prikryl, P.M. Muller, and T.B. Dietrich. 1993. Experimental study of uranium(6+) sorption on the zeolite mineral clinoptilolite. *Materials Research Society Symposium Proceedings: Scientific Basis for Nuclear Waste Management - XVI*. C. Interrante and R. Pabalan, eds. Pittsburgh, PA: MRS: 777-782.
- Papelis, C., K.F. Hayes, and J.O. Leckie. 1988. *HYDRAQL: A Program for the Computation of Chemical Equilibrium Composition of Aqueous Batch Systems Including Surface-Complexation*

Modeling of Ion Adsorption at the Oxide/Solution Interface. Technical Report No. 306. Stanford University: Stanford, CA: Department of Civil Engineering.

- Payne, T.E., and T.D. Waite. 1991. Surface complexation modelling of uranium sorption data obtained by isotope exchange techniques. *Radiochimica Acta* 52/53: 487-493.
- Payne, T.E., K. Sekine, J.A. Davis, and T.D. Waite. 1992. Modeling of radionuclide sorption processes in the weathered zone of the Koongarra ore body. *Alligator Rivers Analogue Project Annual Report, 1990-1991*. P. Duerden, ed. Australian Nuclear Science and Technology Organization: 57-85.
- Phillips, S.L., F.V. Hale, L.F. Silvester, and M.D. Siegel. 1988. *Thermodynamic Tables for Nuclear Waste Isolation: Aqueous Solutions Database*. NUREG/CR-4864. Washington, DC: NRC.
- Rai, D., J.M. Zachara, L.E. Eary, C.C. Ainsworth, J.E. Amonette, C.E. Cowan, R.W. Szelmezcza, C.R. Resch, R.L. Schmidt, D.C. Girvin, and S.C. Smith. 1988. *Chromium Reactions in Geologic Materials*. EPRI-EA-5741. Palo Alto, CA: Electric Power Research Institute.
- Rard, J.A. 1983. *Critical Review of the Chemistry and Thermodynamics of Technetium and Some of its Inorganic Compounds and Aqueous Species*. UCRL-53440. Livermore, CA: Lawrence Livermore National Laboratories.
- Rard, J.A. 1984. *Errata Sheet to UCRL-53440*. Unpublished Note, March 1984: Lawrence Livermore National Laboratories.
- Rard, J.A. 1985a. Chemistry and thermodynamics of ruthenium and some of its inorganic compounds and aqueous species. *Chemical Review* 85: 1-39.
- Rard, J.A. 1985b. Chemistry and thermodynamics of europium and some of its simpler inorganic compounds and aqueous species. *Chemical Review* 85: 555-582.
- Rard, J.A. 1987a. *Thermodynamic Data Bases for Multivalent Elements: An Example for Ruthenium*. UCRL-96555. Livermore, CA: Lawrence Livermore National Laboratories.
- Rard, J.A. 1987b. *Update of the Europium Data Base, October, 1987*. Internal Memorandum: Lawrence Livermore National Laboratories.
- Reardon, E.J. 1981. K_d 's—Can they be used to describe reversible ion sorption reactions in contaminant migration? *Groundwater* 19: 279-286.
- Regazzoni, A.E., M.A. Blesa, and A.J.G. Maroto. 1983. Interfacial properties of zirconium dioxide and magnetite. *Journal of Colloid and Interface Science* 91: 560-570.
- Rickard, D.T., and J.O. Nriagu. 1978. Aqueous environmental chemistry of lead. *The Biochemistry of Lead in the Environment*. J.O. Nriagu, ed. NY: Elsevier.

- Riese, A.C., 1982. *Adsorption of Radium and Thorium onto Quartz and Kaolinite: A Comparison of Solution/Surface Equilibria Models*. Ph.D. Dissertation. Golden CO: Colorado School of Mines.
- Righetto, L., G. Bidoglio, B. Marcandalli, and I.R. Bellobono. 1988 Surface interactions of actinides with alumina colloids. *Radiochimica Acta* 44/45: 73-75.
- Righetto, L., G. Bidoglio, G. Azimonti, and I.R. Bellobono. 1991. Competitive actinide interactions in colloidal humic acid-mineral oxide systems. *Environmental Science and Technology* 25: 1913-1919.
- Robie, R.A., B.S. Hemingway, and J.R. Fisher. 1979. *Thermodynamic Properties of Minerals and Related Substances at 298.15 K and 1 bar (10⁵ Pascals) Pressure and At Higher Temperatures*. USGS Bull. 1452. Reston, VA: U.S. Geological Survey.
- Rogers, P.S.Z., and A. Meijer. 1993. Dependence of radionuclide sorption on sample grinding, surface area, and water composition. *Proceedings of the Fourth Annual International Conference on High Level Radioactive Waste Management*. La Grange Park, IL: American Nuclear Society: 1509-1516.
- Rundberg, R.S. 1992. A suggested approach toward measuring sorption and applying sorption data to repository performance assessment. *Radionuclide Sorption From the Safety Evaluation Perspective, Proceedings of an NEA Workshop*. Nuclear Energy Agency, Paris: Organization for Economic Cooperation and Development: 187-215.
- Sanchez, A.L., J.W. Murray, and T.H. Sibley. 1985. The adsorption of plutonium IV and V on goethite. *Geochimica et Cosmochimica Acta* 49: 2297-2307.
- Schwab, A., and A. Felmy. 1982. *Review and Reevaluation of Pu Thermodynamic Data, Draft Manuscript*. PNL-SA-10731. Richland, WA: Pacific Northwest Laboratory.
- Siegel, M.D., V.S. Tripathi, M.G. Rao, and D.B. Ward. 1992. Development of a multi-site model for adsorption of metals by mixtures of minerals: 1. Overview and preliminary results. *Water-Rock Interaction: Proceedings 7th International Symposium on Water-Rock Interaction*. In Y.F. Kharaka and A.S. Maest eds. Rotterdam, Netherlands: A.A. Balkema
- Smith, R.M., and A.E. Martell. 1976. *Critical Stability Constants. Volume 4: Inorganic Complexes*. NY: Plenum Press.
- Smith, R.W., and E.A. Jenne. 1988. *Compilation, Evaluation, and Prediction of Triple-Layer Model Constants for Ions on Fe(III) and Mn(IV) Hydrous Oxides*. PNL-6754. Richland, WA: Pacific Northwest Laboratory.
- Smith, R.W., and J.A. Jenne. 1991. Recalculation, evaluation, and prediction of surface complexation constants for metal adsorption on iron and manganese oxides. *Environmental Science and Technology* 25: 525-531.

- Smith, R.W., and J.A. Jenne. 1992. Reply to: "Comment on: Recalculation, evaluation, and prediction of surface complexation constants for metal adsorption on iron and manganese oxides." *Environmental Science and Technology* 26: 1253-1254.
- Sposito, G. 1992. Experimental validation of surface speciation models. *American Geophysical Union 1992 Annual Meeting*. American Geophysical Union. Washington, DC: 597.
- Sprycha, R. 1984. Surface charge and adsorption of background electrolyte ions at anatase/electrolyte interface. *Journal of Colloid and Interface Science* 102: 173-185.
- Sprycha, R. 1989. Electrical double layer at alumina/electrolyte interface. *Journal of Colloid and Interface Science* 127: 1-11.
- Stammose, D., and J.M. Dolo. 1990. Sorption of americium at trace levels on a clay mineral. *Radiochimica Acta* 51: 189-193.
- Sverjensky, D.A. 1990. Progress report for geochemical investigation of uranium mobility in the Koongarra ore deposit—A natural analog for the migration of radionuclides from a nuclear waste repository. In: P. Duerden (ed.) Alligator Rivers Analogue Project Progress Report: 1 September 1989 -30 November 1989. Australian Nuclear Science and Technology Organization: 35-40.
- Swallow, K.C. 1978. *Adsorption of Trace Metals by Hydrous Ferric Oxide*. Ph.D. Dissertation. Cambridge, MA: Massachusetts Institute of Technology.
- Tripathi, V.S. 1984. *Uranium(VI) Transport Modeling: Geochemical Data and Submodels*. Ph.D. Dissertation. Stanford, CA: Stanford University.
- Tripathi, V.S. and G.A. Parks. 1992. Factors governing reliability of stability constants. *Materials Research Society 1992 Fall Meeting*. Pittsburgh, PA, MRS: 597.
- Turner, D.R. 1991. *Sorption Modeling for High-Level Waste Performance Assessment: A Literature Review*. CNWRA 91-011. San Antonio, TX: Center for Nuclear Waste Regulatory Analyses.
- Turner, D.R., T. Griffin, and T.B. Dietrich. 1993. Radionuclide sorption modeling using the MINTEQA2 speciation code. *Materials Research Society Symposium Proceedings: Scientific Basis for Nuclear Waste Management—XVI*. C. Interrante and R. Pabalan, eds. Pittsburgh, PA: MRS: 783-789.
- Venkataramani, B., and A.R. Gupta. 1991. Effect of anions on the sorption of uranyl ions on hydrous oxides: Application of the surface hydrolysis model. *Colloids and Surfaces* 53: 1-19.
- Viani, B.E., and C.J. Bruton. 1992. Modeling ion exchange in clinoptilolite using the EQ3/6 geochemical modeling code. *Proceedings of the Seventh International Symposium on Water-Rock Interaction. Volume 1: Low Temperature Environments*. Rotterdam, Netherlands: A.A. Balkema.: 73-77.

- Wagman, D.D., W.H. Evans, V.B. Parker, R.H. Shumm, I. Halow, and S.M. Bailey et al. 1982. *The NBS Tables of Chemical Thermodynamic Properties. Selected Values for Inorganic and C1 and C2 Organic Substances in SI Units*. New York, NY: American Chemical Society.
- Wanner, H. 1988 The NEA thermochemical data base project. *Radiochimica Acta* 44/45: 325-329.
- Westall, J.C., J.L. Zachary, and F.M.M. Morel. 1976. *MINEQL, A Computer Program for the Calculation of Chemical Equilibrium Composition of Aqueous Systems*. Tech. Note 18. Cambridge, MA: Department of Civil Engineering, Massachusetts Institute of Technology.
- Westall, J.C. 1982a. *FITEQL: A Computer Program for Determination of Chemical Equilibrium Constants From Experimental Data, Version 1.2*. Rpt. 82-01. Corvallis, OR: Department of Chemistry, Oregon State University.
- Westall, J.C. 1982b. *FITEQL: A Computer Program for Determination of Chemical Equilibrium Constants From Experimental Data, Version 2.0*. Rpt. 82-02. Corvallis, OR: Department of Chemistry, Oregon State University.
- Westall, J.C., and H. Hohl. 1980. A comparison of electrostatic models for the oxide/solution interface. *Advances in Colloid and Interface Science* 12: 265-294.
- Wolery, T.J., K.J. Jackson, W.L. Bourcier, B.E. Bruton, K.G. Knauss, and J.M. Delany. 1990. Current status of the EQ3/6 software package for geochemical modeling. *Chemical Modeling of Aqueous Systems II*. D. Melchior and R.L. Bassett, eds. ACS Symposium Series 416. Washington, DC: American Chemical Society: 104-116.
- Yates, D.A. 1975. *The Structure of the Oxide/Aqueous Electrolyte Interface*. Ph.D. Dissertation. Melbourne, Australia: University of Melbourne.
- Yates, D.A., and T.W. Healy. 1975. Mechanism of anion adsorption at the ferric and chromic oxide/water interfaces. *Journal of Colloid and Interface Science* 52: 222-228.
- Yeh, G.T., and V.S. Tripathi. 1989. A critical evaluation of recent developments in hydrogeochemical transport models of reactive multichemical components. *Water Resources Research* 25: 93-108.
- Zachara, J.M., D.C. Girvin, R.L. Schmidt, and C.T. Resch. 1987. Chromate adsorption on amorphous iron oxyhydroxide in the presence of major groundwater ions. *Environmental Science and Technology* 21: 589-594.